Title page

- Student Name: Jennifer Chau
- Title of the thesis: Contrast Enhanced Computed Tomography (CT) Of The Hepatobiliary Systems In Dogs And Cats: Protocols For Imaging Studies
- Faculty name: Science
- University's full name – The University of Sydney
- Submission statement: A thesis submitted in fulfilment of the requirements for the degree of Doctor of Philosophy

Statement of originality

- *This is to certify that to the best of my knowledge, the content of this thesis is my own work. This thesis has not been submitted for any degree or other purposes.*
- *I certify that the intellectual content of this thesis is the product of my own work and that all the assistance received in preparing this thesis and sources have been acknowledged.*

Student Name: Jennifer Chau

Date: 29.9.23

Authorship attribution statement

(The corresponding author is listed as the first author).

Chapter 1 *of this thesis is published as Chau et al, 2016 and Makara et al, 2015. For the first study (Chau et al, 2016), I designed the study, collected and analysed the data and wrote the drafts of the manuscript.*

For the second study (Makara et al, 2015), I co-designed the study with the co-authors, collected the data, interpreted the analysis and was involved with editing the manuscript.

Chapter 2 *of this thesis is published as Thierry et al, 2018. This was a multicentre collaboration study. I co-designed the study with the co-authors, collected data, interpreted the analysis and was involved with editing the manuscript.*

Chapter 4 *of this thesis is published as Chau et al, 2017 and Pilton et al, 2019.*

For the first study (Chau et al, 2017), I designed the study, collected and analysed the data and wrote the drafts of the manuscript.

For the second study (Pilton et al, 2019), I co-designed the study with the co-authors, contributed to data collection and analysis.

Attesting your authorship attribution statement

In addition to the statements above, in cases where I am not the corresponding author of a published item, permission to include the published material has been granted by the corresponding author. I understand that if the thesis is accepted, then the thesis will be lodged with the University Librarian and made available for immediate use.

Student Name: Jennifer Chau

Date: 29.9.23

As supervisor for the candidature upon which this thesis is based, I can confirm that the authorship attribution statements above are correct.

Supervisor Name: Dr Craig Ruaux

Date: 29.09.2023

Thesis abstract

Introduction:

Contrast enhanced computed tomography (CECT) of the abdomen in dogs and cats is an increasingly common diagnostic imaging study that may be performed in clinical practice. CT is a rapid acquisition advanced imaging modality that provides cross sectional anatomy in high resolution. After the injection of an intravenous contrast agent, multiple phases of enhancement can be captured during CECT for vascular and parenchymal imaging.[1,2,3,4] It is commonly indicated for detection of congenital portosystemic shunt in dogs and cats and for focal liver disease (e.g. primary or metastatic liver cancer).[5] Abnormalities of the biliary system that may require advanced diagnostic imaging include biliary obstruction or rupture secondary to trauma or recent liver surgery.[6,7]

Aims:

1. Evaluate the influence of contrast injection technique on timing of enhancement of the liver in normal dogs and cats.
2. Develop a standardised protocol for multiphase abdominal CT imaging in dogs and compare protocols between various veterinary institutions.
3. Refine contrast CT imaging in cats: Identify the Ideal Dose of Iohexol
4. Develop a protocol for CECT of the biliary tract using a novel gadolinium-based contrast agent.

Method: Multiphase CECT will be performed in dogs and cats at the University Veterinary Teaching Hospital Sydney as a prospective clinical study. A multicentre collaborative study will be performed to compare different protocols for multiphase CECT in dogs. CT cholangiography will be performed experimentally in healthy research dogs.

Results: We proved that patient body weight, contrast injection technique and contrast dose in dogs and cats are significant factors to consider when planning multiphase CECT. A standardised protocol for multiphase CECT was developed using a regression formula to predict optimal timing of the arterial and liver parenchymal phase. A lowered dose rate for iohexol is recommended in cats based on our research. Biliary CT imaging using a gadolinium-based contrast agent was feasible in dogs but was cost prohibitive, and not feasible in cats.

Conclusion: The standardised protocol for multiphase CECT developed in this research project was proven to be easily reproducible and effective when compared to other CT protocols. Our standardised protocols can overcome the unique challenges when facing veterinary patients that differs to human patients.

Abstract References:

1. Bae KT. Intravenous contrast medium administration and scan timing at CT: considerations and approaches. Radiology. 2010 Jul;256(1):32–61.
2. Makara M, Dennler M, Kuhn, K et al Effect of contrast medium injection duration on peak enhancement and time to peak enhancement of canine pulmonary arteries Vet Radiol and Ultrasound 2011; 52(6): 605–610.
3. Mai W, Suran JN, Caceres AV, Reetz JA. Comparison between bolus tracking and timing-bolus techniques for renal computed tomographic angiography in normal cats Vet Radiol and Ultrasound 2013; 00 (0): 1-8
4. Zwingenberger AL and Schwarz T. Dual-phase CT Angiography of the Normal Canine Portal and Hepatic Vasculature. Veterinary Radiol and Ultrasound 2004; 45(2):117–124
5. d'Anjou, MA. Liver. In: Penninck DA and d'Anjou, MA. Atlas of Small Animal Ultrasonography. Iowa: Blackwell Publishing 2008; 217-262.
6. Lee NK, Kim S, Lee JW, Lee SH, Kang DH, Kim GH, et al. Biliary MR Imaging with Gd-EOB-DTPA and Its Clinical Applications1. RadioGraphics. Radiological Society of North America; 2009 Oct;29(6):1707–24.
7. Suter PF, Olsson SE. The diagnosis of injuries to the intestines, gallbladder and bile ducts in the dog. J Small Anim Pract. 1970 Sep;11(9):575–84.

Table of Content:

SECTION 1. List of Publications

Publication 1

Authors: Jennifer Chau, Alex Young, Navneet Dhand and Mariano Makara

Title: Estimation of time to peak contrast enhancement of the aorta and liver for dual-phase computed tomography on the basis of contrast medium arrival time, injection duration, and injection technique in dogs

Year of Publication: 2016

Journal: American Journal of Veterinary Research

Publication 2

Authors: Mariano Makara, Jennifer Chau, Evelyn Hall, Heide Kloeppel, Juan Podadera and Vanessa Barrs.

Title: Effects of two contrast injection protocols on feline aortic and hepatic enhancement using dynamic computed tomography

Year of Publication: 2015

Journal: Veterinary Radiology and Ultrasound

Publication 3

Authors: Florence Thierry, Jennifer Chau, Mariano Makara, Swan Specchi, Edoardo Auriemma, Maurizio Longo, Ian Handel, Tobias Schwarz

Title: Vascular conspicuity differs among injection protocols and scanner types for canine multiphasic abdominal computed tomographic angiography

Year of Publication: 2018

Journal: Veterinary Radiology and Ultrasound

Publication 4

Authors: Jennifer Chau, Juan M Podadera, Alex Young and Mariano Makara

Title: Use of gadoxetic acid for computed tomographic cholangiography in healthy dogs

Year of Publication: 2017

Journal: American Journal of Veterinary Research

Publication 5

Authors: Joanna L Pilton, Jennifer Chau, Timothy S Foo, Evelyn J Hall, Fernando Martinez-Taboada, Juan M Podadera, Mariano A Makara

Title: Hepatic computed tomography and cholangiography by use of gadoxetic acid in healthy cats

Year of Publication: 2019

Journal: American Journal of Veterinary Research

Manuscript

Authors: Jennifer Chau, Evelyn Hall and Mariano Makara.

Title: Reduced dose of iohexol in abdominal computed tomography in cats

SECTION 2. Literature Review

Since its introduction to the veterinary market in the late 1980's, computed tomography (CT) has revolutionized diagnostic decision making. CT is a cross sectional advanced imaging modality that produces a series of high resolution images of the internal structures of a patient. This is achieved by using a rotating xray tube that circulates around the patient as the table translates through the bore of the CT machine. CT scanners have become an essential piece of diagnostic equipment in specialist veterinary hospitals and some general practices. The global market for veterinary CT scanners is expected to reach 173.7 million USD by 2022, increasing from 122.3 million USD in 2017 (Veterinary CT Scanner Market, 2017). CT has improved the identification of disease, enhanced evaluation of acute trauma patients, progressed cancer diagnosis, surgical planning and treatment. As a cross sectional imaging modality, CT is composed of a series of topographic images, each projection is a thin slab of the patient's anatomy that can be digitally reformatted and viewed in multiple planes. Unlike conventional radiographs, CT images are free from superimposition of surrounding tissues and have superior contrast resolution. In comparison with ultrasound, the size of the patient and interference from gas in the digestive tract does not affect CT image quality. CT has proven to be superior to ultrasound for the detection of clinically relevant lesions in dogs greater than 25kg and has 100% accuracy for differentiating surgical versus non-surgical abdominal disease in dogs (Fields et al 2012, Shanaman et al 2012). CT was more sensitive for the detection of pneumoperitoneum and gastrointestinal foreign bodies compared to ultrasound. CT showed a trend toward a relatively higher total number of lesions detected (Shanaman et al 2012). The sensitivity of CT for the detection of liver cancer in dogs was 73% compared to 45% sensitivity when using ultrasound (Irausquin et al 2008). Ultrasound was found to underestimate the size and number of specific lesions compared to contrast enhanced CT (Shanaman et al 2013).

Technological advances in CT have made it an increasingly appealing imaging modality with higher spatial resolution and shorter scan times, leading to vastly increased clinical applications. Over the last decade, CT has undergone rapid technical developments, with the advent of multi-row CT detector arrays as an important turning point. Early generation CT scanners in veterinary clinics started with four-slice to 16-slice, moving to 64-slice and recent models are up to 320-slice (Sabarudin et al 2012). Multi-row detector arrays have drastically increased image acquisition speed, improved the efficiency of x-ray tubes and improved spatial resolution. The main advantage of multiple-row detector systems is their ability to cover large volumes in short scan times (Mahesh, 2002). The development of helical or spiral CT was another notable advancement in CT scanning that finally allowed true 3D image acquisition in a single breath hold. The technique involves the continuous acquisition of projection data through a 3D volume of tissue by continuous rotation of the x-ray tube and detectors, and simultaneous translation of the patient through the gantry opening. Three technological developments were required: slipring gantry designs (allow the scan frame to rotate continuously with no need to stop between rotations), very high-power x-ray tubes, and interpolation algorithms to handle the noncoplanar projection data. Current CT machines can acquire a complete CT exam of a body region within seconds that is free from

respiratory motion. As a result, the clinical usefulness of this imaging tool and rapid acquisition technology has been a driving force behind the ongoing development of new applications for CT and improved imaging techniques (Ohlerth and Scharf, 2007).

Most clinical applications for veterinary CT require multiphase contrast enhanced CT (CECT), which has been made possible due to the advances in technology allowing increased scan speed, shorter scan times and less interscan delays. The CT scanner is timed and triggered to scan the patient multiple times after a single intravascular injection of contrast medium. Image acquisition should be precisely timed to capture the first pass of contrast in the arterial system (arterial phase), maximal enhancement of the portal venous system (venous phase) and maximal enhancement of the target organ (parenchymal phase). The objective of the arterial phase is to synchronize image acquisition of the liver with the short time interval during which there is peak enhancement of the arteries but before the contrast medium recirculates through the portal system. The goal of the portal venous phase is to scan the patient during peak enhancement of the portal vein. The arterial and portal venous phases of the liver are used to evaluate the abdominal vasculature, which has become the preferred diagnostic tool in cases of congenital vascular malformations such as portosystemic shunts, hepatic arteriovenous fistula and malformations of the caudal vena cava (Zwingenberger and Schwarz, 2004; Zwingenberger et al, 2005; Bertolini et al, 2006; and Fischetti and Kovak, 2008).As portal enhancement plateaus or slowly declines, the liver reaches peak parenchymal enhancement, which can be captured on CT as the hepatic phase. CECT can be used to target different abdominal organs such as the liver, pancreas, spleen, adrenal glands and gastrointestinal tract. For CECT of the liver, the hepatic phase of contrast enhancement depicts peak accumulation of contrast in the liver which is useful for lesion detection and characterization of disease. Multiphase CECT is the imaging modality of choice for presurgical evaluation of patients with abdominal disease and cancer due to its high sensitivity for lesion detection (Oliver et al, 1996; Ohashi et al, 1993; Hollett et al, 1995 and Irausquin et al, 2008). After the introduction of multiphase CECT of the abdomen, there was more emphasis on accurate CT scan timing, optimisation of contrast injection protocols and developing standardised imaging techniques to make arterial/venous and parenchymal phase acquisitions easily reproducible and comparable between patients.

From a clinical perspective, there are many indications for abdominal CT in veterinary patients. Small animals commonly present for CT examination due to abdominal distension, organomegaly, palpable abdominal mass, cancer staging, investigation of congenital vascular anomalies, draining sinus tract due to a suspected migrating foreign body or acute abdomen. Relating to the hepatobiliary system, common clinical signs that are reported include inappetence or anorexia, lethargy, weight loss, vomiting, abdominal pain, icterus, and often elevations in serum biochemical markers for hepatobiliary disease. Most of these clinical signs are not pathognomonic for hepatobiliary disease and overlap with diseases of other organ systems. Diagnostic imaging is a useful tool to identify structural changes of the hepatobiliary system, determine the location, extent, and severity of disease, characterize the nature of the problem and if possible, facilitate guided tissue

sampling for cytology or histopathology. Ultrasound is commonly used as an initial imaging tool to assess hepatobiliary disease and is extremely helpful for guiding fine needle aspiration of the liver or any focal lesions. Changes identified in the liver may be diffuse, focal or multifocal. Common pathologies that share imaging features include hepatobiliary neoplasia (primary or metastatic) and hyperplasia. Focal liver lesions are common in dogs, especially in older patients. Benign focal liver lesions are mostly nodular hyperplasia, extramedullary haematopoiesis, hepatocellular adenoma and bile duct adenoma. In a canine study comparing the incidence of benign versus malignant hepatic masses, 38% of hepatic masses were benign (most commonly nodular hyperplasia), and 54% had malignant neoplasia (Fernando, et al 2018). The most common malignant cause for focal liver disease in dogs is metastatic neoplasia (e.g. pancreatic, splenic and gastroenteric tract) followed by primary hepatocellular carcinoma (Burti et al, 2021). CT is useful to determine the extent of tumours for surgical planning and to identify possible metastatic lesions for prognostication. At times, large structural abnormalities in the liver can be challenging to characterize using ultrasound, particularly in large dogs or if visualisation of the liver is impeded by gas in the stomach. Large space occupying lesions compress and displace adjacent organs. The involvement of nearby structures such as arteries and bile ducts can be difficult to clearly evaluate. This will have important clinical implications in terms of prognosis and surgical treatment.

Common abnormalities associated with the biliary system that require diagnostic imaging include biliary obstruction or biliary tract rupture. The integrity of the biliary system is an important clinical question following abdominal trauma such as dog fight wounds and vehicle trauma, and for patients that develop jaundice after hepatobiliary surgery (Lee et al, 2009; Suter and Olsson, 1970). The clinical signs of biliary leakage can be insidious in onset and the acute stage can be masked by other concurrent problems in cases of trauma such as fractures or abdominal haemorrhage. The prognosis of bile peritonitis is often guarded and careful radiological assessment at an early stage is recommended. Ultrasound is often the first imaging modality used to screen patients with evidence of biliary disease. It is a helpful tool for identifying dilation of the biliary tree, and signs of bile peritonitis such as steatitis and peritoneal effusion around the gallbladder. Other imaging options may be required if the underlying cause of bile duct obstruction remains unclear, or if bile peritonitis is suspected but more information is required for confirmation or to determine the site of leakage. Advanced imaging techniques described for the biliary tract include MRI cholangiography (MRCP; Marolf et al, 2011) and endoscopic retrograde cholangiopancreatography (ERC; Spillman et al, 2013). MRCP highlights fluid within the biliary tract and pancreatic ducts to diagnose intrahepatic and extrahepatic biliary tract inflammation or obstruction. It has been described in cats with high resolution sequencing, allowing consistent visualisation of the bile ducts. Unfortunately, this technique requires a high field magnet that is of limited availability in the veterinary field and MR sequences were acquired during suspended ventilation for up to 2 minutes, which is not always feasible. ERC has been reported in dogs and cats, but success is influenced by operator experience, and the procedure is technically difficult in dogs < 10kg and cats due to the small diameter of the duodenum that limits manoeuvrability of the endoscope. Cholangiography using iodinated contrast medium given orally, percutaneously, or intravenously has been performed experimentally in dogs and cats, however, various problems have been

reported relating to side effects and efficacy. Biliary uptake of contrast is expected after oral administration of ipodate calcium or ipodate sodium. Contrast can be visualised in the gall bladder on radiographs, however there was no opacification of the intrahepatic bile ducts and variable enhancement of the extrahepatic bile ducts (Allan and Dixon, 1975). The optimal time for imaging post oral administration was 12-14 hours which is a suboptimal delay for patients with biliary disease that may require laparotomy (Gaschen, 2009; Allan and Dixon, 1975). Percutaneous injection of iodinated contrast directly into the gall bladder has been performed followed by radiographs to visualise the gallbladder. Occasionally resulted in retrograde leakage of contrast into the peritoneal cavity from the injection site (Wrigley and Reuter, 1982). Some intravenous contrast agents are partially excreted via the biliary tract. Iodipamide is highly bound to plasma protein and is taken up by the liver and excreted into bile. Use of iodipamide in dogs has given variable results with some reporting minimal or no radiographic opacification of the biliary tract after 3 hours (Suter and Olsson, 1970; Gaschen 2009). Side effects from intravenous cholangiographic contrast such as licking, vomiting and defecation were frequently observed, which has been thought to be the result of rapid intravenous administration (Allan and Dixon, 1975; Maiti et al, 2011). At the time of planning this research project, specific biliary contrast media coupled with CT imaging had not been reported.

Multiphase CECT of the abdomen utilises a contrast agent administered intravenously. Different types of intravenous contrast agents are available to enhance the diagnostic capability of a CT study by improving the contrast resolution of soft tissue structures. In the absence of intravenous contrast, CT provides limited information on the internal architecture of parenchymatous organs and vessels. The addition of intravenous contrast dramatically improves visualization of soft tissue detail due to the differential uptake of contrast by adjoining organs and their connecting structures such as arteries, veins and ducts. Structures that fill with radiopaque intravenous contrast media will absorb most of the x-ray energy emitted during a CT scan, and adjacent structures that have less or no uptake of contrast media will allow the x-ray energy to pass through. Absorption of x-ray energy occurs with compounds that have a high atomic number. There are iodine and gadolinium-based contrast agents available for intravenous use. Contrast agents can be selected based on their safety, cost, distribution properties within the body and the mode of excretion that allows it to accumulate in a target organ. The iodinated contrast agent, iohexol, is the mainstay for CT vascular and parenchymal imaging and there is no question of its effectiveness. It is exceptionally well tolerated in domestic animals and humans for CT imaging with rapid renal excretion, ready accessibility and low cost (Mortele et al, 2004). Less commonly used agents in animal CT studies include other types of iodinated contrast and gadolinium-based contrast agents that can be used for biliary imaging due to their excretion pathway.

Iodinated contrast for vascular and parenchymal imaging

The current intravenous dose rate for iodinated contrast used in multiphase CECT of the abdomen in dogs and cats has derived from early radiographic contrast studies including urograms and non-selective angiograms (Feeney et al, 1982, Wise, 1982). The recommended dose is 600-880mg I/kg with slight variation in the volume depending on the concentration of the formulation (average 2ml/kg) (Schwarz and Saunders, 2011). Reduced dose rates have been reported for iohexol clearance studies using dynamic CT to calculate glomerular filtration rates in cats. Dose rates of 0.25ml to 1.5ml/kg for iodinated contrast were reported and sufficient enhancement of the kidneys was achieved. However, evaluation of the remainder of the abdomen using these lower doses is lacking. We know that circulating blood volume as a ratio of body weight area varies between domestic animals. In dogs, the circulating blood volume is 79mls/kg compared to cats at approximately 65mls/kg (Courtice, 1943). Therefore, the contrast dose (mls/kg) required to achieve the same degree of vascular enhancement may differ between cats and dogs, however currently there are no recommendations for variation in dosing between different species of veterinary patients. Using bodyweight alone in human patients may lead to excessive contrast administration in obese human patients. In humans, there was a strong negative linear correlation between the dose of injected iodine and patient weight (Gbande et al, 2023). Obese patients received a lower dose of iodine, whereas underweight patients received a dose above the recommended range. Although there are no recommendations for obese patients, radiologists had subjectively reduced the iodine dose in these human patients as a precautionary measure. An obese patient has a high proportion of body fat, a proportionally small blood volume compared to total body weight, and a small and well- perfused extracellular compartment (Gbande et al, 2023).

Ninety-five percent of iohexol is excreted via the kidneys after intravenous injection. There is a clinical preference towards using reduced contrast dose rates to avoid exacerbating renal dysfunction, particularly in the feline population due to a high incidence of pre-existing renal disease. The reported incidence of contrast induced acute renal failure in animals is low, mainly associated with ionic forms of iodinated contrast. The incidence is much higher in human patients with contrast induced nephropathy as one of the leading causes of acute renal failure in hospitalised patients (Stokes and Bartges, 2006). A recent study of feline renal function post administration of iodinated and gadolinium-based contrast showed no significant changes in renal parameters with the exception of proteinuria in 11% of cases (Prullage et al, 2022). Despite the low incidence of reported renal side effects, veterinary clinicians remain cautious and prefer to avoid intravenous contrast or request a reduced dose rate when considering contrast enhanced CT studies for elderly feline patients with pre-existing renal disease.

Radiodense contrast agents can effectively absorb x-ray energy. Organs that uptake the contrast agent will attenuate the x-ray energy (e.g. vessel), and surrounding tissues that do not uptake contrast will allow x-ray penetration. This differential absorption of x-ray energy is key to improving contrast resolution of soft tissues during CECT. Contrast agents can absorb x-ray energy by photoelectric effect.

The chance of a photoelectric effect occurring is proportional to the third power of the atomic number. Iodine has an atomic number of 52 and gadolinium is 64. As a result, the CT attenuation of gadolinium is 40% higher than that of iodine (Schmitz et al, 1997a). The chance of a photoelectric effect occurring is also inversely proportional to the third power of the X-ray photon energy (1/E3). The photoelectric effect is more likely to occur if the x-ray energy approaches the binding energy of the inner shell electron. Lower x-ray tube voltages that approximate the electron binding energy of contrast agents have been used to achieve higher CT attenuation levels from iodinated contrast. Human clinical studies have trialled lower x-ray energies to enhance the CT attenuation of contrast media. A lowered radiation exposure energy (80kVp) was coupled with a reduced contrast dose, compared to regular radiation exposure energy (120kVp) coupled with a full contrast dose. These studies showed that a similar degree of CT contrast enhancement could be reached in both patient groups even with reduced dose of contrast medium (Schmitz et al, 1997b). There was no significant difference in image noise or signal to noise ratio and reducing contrast did not interfere with vascular conspicuity or diagnostic confidence.

Gadolinium and other intravenous contrast agents for biliary imaging

One of the newer hepatobiliary biliary specific contrast agents, Gadoxetic acid (also known as gadoxetate disodium or Gd-EOB-DTPA), undergoes approximately 50% excretion through the hepatobiliary route and 50% renal excretion after intravenous administration. Hepatobiliary specific contrast agents can concentrate in the liver because they are coupled with an alipophilic ethobenzyl group that allows them to readily enter hepatocytes or Kupffer cells. Preclinical safety trials in healthy dogs and clinical trials in diseased dogs have shown no adverse clinical side effects (Marks et al, 2014; Yonetomi, et al, 2012; Dohr et al, 2007). The most common application for gadoxetic acid is for hepatobiliary imaging in humans using magnetic resonance (MRI) because of its paramagnetic properties. However, gadolinium in gadoxetic acid is an effective absorber of x-rays because of its high atomic number (64). As a contrast medium, it can effectively absorb x-ray energy in CT to improve contrast resolution. Previous experimental studies have proven that gadolinium contrast can be visualised in the liver and biliary tract of dogs using CT (Schmitz et al, 1997a; Schmitz et al, 1997b). No published studies have evaluated the feasibility and diagnostic quality of using gadoxetic acid as a cholangiographic contrast agent in dogs.

There are limited options for other types of contrast enhanced imaging of the biliary tract and none have gained widespread use due to variable success rates, side effects and prolonged biliary excretion times. Contrast agents that excrete into the biliary system are uncommon. The only iodinated intravenous cholangiographic agent currently available in Australia is Biliscopin (meglumine iotroxate). Early studies describing the use of iotroxate in cats for cholangiography reported side effects in 50% of cases, including vomiting, defecation and increased liver enzymes (Fujita and Orima, 1994). Recent studies have reported iotroxate use in dogs and cats as a slow intravenous infusion, providing contrast enhancement of the biliary tree after 60 minutes (Hayakawa et al, 2018; Tanaka et al, 2018).

Multiphase CECT of the liver increases lesion prominence by taking advantage of the dual blood supply to the liver from the arterial and portal system. In the normal liver, most of the blood flow to the liver comes from the portal vein, making up 70-75% of hepatic blood flow, and the remainder comes from the hepatic artery. In the case of liver tumours and metastatic tumours, it has been shown in humans that these lesions are supplied mainly by the hepatic artery. The arterial blood supply is even stronger when tumours increase their size. The results of an experimental study on mice with hepatic adenocarcinoma showed that the portal vein was only responsible for 4% of the blood supply (Stehlik et al, 2021). Lesions with an arterial blood supply will appear hyperattenuating against a background of liver tissue that is minimally enhanced in the arterial phase. These hypervascular lesions will be less obvious and indistinct in the portal phase when the liver tissue surrounding the lesion is also at maximal enhancement. It is this unique, momentary feature of differential contrast uptake between lesions and the surrounding liver tissue that allows CT to capture focal nodules or masses in parenchymal organs such as the liver and pancreas, and therefore increases sensitivity for lesion detection. In dogs, the sensitivity of detecting focal lesions is increased with multiphase CECT of the liver compared to ultrasound (Shanaman et al, 2012; Irausquin et a, 2008).

Characterising the type of disease present in the liver relies on focal hepatic lesions exhibiting a specific pattern of enhancement during the different contrast phases. In human radiology, multiphase CECT of focal liver disease is essential for the non-invasive detection and classification of lesions into different categories such as hepatocellular carcinoma, liver metastases, benign non-inflammatory focal liver lesions (e.g. hemangiomas, adenomas or nodular hyperplasia) and hepatic abscesses (Cao et al, 2020). These different diseases exhibit specific enhancement features on multiphase CECT. In humans, lesions greater than 2cm can be confidently diagnosed as hepatocellular carcinoma based on contrast enhancement in the arterial phase that 'washes-out' in the venous phase with a residual ring enhancement pattern. Focal nodular hyperplasia demonstrates strong, homogenous contrast enhancement during the arterial phase and a central scar (Carlson et al, 2000). The unique features of focal liver disease on multiphase CECT have been used in recent years to create data sets for artificial intelligence software that have demonstrated precision values between 81-84% (Cao et al, 2020, Yoshinobu et al, 2020). However, this is different in veterinary radiology and there is a lack of consistent information to characterise disease type based on multiphase CECT. Currently, there is no clear consensus on the enhancement characteristics of benign versus malignant hepatic lesions in dogs (see table below). A published meta-analysis of canine focal liver lesions compared 8 studies using multiphase CECT to diagnose and characterise the type of disease (Table 1). The protocols for multiphase CECT in veterinary patients are not standardised, and the parameters vary between different veterinary hospitals. A comparison of the CT protocols in Table 1 (dogs) and Table 2 (cats) shows a lack of agreement on the injection technique and scan delay times. In the veterinary literature, there is no mention of the effect of CT protocol on the pattern of lesion enhancement and reproducibility of the study.

Table 1. Multiphase CECT studies of canine focal liver lesions

Reference	Body weight	Injection rate	Injection duration	Contrast dose	Contrast concentration	Contrast arrival time measurement	Bolus tracking /test bolus	Scan timing	Lesion characterisation
Taniura et al 2009	Not provided	According to injection duration	15-20s	2ml/kg	300mg/ml or 350mg/ml	None	None	Arterial phase - 15sec Portal phase - 20 sec Delayed phase - 90sec	Hepatocellular carcinoma – up to 25/76 dogs showed characteristic changes including capsule formation, septum formation and dilated blood vessels, which were not seen in nodular hyperplastic lesions
Fukushima et al 2012	1.5-38.5kg	According to injection duration	5-10s	2ml/kg	300mg/ml	None	None	Arterial phase - 13sec Portal phase -30 sec Delayed phase - 120sec	Hepatocellular carcinoma – up to 95% (33 dogs) showed rim enhancement in the arterial phase, cyst like lesions, capsule formation and hypoattenuation in the portal/delayed phases. Hepatic adenomas or nodular hyperplasia: diffuse enhancement in arterial phase in 57-60%
Kutara et al 2013	5.7-23.9kg	According to injection duration (0.3–3 ml/s)	15-20sec	2.5ml/kg	300mg/ml	None	None	Arterial phase - 20sec Portal phase - 40sec Delayed phase -120 sec	Hepatocellular carcinoma – heterogenous in the arterial and portal phases Hypoattenuating (105-121HU) in portal/delayed phases Nodular hyperplasia – homogenous in portal and delayed phases (13/14). Hyperattenuating (111HU) in arterial phase Metastatic lesions lowest HU (65-85HU) in arterial and portal phases.
Jones et al 2016	4-54kg	2ml/s	Variable	2ml/kg	300mg/ml	None	None	Arterial phase <30sec Delayed phase <60 sec (as recommended in human	Substantial overlap in appearance of malignant and non-malignant liver and splenic masses.

								protocols)	
Griebie et al 2017	Not provided	1.0 to 3.5 mL/s	Variable	2ml/kg	385mg/ml	Yes	Bolus tracking (180HU)	Arterial phase -(immediately post trigger) Venous phase - 20sec Delayed phase - 90 sec	An equation that included only the lowest delayed-phase absolute enhancement of the mass could be used to correctly classify 42 of 46 (91.3%) masses (with expectation of malignancy if this value was < 37 Hounsfield units).
Leela-Arporn et al 2019	2.6-15.8kg	According to injection duration	20-30secs	2ml/kg	300mg/ml	Yes	Bolus tracking (200HU)	Arterial phase - 20 sec post trigger Portal phase - 20 sec after the arterial phase Delayed phase - 180secs	Malignant liver lesions were more likely heterogenous and >4.5cm in the delayed phase.
Stehlik et al, 2020	12.5-34.1kg	2ml/s	Variable	2ml/kg	300mg/ml	None	None	Arterial phase - 10-15sec Portal phase - 30-40sec Delayed phase - 90 sec	No significant differences were identified between the benign and malignant liver lesions, nor between the individual histological types of lesions. The conclusion from this study is that triple-phase contrast-enhanced computed tomography cannot differentiate between benign and malignant liver lesions.
Burti et al 2021	Not provided	Variable (hand injection)	Variable	2ml/kg	350mg/ml	None	None	Delayed phase only 60-120sec	Hepatocellular carcinoma and other malignant lesions – heterogenous enhancement in 68-100% (13/13) , however they also reported diffuse enhancement in 84% (11/13 cases). A cyst like appearance (92%, 12/13)
Magistris et al 2022	Not provided	Hand injection or 2-5ml/s	Variable	2ml/kg	300mg/ml	Not measured	None	16 dogs had an Early phase - 30-40sec and Late phase – 60sec 25 dogs had a single post contrast study	Characterisation of differential types of GIT tumours (epithelial, spindle or round cell).

Table 2. Multiphase CECT studies of cats

Reference	Body weight	Injection rate	Injection duration	Contrast dose	Contrast concentration	Contrast arrival time measurement	Bolus tracking/test bolus	Scan timing	Study purpose
Bouma 2003	10 healthy cats (mean weight of 4.5kg)	Unknown (Hand injection)	Unknown	2.2ml/kg	240mg/ml	Yes	Test bolus (0.22ml/kg)	Arterial phase - 10 sec Venous phase immediately after the first	Characterise renal vessels for renal transplantation.
Secrest et al, 2018	3-6.4kg	5ml/s	Variable	2ml/kg	350mg/ml	Yes	Test bolus	Arterial phase (set as contrast arrival time) Portal phase set as time to peak portal enhancement from test bolus Delayed phase – 180 sec	Describe triple phase CT of the feline pancreas in normal cats
Cordella and Bertolini, 2021	4 Dogs 1 cat Unknown weights	2ml/s	Variable	2ml/kg	320mg/ml	Yes	Bolus tracking (100 HU)	Arterial phase – auto min. post trigger Portal phase - 20 sec after end of arterial phase Delayed phase – 120-180sec	Describe portal venous gas and pneumobilia.
Noh et al, 2022 (8 dogs and 2 cats)	Dogs 2. 2-30kg and cats 3.1-3.6kg	According to injection duration	20 secs	2ml/kg	300mg/ml	No	N/a	Arterial phase - 20sec Portal phase - 40sec Delayed phase - 60 sec	Describe CT appearance of renal tumours in dogs and cats
Li 2022	3.5-4.5kg	0.5ml/s	Variable	1.5ml/kg	350mg/ml	Yes	Bolus tracking (200HU)	Arterial phase - 0, 2 and 4s post trigger Portal phase (5, 7 and 9s post trigger)	Evaluate the optimal delay for triple phase hepatic CT using

								Delayed (60, 62, 64s post trigger)	bolus tracking in cats (concluded that best results seen at 2s arterial phase, 7s portal phase and 62s delayed phase).

Multiphase CECT of the abdomen: variation in scan timing

The start of the arterial, portal and delayed CT scan phases varied between different institutions. Arterial phase start times ranged from 13-30 sec in dogs, and 0-10sec in cats after contrast injection. This variation in timing is significant given that modern multi-row CT machines can finish an abdominal CT scan within 5-10 secs. The portal or venous phase ranged from 20-60secs in dogs and 7-40secs in cats. Some institutions labelled the 60 sec scan the delayed phase (Burti et al 2021). The delayed phase varied from 60-180sec in dogs and cats. The definition of an arterial phase, compared to a portal/venous phase or delayed phase is not clearly described in these studies. According to a veterinary textbook on multi-row CT in small animals (Bertolini 2017), the hepatic arterial phase (HAP) can be subdivided into a pure early arterial phase (EAP) and a late arterial phase (LAP), with no or minimal enhancement of the hepatic parenchyma. The EAP provides important information in cases of vascular malformation (arterio- venous malformations and arterioportal fistulas). In the LAP, inflow in the portal vein can be observed, and the arterial vascular component still shows excellent opacification. Benign and malignant hypervascular lesions generally show maximum enhancement during this phase. However, in the veterinary studies evaluating the CT appearance of focal liver lesions, it is unclear if the CT protocols achieved an early or late arterial phase. The portal venous phase corresponds to the maximum enhancement of the liver parenchyma and takes approximately 35–40 s from the start of contrast medium injection. The delayed phase (also termed interstitial or equilibrium phase) can be acquired approximately 120 s after the start of contrast medium injection. This phase is important in the assessment of pathological changes with absent or minimal vascular supply, such as hepatic cysts, abscesses, and biliary dilations, as well as in the evaluation of venous thrombosis and tumoral invasion of the hepatic veins and hepatic vena cava.

For a successful multiphase CECT study, the CT machine needs to be triggered to scan at the right time. Scan timing should be aimed at centring the scan phase on the peak of vascular enhancement (arterial or venous) or parenchymal enhancement (e.g. liver) to maximise contrast differentiation between the vessels and surrounding soft tissues, and to maintain homogenous enhancement throughout the scan phase. In humans, it has been clearly described that an arterial phase should aim to capture the first pass of contrast in the arterial system with contrast attenuation in the aorta reaching at least 250 Hounsfield Units (HU) (Gbande et al, 2022 and Bae 2010). The portal phase (also termed hepatic phase) should capture contrast enhancement of the portal veins and hepatic veins and peak liver enhancement (satisfactory if 50-60HU above precontrast level, or good if >60HU above precontrast level) (Gbande et al, 2022). So far, there are no veterinary studies that have assessed the accuracy of their multiphase CECT studies at capturing a true arterial and portal/hepatic phase. The delayed phase in human radiology (also termed the equilibrium phase) is obtained at 3 to 5 minutes after contrast injection. During this phase, contrast has equilibrated between the intravascular and interstitial water of the liver (Kulkarni et al, 2021).

Multiphase CECT of the abdomen: variation in patient body weight:

A common feature of the canine population in these studies is variation in body weight. In one study, the heaviest dog weighed 25 times more than the lightest dog (Fukushima et al 2012). Therefore, when using a contrast dose tailored to body weight (typically 2ml/kg), the total contrast volume increased by 25-fold. In human imaging facilities, body weight categories are sometimes used to guide the contrast dose; patients weighing 64-109 kg receive 40-50mls of contrast, 110-136 kg receive 50-60mls and the dose is capped at 60-70mls for patients >136kg. In this model, the difference in contrast volume between light and heavy patients can increase by a maximum of 1.75-fold. By comparison, in veterinary patients there is no recommendation for a contrast dose cap. As a result, large breed dogs receive a significantly greater contrast volume. This will in turn affect the length of time required to administer the total volume to the patient (i.e. injecting 100mls of contrast medium through a 20G catheter is rate limited). Controlling the rate and duration of contrast injection is important as this critically affects the timing of vascular enhancement in the patient. In human radiology, variation in timing of enhancement due to changes in contrast volume and patient body weight, are controlled by standardising the injection duration. One recent study in human imaging reported the contrast medium parameters in abdominal CT scans for cancer assessment (Gbande et al 2022). Across 218 humans, the body weight ranged from 55 to 85 kg, leading to changes in the contrast volume (ranging from 20-95mls). However, the injection duration operated within a small range (23-37 secs injection duration).

Multiphase CECT of the abdomen: variation in injection technique:

Comparing multiphase CECT studies of canine focal liver lesions, 4 studies used a standard injection duration (although the chosen injection duration varied between different institutions, ranging from 5-30secs) and 2 studies used fixed injection rates (commonly 2ml/s and up to 3.5mls) and one study used a hand injection technique with no precalculated injection rate or duration. The inconsistent contrast injection technique may have caused variation in the intensity and timing of contrast enhancement, both within study groups (between patients) and between different institutions. Experimental studies in humans and animals have proven that injection techniques are important factors to consider because they critically influence the rate and distribution of contrast in the patient's body. Injection rate is the speed at which contrast is administered over time. Injection duration is defined as the time taken to administer the total volume of contrast. For a fixed contrast volume, a long injection duration requires a slow (low) injection rate, and a short injection duration leads to a faster (higher) injection rate. Maximal contrast enhancement on CT is only achieved when the total volume of contrast volume has been administered to the patient, after the end of the injection duration. There is a strong positive correlation between time to peak arterial enhancement and injection duration (Bae, 2010; Awai and Hori, 2003; Ichikawa et al 2000; Makara et al 2011). Longer injection durations will prolong the delivery of intravenous contrast medium to the patient and the peak will only occur after all the contrast medium has been administered. Long injection durations occur when using a fixed injection rate (e.g. 2ml/s) in heavy body weight patients. For example, a large dog weighing 40kg requires a greater volume of contrast (e.g. standard contrast dose of 2ml/s will equate to 80mls of contrast). The injection duration for this large dog will be 40secs when administering at a fixed rate of 2ml/s

(i.e. 80mls divided by 2ml/s). In comparison, a small dog would require less contrast volume (e.g. 5kg dog at a standard contrast dose of 2ml/s will require 10mls). The injection duration for this small patient will be 5secs (i.e. 10mls divided by 2ml/s). The time to peak arterial enhancement will occur earlier in the small patient (given that the total contrast volume will be administered in a short period of time). The time to peak arterial enhancement will occur later in the heavy patient. The consequence of a very fast injection of a small contrast volume is early enhancement which can be easily missed. In a population of cats that underwent CT renal angiography, the first pass of contrast was missed in the scanned arterial phase and contrast was already present in the veins (Mai et al, 2013). Therefore, rapid injection rates leading to early enhancement can be undesirable. There is also a limit to how much the rate of contrast delivery can perturb the time to peak enhancement due to right heart filling pressure. In humans, injections rates of 8-10ml/s lead to retrograde reflux of contrast into the caudal vena cava. The effect of contrast injection technique on arterial and liver enhancement has not been evaluated in dogs and cats. Experimental studies in human radiology have used dogs as models, however, a clinical study in dogs and cats has not been performed. The effect of variation in canine breed and body weight has not been examined in veterinary radiology.

Multiphase CECT of the abdomen: variable consideration of contrast arrival time in the aorta:

In veterinary studies on multiphase CECT of the liver, the time taken for contrast to transit from the peripheral venous injection site to the abdominal aorta was frequently not measured. The length of this transit period is affected by the patient size and cardiac output. This is termed the contrast arrival time. In humans, contrast arrival time is inversely proportional to the cardiac output, that is a longer contrast arrival time is seen with reduced cardiac output. The contrast arrival time can be measured by two methods: test bolus and bolus tracking. The test bolus technique requires administration of a small volume of contrast (usually a quarter of the diagnostic contrast dose) to identify the contrast arrival time prior to acquisition of the diagnostic images. The test bolus is given to the patient and a series of single slice CT images is obtained at the same level (usually cranial abdominal aorta) at a rate of 1 image/sec. This creates a cine loop that captures aortic enhancement over time (60 secs). A time vs attenuation curve can be generated and the point at which the aorta reaches 100-150HU is labelled the contrast arrival time. This information is used to plan the multiphase CECT scan and decide the scan delays for the arterial and hepatic phases. Alternatively, the bolus tracking technique uses a single contrast injection, and the contrast arrival time is only identified during the diagnostic CT scan. The full contrast dose is given to the patient, and a real time cine loop of the aorta is acquired (similar to the test bolus) to monitor the arrival of contrast. As soon as enhancement reaches a minimum threshold (usually 100-150HU), the beginning of the multiphase diagnostic CT scan is triggered. Therefore, if the bolus tracking technique is used, the scan delays must be preset into the CT machine before injecting contrast into the patient. When using bolus tracking technique in multiphase CECT, the arterial and hepatic phases are set with post trigger scan delays.

Currently in the veterinary literature, there is a lack of agreement on the minimum aortic density threshold. Griebie et al 2017 and Leela-Arporn et al 2019 used a minimum threshold of 180HU and 200HU, respectively. In comparison, the aortic threshold density is set at <150HU in humans (Kulkarni er al, 2021; Bae, 2010). An aortic density threshold that is too high may prolong the start of the CT scan and result in inappropriate diagnostic enhancement.
The test bolus method is used differently between institutions and the reliability of this technique has been questioned. A veterinary study that was one of the first to publish on multiphase CECT of the canine liver described the use of the test bolus technique to premeasure the contrast arrival time in the aorta (Zwingenberger and Schwarz, 2004). This contrast arrival time was then chosen as the scan delay for arterial phase and the injection duration was not taken into consideration (i.e. the arterial phase scan was set to start when contrast first appeared in the aorta). The maximum point of arterial enhancement may or may not have been captured (depending on the injection duration) because it is expected to occur after the total volume of contrast is administered. Another veterinary study used the test bolus method to measure time to peak aortic enhancement. The time to peak enhancement from the test bolus was then used as the scan delay for the arterial phase. This presumed that the time to peak aortic enhancement of the test bolus would be the same as the diagnostic bolus. In theory, this technique can be inaccurate because the TPE from a test bolus will change in the diagnostic bolus due to differences in the contrast volume and injection duration. The injection duration changes between the test bolus (1ml/kg) and the diagnostic bolus (2ml/kg), but both volumes are injected at the same fixed rate (e.g. 2ml/s). For example, a dog weighing 40kg would receive 40mls in the test bolus, and 80mls in the diagnostic bolus. When given at the same fixed injection rate such as 2ml/s, the injection duration would be 20s and 40s for the test bolus and diagnostic bolus respectively. This change in volume and injection duration will alter the timing of contrast distribution in the body. As such, using the TPE from a test bolus as the scan delay may result in prematurely finishing the CT scan before peak enhancement in the aorta occurs. Mai et al (2013) identified this anomaly in 3/9 cats when using the test bolus method; there was no arterial or venous enhancement at the scanned arterial phase, indicating that iodine had not yet arrived in the region of interest.

A limitation of current multiphase CECT protocols is that there is no standardised injection technique or CT scan protocol. Protocols vary from one institution to another, the arterial, hepatic and delayed scan times are different. This seems particularly important when using fast, multi-row CT technology. It is more challenging to accurately synchronise the CT scan with optimal enhancement of the target organ. And it is also very important when the momentary enhancement features of focal lesions are used to classify the type of disease present, including primary liver neoplasia versus metastasis or nodular hyperplasia. To accurately classify the specific CT enhancement features of different diseases, CT protocols for multiphase studies should be standardised so that the arterial and hepatic phases can be reliably and repeatedly captured. There are no veterinary studies evaluating the reliability of the different CT protocols currently in use.

Veterinary radiologists have attempted to characterise the nature of focal liver lesions on multiphase CECT based on their enhancement characteristics, trying to align with research in human radiology. However, the results from veterinary studies on multiphase CECT of canine liver lesions are conflicting. Two of 8 studies on CT enhancement characteristics of canine liver lesions found no significant differences were identified between the benign and malignant liver lesions, nor between the individual histological types of lesions (Jones et al 2016; Stehlik et al, 2020). These two studies used a fixed injection rate (resulting in variable injection duration), they did not take into consideration the contrast arrival time, and the scan times for the arterial, hepatic and delayed phases were different (see Table 1). Two of 8 studies reported heterogenous enhancement of hepatocellular carcinomas in the delayed phase (Leela-Arporn et al, 2019; Burti et al, 2021), however the injection technique was variable, and consideration of contrast arrival time was also inconsistent between these studies. Two of 8 studies reported rim enhancement in hepatocellular carcinomas in the arterial phase, which was not identified with nodular hyperplasia; these studies used a standardised injection duration (Taniura et al, 2009; Fukushima et al, 2012).

There are multiple other veterinary publications that aim to characterise the CT enhancement features of other organ lesions. Multiphase CECT for the detection of pancreatic insulinoma is highly sensitive (Iseri et al 2007, Mai and Caceres 2008 and Fukushima 2015). Two of these earlier studies agreed that pancreatic insulinomas were contrast enhancing in the arterial phase and this was the most useful scan phase (Iseri et al 2007; Mai and Caceres 2008). Both studies used the same injection rate (5ml/s) and a test bolus to estimate contrast arrival time or time taken to reach peak arterial enhancement. A later study (Fukushima et al, 2015) used a different CT protocol (standardised injection duration over 5-10 secs). This study found that hypo-attenuation was as common as hyperattenuation in dogs with insulinoma in triple-phase CT, and mass lesions were conspicuous not only in the arterial phase but in the pancreatic and later phases in some cases. A fourth study (Buishand et al, 2018) agreed that triple phase CT had the highest sensitivity for lesion detection (including metastases to the lymph nodes and liver), and that there was no single post contrast phase in which insulinomas could be best visualised.

Blaser et al (2016) assessed different injection protocols for CT of the adrenal glands in 9 healthy dogs. They used an injection protocol delivering 2ml/kg of contrast over 20 seconds, with scans obtained approximately 30 seconds after starting contrast medium injection. This provided images with maximum adrenal gland attenuation values. Another multiphase CECT study in 36 dogs with adrenal tumours also used a standard injection duration of 20 secs. This study found that cortical adenocarcinomas had significantly lower attenuation in the arterial phase compared to adenomas and phaeochromocytoma (Yoshida et al, 2016). On the contrary, a separate study in 17 dogs with adrenal masses, used a different protocol for delivering contrast (fixed injection rate at 2 ml/s, and therefore variable injection duration between dogs). This study concluded that the overlapping characteristics between tumor types limited the potential for reliably distinguishing them based on CT alone (Gregori et al 2015).

Other multiphase CECT studies in dogs tried to characterise lesions in the spleen (Cordella et al 2020) and stomach (Tanaka et al, 2019). Cordella et al (2019) found that splenic extramedullary haematopoiesis consists of multiple nodules hyperattenuating to the normal spleen, best visualized in the arterial and portal phases. This study used a variable injection rate, variable injection duration and contrast arrival time was measured using bolus tracking. By comparison, Jones et al (2016) assessed the multiphase CECT features of splenic lesions and concluded that there was substantial overlap in appearance of malignant and non-malignant splenic masses. This study used a fixed injection rate of 2 ml/s (therefore variable injection duration) and did not measure contrast arrival time.

In human radiology, the recommendation for multiphase CECT for diagnosis of liver disease is embedded in the AASLD (American Association for the Study of Liver Diseases), EASL (European Association for the Study of the Liver), OPTN (Organ Procurement and Transplantation Network), Asian Pacific Association for the Study of the Liver, JSH (Japan Society of Hepatology), National Comprehensive Cancer Network, and other organizations (Kim et al, 2019; Marrero et al 2019; Shi et al 2020; Mitchell et al 2014). They specify imaging criteria such as “arterial phase hyperenhancement” and “venous or delayed phase washout” as diagnostic of hepatocellular carcinoma. The 1-year survival rate of hepatocellular carcinoma was 25% in 1992 and has improved to 47% in 2004, and the 5-year survival from 40% to 70%, an improvement attributed to diagnosis of the cancer at an early stage (Tang et al 2015). Imaging diagnosis is preferred over biopsy due to risk of significant bleeding attributable to the hypervascular nature of hepatocellular carcinomas, risk of mortality, risk of false-negative biopsies and a risk of tumor seeding along the biopsy tract (Tang et al 2015). In a human study with 96 patients, the combination of arterial phase and delayed phase yielded the highest specificity (99%) and sensitivity (57%) (Janq et al 2013). In another study with 100 patients with focal liver lesions, only malignant lesions (hepatocellular carcinoma and metastasis) demonstrated the abnormal internal vessels or variegated pattern of enhancement on the arterial phase (Nino-Murcia 2000). Complete ring enhancement pattern was mostly seen with metastasis (82%), hepatocellular carcinoma (14%), cholangiocarcinoma (2%) and abscess (2%). They reported that occasionally metastasis and hepatocellular carcinoma exhibited no enhancement. For both human studies, the CT protocol was similar; injection rate of 5ml/s, using either a fixed contrast volume (150mls) or contrast dose of 2ml/kg but capped at 180mls, scan timing was also similar between studies (arterial phase 20-25sec, portal phase 60 sec). Similarly, another study of 60 malignant liver tumours used a fixed injection volume of 150mls and an injection rate of 4-5mls, additionally bolus tracking was used to assess contrast arrival time; arterial phase was started 12 secs post trigger, venous phase 70 secs and delayed phase 180 secs.

The CT protocol including contrast injection volume, technique and CT scan timing is relatively standardised in human radiology. In comparison, protocols for multiphase CECT of the abdomen remains variable in the veterinary literature. Contrast injection techniques are variable (different injection rates or some using standardised injection duration). The scan delays for the arterial, hepatic and delayed phases are inconsistent in the veterinary literature, and the definition of each phase is inconsistent. The contrast arrival time is infrequently measured in veterinary studies, this has been proven to be a significant factor to consider in multiphase CECT in humans. There are no studies in animals comparing the reliability and successfulness of different veterinary CT protocols. It is unclear if the same CT protocol used in human radiology can be reliably applied to dogs and cats. Given that there is a wide range in canine size due to breed, veterinary imaging is faced with significant variation in patient bodyweight. As mentioned previously, bodyweight affects the total contrast volume when using a contrast dose tailored to body weight. Changing the contrast volume will vary the duration of time required to administer the total volume of contrast to the patient, and this will in turn affect time to vascular and parenchymal enhancement. So far, there are no clinical studies in dogs and cats to assess the effect of animal body weight on time to peak enhancement.

The purpose of this thesis is to analyse the technical factors affecting CECT of the hepatobiliary tract in dogs and cats. We aimed to understand how these factors influence the timing and intensity of contrast enhancement in the abdominal aorta, portovenous system and liver and biliary tract. Regarding the intravenous contrast agent, the factors of interest included the effect of contrast dose (particularly for cats), injection rate, and injection duration in both dogs and cats. Regarding the CT machine, factors assessed include the use of bolus tracking software or test bolus injection to help predict timing of contrast arrival in the aorta and determine optimal CT scan delays for multiphase CECT imaging. Regarding the patient, the effect of patient species (canine or feline) and the effect of patient body weight were assessed. A comprehensive analysis was carried out, with the intention of identifying the key players that can perturb contrast distribution in the body. We hypothesised that the key factors affecting timing of enhancement could be used to develop standardised protocols for multiphase CECT in both dogs and cats. Chapter 1 of this thesis includes two research studies on contrast medium and patient related factors that affect timing of enhancement in multiphase CECT of the liver imaging in dogs and cats. Chapter 2 applies the information gained from the previous chapter, adopting a multicentre comparison study to critically evaluate different protocols for multiphase CECT of the abdomen in dogs, assessing the performance of these CT protocols and their diagnostic quality. Chapter 3 of the thesis aims to refine contrast CT imaging protocols in cats with a particular focus on dose reduction. Chapter 4 is an experimental study, exploring an alternative, gadolinium-based contrast agent for biliary CT imaging in dogs in cats with the aim of identifying the optimal contrast dose and timing for CT imaging.

SECTION 3 – Research Chapters (1-4)

Chapter 1. Influence of contrast injection technique on timing of enhancement of the liver in normal dogs and cats.

The pattern of contrast distribution in the body as it flows from the vascular compartment to targets organs, can be analysed on a bolus geometry curve. The curve is derived from plotting and measuring the degree enhancement of a selected area of interest over time (e.g. aorta, liver). The bolus geometry of the aorta and liver has been studied in dogs used as models for human imaging studies, and also in the veterinary clinical setting when a test bolus is used to monitor timing of enhancement. There are differences in the bolus geometry of the aorta compared to the liver. The aortic enhancement curve is expected to occur early with a rapid rise, short peak and rapid decline in enhancement as the contrast medium is diluted by blood in the intravascular space and flows into the extravascular space. The bolus geometry of the liver has a shallow, broad peak that occurs later when the contrast medium flows into the interstitial space. The contrast bolus is subject to the hemodynamics of the circulatory system such as heart rate, cardiac output and the length of the circulatory paths. The bolus geometry can also be influenced by external factors such as contrast medium injection rate, injection duration and volume. Based on experimental research studies, bolus geometry can be disturbed by increased contrast volume administered rapidly using a fast injection rate. The bolus geometry is compressed with the peak of enhancement occurring earlier (Bae, 2010). This corresponds with findings from a canine CT study of the thorax, where the bolus geometry of the pulmonary artery was shifted by a rapid injection rate and time to peak enhancement occurred earlier. Small dogs with low body weight were particularly susceptible to this shift, and we hypothesised that the same effect would be seen in the feline population. The bolus geometry of the pulmonary artery was significantly different between dogs of different body size when using a fixed, rapid injection rate (Makara et al, 2011). Conversely, the bolus geometry remained relatively unchanged when a slower injection rate was used with contrast administered over a fixed duration (Makara, 2011). These findings were replicated in an experimental study using Beagle dogs from a research facility. Fixing the injection duration resulted in reproducible contrast timing (Tateishi et al, 2008). We hypothesised that the bolus geometry of the splanchnic vessesls and liver could be similarly affected by changes in injection rate and injection duration. The added interaction of patient body weight and size is also in question, given that changes in body weight in turn affects contrast volume and injection rate or duration. We aimed to identify the significant variables that affect bolus geometry in the splanchnic vessels and liver in dogs that varied in body weight and in feline patients. Focus is given to the time taken to reach peak enhancement in the splanchnic vessels and liver. The ability to predict time to peak enhancement offers the potential to make standardised recommendations for CT scan timing when acquiring abdominal multiphase CECT studies.

Estimation of time to peak contrast enhancement of the aorta and liver for dual-phase computed tomography on the basis of contrast medium arrival time, injection duration, and injection technique in dogs

Jennifer Chau BVSc
Alex C. Young BVSc
Navneet Dhand PhD
Mariano A. Makara Dr Med Vet

Received June 18, 2015.
Accepted December 7, 2015.

From the Department of Diagnostic Imaging, Faculty of Veterinary Science, University of Sydney, Sydney, NSW 2006, Australia.

Address correspondence to Dr. Makara (mariano.makara@sydney.edu.au).

OBJECTIVE
To evaluate the accuracy of estimating time to peak enhancement (TPE) of the aorta and liver parenchyma on the basis of contrast medium arrival time in the aorta, injection duration, and injection technique in dogs.

ANIMALS
18 dogs of specific body weight categories (≥ 2 dogs/category) with no liver abnormalities detected via CT.

PROCEDURES
Dogs were randomly assigned within weight categories to receive contrast medium IV at a fixed injection rate (5 mL/s) or fixed injection duration (20 seconds). Time–contrast attenuation curves were generated from dynamic CT scans acquired at the hepatic hilus. Data collected for contrast medium arrival time and injection duration were used to estimate TPEs of the aorta and liver, and results were compared with the observed TPEs for the aorta and liver.

RESULTS
Contrast medium arrival time, injection duration, and injection technique were significantly associated with observed values for aortic TPE and explained 96.1% of variation in TPE. For the fixed rate technique, the regression equation for estimating aortic TPE was 0.8 X (injection duration + contrast medium arrival time) + 1.6. For the fixed duration technique, the regression equation changed by only the constant (−2.6). However, the hepatic TPE estimated from the 3 predictor variables was not significantly different from the mean of observed TPEs.

CONCLUSIONS AND CLINICAL RELEVANCE
Aortic TPE could be accurately estimated from contrast medium arrival time, injection duration, and injection technique in dogs with apparently healthy livers. The regression equations derived from this relationship can be used to improve the efficiency of dual-phase CT of the liver in dogs. (*Am J Vet Res* 2016;77:1093–1100)

The applications for contrast CT of the abdomen include vascular and parenchymal imaging. Vascular CT imaging has been used for angiographic evaluation of clinically normal dogs and is a useful technique for the diagnosis of congenital vascular malformations such as portosystemic shunts, hepatic arteriovenous fistulas, and malformations of the caudal vena cava.[1–6] More recently, multiple studies[7–9] have been conducted to explore applications for parenchymal CT imaging, particularly of the liver and pancreas in dogs. The advent of fast, multidetector CT technology has enabled acquisition of data pertaining to both arterial and parenchymal phases of contrast enhancement after a single contrast injection. Dual-phase contrast CT of the liver and pancreas in people is performed to increase the sensitivity for lesion detection and to enable characterization of disease.[10–14]

ABBREVIATIONS
HU Hounsfield unit
ROI Region of interest
TPE Time to peak enhancement

The principal goal of dual-phase CT is to acquire images when optimal contrast resolution of the structure of interest is evident following contrast medium injection.[12] This occurs when there is differential enhancement between the focal lesion and the surrounding parenchyma. When contrast resolution is optimized, the sensitivity increases for detecting focal lesions in organs such as the liver and pancreas.[7–9] Focal hepatic lesions that are hypervascular will increase in conspicuity during the arterial phase be-

cause the surrounding hepatic parenchyma will be slower to have contrast enhancement. Subsequent diffuse parenchymal enhancement will render these lesions nonvisible, but other types of lesions that are hypovascular will be more evident during the parenchymal phase.[12,15] The timing of image acquisition following contrast medium injection is therefore of paramount importance when assessing the liver via CT.

The aim of dual-phase CT imaging is to capture peak arterial enhancement during the arterial phase and peak parenchymal enhancement during the hepatic phase. As a result, TPE of the arteries and parenchyma is an important consideration when planning CT scans.[16,17] Operators attempt to synchronize the early and late CT scan with TPE of the arteries and parenchyma, respectively. Achieving an accurate early CT scan that captures peak arterial enhancement is particularly challenging because of the inherently narrow temporal window of peak contrast enhancement.[17]

Various techniques for contrast medium injection and protocols for CT timing exist for dual-phase hepatic CT imaging in veterinary patients; however, the accuracy of these methods has not been objectively measured. A commonly used technique for contrast medium administration is IV injection by hand followed immediately by CT scanning. This technique has been used for angiographic evaluations to characterize normal anatomy and portosystemic shunts but not for dual-phase evaluations of parenchymatous organs.[6,18,19] The main limitation of administering contrast medium by hand is that there is no control over the injection duration, which is one of the most important factors in the calculation of TPE.[17,20–22]

A second contrast injection technique via a fixed injection rate (3 to 5 mL/s) has been used for dual-phase CT scans of the liver and pancreas.[1,9] Likewise, this technique does not take injection duration into account for estimating TPE of the aorta and liver. The technique for achieving a fixed injection rate has been used in conjunction with a test bolus procedure to estimate TPE. The test bolus procedure involves a small dose (eg, 0.5 to 1 mL/kg) of contrast medium administered IV to gauge the timing of enhancement in a subject prior to administration of the diagnostic bolus (2 mL/kg, IV). However, when 2 different volumes of contrast medium are given at the same injection rate, the injection duration is subsequently modified. Therefore, the information provided by the test bolus is considered a poor estimate of TPE but a good estimate of the time required for contrast medium to circulate from the venous injection site to the aorta (contrast medium arrival time).[17]

A third type of technique for contrast medium injection involves a fixed injection duration.[7,8] Contrast medium is administered at a fixed injection duration of 15 to 20 seconds, and the CT scan is started after a fixed delay period. The fixed scan delay for the early and late CT scans is the same for every subject. This technique may result in asynchrony between the CT scan and peak enhancement because of intersubject differences in blood circulatory time and cardiac output. Subjects with low cardiac output caused by cardiac disease or anesthetic depth are expected to have slower circulatory times, resulting in a delay in TPE. These variations in circulatory times can be estimated by measuring the contrast medium arrival time.[17]

Dual-phase CT is routinely performed for hepatic imaging of humans, and accurately estimating TPE is an important part of the procedure. An estimated value for TPE is calculated as a function of contrast medium arrival time and injection duration.[16,17,21,23] This calculation is a simple procedure that could be used in a clinical setting to improve the efficiency and accuracy of dual-phase CT of the liver in veterinary patients. Knowledge of the TPE is important for determining the necessary CT scan delay after contrast medium injection to allow synchronization of image acquisition with peak enhancement. However, this technique has not been validated in veterinary medicine. Furthermore, the accuracy of estimating TPE of the aorta and liver as a function of contrast medium arrival time and injection duration is unknown. The purpose of the study reported here was to measure the accuracy of estimating TPE of the aorta and liver parenchyma for 2 types of injection techniques (fixed injection rate and fixed injection duration), with contrast medium arrival time in the aorta and injection duration used as predictor variables.

Materials and Methods

Animals

Client-owned dogs brought to University Veterinary Teaching Hospital Sydney from May to November 2013 for CT evaluation involving general anesthesia for a problem unrelated to the liver were eligible for inclusion in the study. To qualify for inclusion, dogs were required to have a grossly normal liver as identified via CT, no contraindication to contrast medium administration, and a cephalic vein available for contrast medium injection. The CT assessment criteria for the liver included an unremarkable size, shape, margination, homogeneity on pre- and postcontrast CT scans, and morphology of the hepatic and portal vasculature. Dogs were excluded from the study when they had portosystemic vascular anomalies, congestive heart failure, renal failure, dehydration, or hypertension.

To achieve a uniform distribution of dogs of various body weights, an equal number of dogs of specific body weight categories (0 to 5, 5 to 10, 10 to 15, 15 to 20, 20 to 25, 25 to 30, and > 30 kg) was enrolled to provide a minimum of 2 dogs/category. Owner consent was obtained for all dogs prior to enrollment. The study protocol was approved by the Animal Ethics Committee of the University of Sydney.

Study protocol

Dogs in each body weight category were randomly allocated by drawing of numbers into 1 of

2 groups: group A received contrast medium at a fixed injection rate of 5 mL/s, and group B received contrast medium at a fixed injection duration of 20 seconds. These 2 methods of injection were adopted from techniques used in veterinary radiology. For the procedure, dogs were sedated with butorphanol tartrate[a] (0.2 mg/kg, IM). A 23-gauge IV catheter was placed into a cephalic vein, and anesthesia was induced with alfaxalone[b] (1 to 2 mg/kg, IV). Dogs were endotracheally intubated, and anesthesia was maintained with isoflurane[c] in oxygen, with dogs breathing spontaneously. Hartmann solution[d] was administered at 5 mL/kg/h from the beginning of anesthetic induction through to the point of contrast medium administration. Anesthetic variables that were monitored during the procedure included noninvasively measured arterial blood pressure, heart rate, respiratory rate, end-tidal CO_2 concentration, and Spo_2.

All CT scans were performed with a 16-slice multidetector CT scanner.[e] Dogs were positioned in sternal recumbency. Breath-holds were not used for image acquisition. A precontrast helical scan of the abdomen from the cranial aspect of the diaphragm to the pubis was performed, and images were used to evaluate the liver for focal or diffuse disease. If the liver appeared unremarkable, then a dynamic, single-slice transverse CT scan was performed at the level of the hepatic hilus (cranial to the last tributary to the portal vein [the gastroduodenal vein] and caudal to the first intrahepatic portal branch). A total of 30 single-slice transverse scans were acquired every 2 seconds for a fixed duration of 60 seconds. The settings for the dynamic scan were the same for every dog: beam collimation of 4 data channels with a detector-row width of 0.75 mm (4 X 0.75 mm), a tube potential of 120 kVp, and a tube current of 90 mA.

Injection of contrast medium was started simultaneously with initiation of the dynamic CT scan, although there was an inherent machine delay of 1 second before the start of the first transverse scan. All dogs received the same dose (2 mL/kg) of iohexol[f] (350 mg of iodine/mL), which was administered via the cephalic vein by means of an automated injector.[g] The beginning of contrast medium injection was labeled time 0. After completion of the dynamic CT scan, a postcontrast helical CT scan of the abdomen was performed to evaluate the hepatic and portal vasculature and the liver parenchyma for focal hepatic lesions. Other body regions were subsequently scanned, depending on the initial reason the dog was brought for CT evaluation.

The CT images from the dynamic scan were transferred to a designated workstation and reviewed with image-processing software.[h] Image display was standardized among dog evaluations by use of a window level of 40 and window width of 350. The contrast enhancement values for the aorta and hepatic parenchyma were measured in each dog by drawing a circular ROI in all single-slice images from the dynamic CT scan. In the aorta, the ROI occupied approximately 90% of the vessel diameter. In the hepatic parenchyma, 2 ROIs were placed in the left and right portions of the liver (avoiding intrahepatic vessels), and the mean of the 2 measurements was calculated. To reduce observer variability, all measurements of ROI were made by the same investigator (MAM). Data obtained from the ROIs were exported to spreadsheet software[i] to generate time-attenuation curves for the aorta and liver parenchyma in both injection groups.

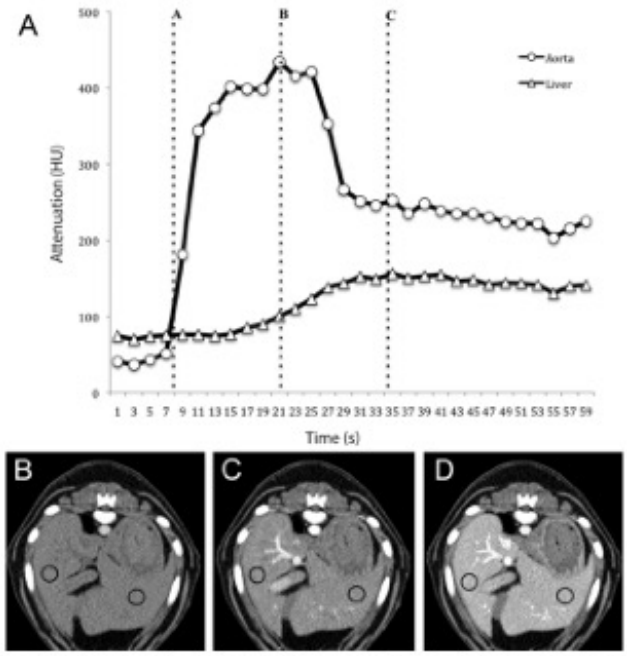

Figure 1—Time-attenuation curve for the aorta and liver during a dynamic CT scan (A) and representative transverse CT images (B–D) at the level of the liver hilus of a dog in which contrast medium (2 mL/kg) was injected IV (beginning at 0 seconds) for a fixed duration (20 seconds). A—The vertical dotted lines represent contrast medium arrival time at the aorta (A), TPE of the aorta (B), and TPE of the liver (C). B—Single-slice image corresponding with contrast medium arrival at the aorta. Notice that no contrast medium is present in other abdominal structures. C—Single-slice image corresponding with peak enhancement of the aorta. Mild diffuse parenchymal enhancement of the liver is evident, caused by perfusion of contrast medium from the hepatic arteries. No vascular enhancement of the hepatic veins is present. D—Single-slice image corresponding with peak enhancement in the liver. In both panels C and D, contrast enhancement of the portal vein is evident.

Information was collected on contrast medium arrival time (from time 0 to the point that aortic enhancement reached 100 HU), TPE of the aorta and liver parenchyma, and peak enhancement values for the aorta and liver parenchyma **(Figure 1)**. Use of 100 HU for estimation of contrast medium arrival time in the aorta was obtained from the human literature.[12] The TPE was defined as the time elapsed from the beginning of the injection to the maximum enhancement value. The peak enhancement value was defined as the maximal value obtained during dynamic CT scanning.

Statistical analysis

Statistical analyses were performed by use of statistical software.[J] Linear mixed models were created to determine the proportion of variation in TPE for aortic and liver parenchymal enhancement that could be explained by contrast medium arrival time, injection duration, and injection technique and to estimate TPE of the aorta and liver parenchyma on the basis of these variables. A block variable representing the 7 body weight groups of dogs was included as a random effect to account for the correlation within each body weight group. Model assumptions were evaluated by creating residual diagnostic plots. If the assumption of linearity appeared invalid, quadratic models were created, but the simpler model was retained if the quadratic model was not statistically superior to the simpler model. All hypothesis tests performed were 2-sided. Values of $P < 0.05$ were considered significant for all analyses.

Results

Animals

Eighteen dogs were included in the study, with 9 dogs in group A (contrast medium administered at a fixed injection rate of 5 mL/s) and 9 dogs in group B (contrast medium administered at a fixed injection duration of 20 seconds). Groups A and B had 2 dogs each in the lowest and highest body weight categories and 1 dog each in the remaining 5 body weight categories. Median body weight in group A was 16 kg (range, 1.5 to 40 kg), and that in group B was 19.8 kg (range, 3.0 kg to 69.4 kg). Group A included 2 Labrador Retrievers and 1 each of Pomeranian, Tibetan Spaniel, Maltese, Cocker Spaniel, Staffordshire Bull Terrier, Australian Shepherd, and Labrador cross. Group B included 2 Labrador Retrievers and 1 each of Miniature Pinscher, Miniature Dachshund, Poodle, Basenji, Shar Pei, Staffordshire Bull Terrier, and Bull Mastiff. Median age in group A was 11 years (range, 6 to 15 years), and that in group B was 11 years (range, 1 to 16 years). Group A included 1 sexually intact female, 2 spayed females, 1 sexually intact male, and 5 neutered males. Group B included 2 sexually intact females, 1 spayed female, 3 sexually intact males, and 3 neutered males. No significant intergroup differences were identified regarding dog age or sex.

Effects of contrast medium injection technique

Values of variables associated with contrast medium administration were summarized by individual dog **(Table 1)**. Contrast medium arrival time ($P < 0.001$), in-

Table 1—Summary of variables for individual dogs with no evidence of liver disease identified via CT in which contrast medium (2 mg/kg) was injected IV at a fixed rate of 5 mL/s (group A) or fixed injection duration of 20 seconds (group B) for dynamic CT scanning.

Dogs	Body weight (kg)	Injection duration (s)	Injection rate (mL/s)	Contrast medium arrival time (s)	TPE of the aorta (s)	Peak aorta enhancement value (HU)	TPE of the liver (s)	Peak liver enhancement value (HU)
Group A								
1	1.5	0.6	5	5	7	778	49	151
2	5	2	5	9	11	754	51	161
3	5.6	2.2	5	7	9	591	31	149
4	14.3	5.6	5	11	15	739	53	136
5	16	6.4	5	9	13	798	37	148
6	21.7	8.4	5	15	21	746	41	140
7	29.9	11.8	5	15	23	900	47	183
8	39	15.6	5	11	23	692	43	157
9	40	16	5	19	31	666	57	183
Median value	16	6.4	5	11	15	746	47	151
Group B								
1	3	20	0.3	11	21	377	51	125
2	5	20	0.5	13	23	511	49	157
3	8.9	20	0.9	7	21	489	55	149
4	11	20	1.1	11	21	607	45	180
5	19.8	20	2	13	25	679	57	173
6	22.5	20	2.2	9	21	434	35	156
7	27.4	20	2.8	13	27	639	57	154
8	49.3	20	4.9	11	23	659	47	192
9	69.4	20	7	13	23	549	51	128
Median value	19.8	20	2	11	23	549	51	156

jection duration ($P < 0.001$), and injection technique ($P = 0.03$) were significantly associated with the observed TPE of the aorta and explained 96.1% of the variation in TPE. The assumptions of linearity, independence of errors, homoscedasticity, and normality of residuals for statistical modeling of the association between aortic TPE and these 3 variables were approximately met. There were no significant outliers or influential observations. The final model was as follows:

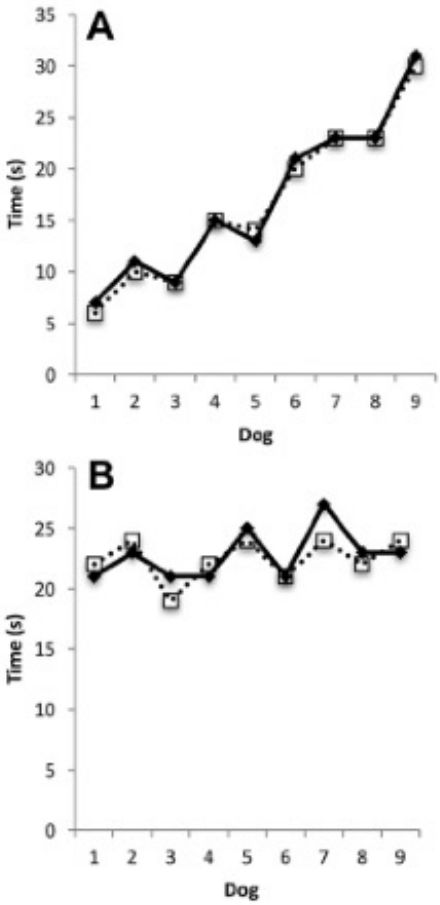

Figure 2—Observed (diamonds) and estimated (squares) TPE of the aorta for individual dogs (ordered by increasing body weight) with no evidence of liver disease identified via CT in which contrast medium (2 mL/kg) was injected IV at a fixed rate of 5 mL/s (A) or fixed injection duration of 20 seconds (B) for dynamic CT scanning. The regression equation for TPE estimates for the fixed injection rate was as follows: 0.8 X (contrast medium arrival time + injection duration)+1.6. The regression equation for TPE estimates for the fixed injection duration was as follows: 0.8 X (contrast medium arrival time + injection duration) − 2.6.

Estimated aortic TPE = (0.8 X contrast medium arrival time) + (0.8 X injection duration) − 2.6 + (4.2 X injection technique)

where a value of 1 was assigned when the injection technique was fixed rate and a value of 0 was assigned when the injection technique was fixed duration. Therefore, when the injection technique was via a fixed injection rate, the model for estimated aortic TPE was (0.8 X contrast medium arrival time) + (0.8 X injection duration) − 2.6 + (4.2 X 1). Further simplified, the model was 0.8 X (injection duration + contrast medium arrival time) + 1.6.

When the injection technique was via a fixed duration, the model for estimated aortic TPE was (0.8 X contrast medium arrival time) + (0.8 X injection duration) − 2.6 + (4.2 X 0). This simplified to 0.8 X (injection duration + contrast medium arrival time) − 2.6. Values for estimated aortic TPE for both injection techniques were plotted against observed TPEs collected from the dynamic CT scan **(Figure 2)**.

The equations for estimated aortic TPE were further simplified by consideration of dog body weight and the known dose of contrast medium **(Table 2)**. When a fixed injection duration technique was used for dogs with various body weights, the constant in the equation became fixed and the only unknown variable was contrast medium arrival time. When a fixed injection rate technique was used for dogs with various body weights, the constant in the equation varied with body weight and the contrast medium arrival time remained an unknown variable.

The estimated TPE of the liver as predicted by contrast medium arrival time ($P = 0.21$), injection duration ($P = 0.64$), and injection technique ($P = 0.40$) was not significantly different from the mean of the observed hepatic TPEs. The regression model that included those 3 variables explained only 6.4% of the variation in hepatic TPE.

Discussion

The purpose of the present study was to measure the accuracy of estimating TPE of the aorta and liver parenchyma in dogs by use of dynamic CT, taking into consideration contrast medium arrival time, injection duration, and injection technique as predictor variables. These 3 variables accounted for 96.1% of the variation in aortic TPE but could not explain variations in hepatic TPE. Therefore, contrast medium arrival time and injection duration are important factors to consider when determining aortic TPE during CT. This is in agreement with previous reports[17,24] and can be explained by the physiologic distribution of contrast medium within the body.

Peak enhancement of the aorta is expected to occur after the full dose of contrast medium has been delivered, with additional time allowed for the medium to move from the venous access site to the aorta. For any given injection rate, a constant inflow of contrast medium occurs throughout the injection duration, which contributes to progressive opacification of the aorta. A brief additional period is required

Table 2—Simplified regression equations for estimating TPE of the aorta by contrast medium injection technique and body weight for the dogs in Table 1.

Body weight (kg)	Volume of contrast medium (2 mL/kg)	Injection rate (mL/s)	Injection duration (s)	Expanded equation	Simplified equation
Fixed injection rate					
5	10	5	2	$(0.8 \times T_{arr}) + (0.8 \times 2) + 1.6$	$(0.8 \times T_{arr}) + 3.2$
10	20	5	4	$(0.8 \times T_{arr}) + (0.8 \times 4) + 1.6$	$(0.8 \times T_{arr}) + 4.8$
15	30	5	6	$(0.8 \times T_{arr}) + (0.8 \times 6) + 1.6$	$(0.8 \times T_{arr}) + 6.4$
20	40	5	8	$(0.8 \times T_{arr}) + (0.8 \times 8) + 1.6$	$(0.8 \times T_{arr}) + 8$
25	50	5	10	$(0.8 \times T_{arr}) + (0.8 \times 10) + 1.6$	$(0.8 \times T_{arr}) + 9.6$
30	60	5	12	$(0.8 \times T_{arr}) + (0.8 \times 12) + 1.6$	$(0.8 \times T_{arr}) + 11.2$
35	70	5	14	$(0.8 \times T_{arr}) + (0.8 \times 14) + 1.6$	$(0.8 \times T_{arr}) + 12.8$
40	80	5	16	$(0.8 \times T_{arr}) + (0.8 \times 16) + 1.6$	$(0.8 \times T_{arr}) + 14.4$
Fixed injection duration (s)					
5	10	0.5	20	$(0.8 \times T_{arr}) + (0.8 \times 20) - 2.6$	$(0.8 \times T_{arr}) + 13.4$
10	20	1.0	20	$(0.8 \times T_{arr}) + (0.8 \times 20) - 2.6$	$(0.8 \times T_{arr}) + 13.4$
15	30	1.5	20	$(0.8 \times T_{arr}) + (0.8 \times 20) - 2.6$	$(0.8 \times T_{arr}) + 13.4$
20	40	2.0	20	$(0.8 \times T_{arr}) + (0.8 \times 20) - 2.6$	$(0.8 \times T_{arr}) + 13.4$
25	50	2.5	20	$(0.8 \times T_{arr}) + (0.8 \times 20) - 2.6$	$(0.8 \times T_{arr}) + 13.4$
30	60	3.0	20	$(0.8 \times T_{arr}) + (0.8 \times 20) - 2.6$	$(0.8 \times T_{arr}) + 13.4$
35	70	3.5	20	$(0.8 \times T_{arr}) + (0.8 \times 20) - 2.6$	$(0.8 \times T_{arr}) + 13.4$
40	80	4.0	20	$(0.8 \times T_{arr}) + (0.8 \times 20) - 2.6$	$(0.8 \times T_{arr}) + 13.4$

The equation for the fixed rate technique simplified to 0.8 X (injection duration + contrast medium arrival time) + 1.6, and that for the fixed duration technique simplified to 0.8 X (injection duration + contrast medium arrival time) – 2.6.

T_{arr} = Contrast medium arrival time.

for contrast medium to move from the venous access site to the heart, through the pulmonary vasculature, and then to the aorta. This brief period relates to the contrast medium arrival time in the aorta and is dependent on cardiac output.[17,25]

The regression formula for estimating TPE obtained in the present study (0.8 X [injection duration + contrast medium arrival time] ± a constant) can be used in a clinical setting when planning dual-phase CT evaluation of the liver in dogs. The regression formula will give an accurate estimation of aortic TPE, which can be used to determine the appropriate timing for the arterial phase and ensure optimal synchronization with peak enhancement.

To solve the regression formula for estimating TPE, the injection duration and contrast medium arrival time need to be identified. If a fixed injection rate is used, then the injection duration is obtained by dividing the contrast medium volume by the injection rate. If a fixed injection duration is used, then this value can be directly incorporated into the regression formula. Fixed injection duration has been previously used for dual-phase CT in dogs.[7,8] Second, the contrast medium arrival time can be identified by administering a test bolus. Once the injection duration and contrast medium arrival time are known, then the estimated TPE can be calculated by use of the regression formula. This estimated TPE should not be directly used as the scan delay (the interval from the beginning of contrast medium injection to the time of initial image acquisition) because that would result in the scan starting at the peak of enhancement and would mainly capture a period of progressive decline in contrast. Instead, the estimated TPE should coincide with the middle of the CT acquisition window. To achieve this, the scan delay is calculated as the estimated TPE minus half of the acquisition period.[17] During the arterial phase, scans should be performed in a cranial-to-caudal direction, corresponding with the direction of contrast medium flow in the aorta.

In addition to the use of a test bolus, an alternative method for identifying contrast medium arrival time is the use of bolus tracking. The advantage of this method over the test bolus procedure is that only a single injection of contrast medium is required and the duration of the CT scan procedure can be reduced.[25] Bolus tracking is automatically linked to the start of the diagnostic CT scan, and therefore contrast medium arrival time cannot be predetermined when this technique is used. This represents a problem because contrast medium arrival time is needed to solve the regression formula for estimating aortic TPE. As a solution, we suggest use of a regression coefficient of 1 instead of 0.8 for contrast medium arrival time. As a result, the whole value for contrast medium arrival time as identified from the bolus-tracking procedure would be used in the regression formula, and the remaining TPE would be given by (0.8 X injection duration) ± a constant. This modification may lead to a minimal overestimation of TPE.

None of the 3 variables significantly associated with aortic TPE were associated with TPE of the liver parenchyma of dogs in the present study. The regression formula was no better than the mean of observed values for estimation of TPE of the dogs used. Therefore, we propose using the mean of observed TPE val-

ues (45 seconds for group A and 50 seconds for group B, from the beginning of contrast medium injection) as an estimate of TPE for other dogs. Similar to the arterial phase, the CT scan delay for the hepatic phase is calculated as the estimated TPE of the liver minus half of the acquisition period. Use of the mean observed value as an estimate of hepatic TPE is considered a feasible option on the basis of previous research in which little to no change was demonstrated in the timing of peak enhancement in the liver in various conditions.[15] The results reported here were in agreement with those of previous research, given that the timing of peak liver enhancement was fairly constant regardless of the injection duration or dog body weight. In addition, the period of peak liver enhancement is much broader than that of arterial enhancement, which provides a wider temporal window for synchronization with the hepatic phase scan.[17] For the hepatic phase, scanning should be performed in a caudal-to-cranial direction, corresponding with portal blood flow.

The capability of the CT machine in terms of speed of image acquisition has an impact on the CT scan protocol used for dual-phase CT of the liver.[17] Speed of image acquisition is largely dependent on the number of detector rows, pitch, and rotation time. Matching the duration of image acquisition with injection duration is recommended to ensure sufficient contrast enhancement throughout both scan phases. If injection duration is much briefer than the acquisition window, the TPE is expected to occur early, and the CT scan may either miss peak enhancement or mainly capture a period of progressive decline in contrast enhancement. If injection duration is much longer than the acquisition window, then the scan may have finished before the full volume of contrast medium has been administered, which means some of the dose would not contribute to diagnostic usefulness.

In the present study, a multirow CT scanner with 16 detector rows was used, and the acquisition time for the canine abdomen was up to 20 seconds (for a large-breed dog). Therefore, a fixed injection duration of 20 seconds was selected to match the acquisition window. This injection technique is also one of the published techniques for dual-phase CT of the liver.[7] When a CT scanner with 64 detector rows is used, the acquisition times will be relatively brief, and the injection duration should be reduced to match this. Both an arterial and parenchymal phase would be achievable with this type of rapid CT technology. Conversely, a single-detector row CT scanner would have relatively prolonged acquisition times. The injection duration can be increased to match this and still achieve a parenchymal phase CT scan of the liver. However, an arterial phase would be unlikely to be achieved because the long injection duration is associated with a slow injection rate and this would result in insufficient contrast enhancement of the arteries. Although shortening the injection duration by injecting contrast medium faster will increase the magnitude of contrast enhancement, this practice would not be appropriate when single-slice CT machinery is used because peak enhancement would likely occur much earlier than image acquisition.

The present study had some limitations. Dogs with nonhepatic illnesses were used rather than healthy dogs. This was justified by the fact that multiphase CT evaluations are often indicated for diseased patients. We therefore chose a study population that we believed represented the target clinical population. Although the presence of hepatic disease was excluded through performance of pre- and postcontrast CT scans of the liver, cytologic and histopathologic evaluation of liver samples was not always performed, nor was serum biochemical analysis. Therefore, we could not rule out the possibility that some dogs may have had microcirculatory liver disease, which could have affected the TPE. Finally, multiphasic CT evaluations of the liver are also indicated for patients with macroscopic liver disease, and it is unknown whether the presence of macroscopic disease would alter the flow of contrast medium and affect timing of contrast enhancement. Additional studies may be needed to evaluate the effect of gross liver disease on the timing of contrast enhancement.

The study reported here revealed that contrast medium arrival time, injection duration, and injection technique can be used to estimate aortic TPE. The combination of these variables in a regression formula provides an accurate and relatively quick way of estimating TPE, which can then be used to calculate the necessary scan delay for dual-phase CT scans. Unlike aortic TPE, hepatic TPE could not be significantly explained by these 3 variables.

Acknowledgments

This manuscript represents a portion of a thesis submitted by Dr. Chau to the University of Sydney Faculty of Veterinary Science as partial fulfillment of the requirements for a Master of Veterinary Clinical Studies degree.

Presented in abstract form at the 2015 Scientific Conference of the International Veterinary Radiology Association, Perth, WA, Australia, August 2015.

Footnotes

a. Butorgesic, Troy Laboratories Pty Ltd, Smithfield, NSW, Australia.
b. Alfaxan, Jurox Pty Ltd, Rutherford, NSW, Australia.
c. Isoflo, Abbott Australasia Pty Ltd, Botany, NSW, Australia.
d. Viaflex, Baxter Healthcare Pty Ltd, Toongabbie, NSW, Australia.
e. Philips 16-slice Brilliance CT V2.3, Phillips Medical Systems Netherlands, Eindohoven, Netherlands.
f. Omnipaque, GE Healthcare Australia Pty Ltd, Rydalmere, NSW, Australia.
g. Empower CTA, E-Z-EM Inc, Westbury, NY.
h. Osirix, version 4.1.2, OsiriX Foundation, Geneva, Switzerland.
i. Numbers, version 3.5.2, Apple Pty Ltd, Apple, Cupertino, Calif.
j. SAS, version 9.4, SAS Institute Inc, Cary, NC.

References

1. Zwingenberger AL, Schwarz T. Dual-phase CT angiography of the normal canine portal and hepatic vasculature. *Vet Radiol Ultrasound* 2004;45:117–124.

2. Frank P, Mahaffey M, Egger C, et al. Helical computed tomographic portography in ten normal dogs and ten dogs with a portosystemic shunt. *Vet Radiol Ultrasound* 2003;44:392–400.
3. Bertolini G, Rolla EC, Zotti A, et al. Three-dimensional multislice helical computed tomography techniques for canine extra-hepatic portosystemic shunt assessment. *Vet Radiol Ultrasound* 2006;47:439–443.
4. Zwingenberger AL, McLear RC, Weisse C. Diagnosis of arterioportal fistulae in four dogs using computed tomographic angiography. *Vet Radiol Ultrasound* 2005;46:472–477.
5. Schwarz T, Rossi F, Wray JD, et al. Computed tomographic and magnetic resonance imaging features of canine segmental caudal vena cava aplasia. *J Small Anim Pract* 2009;50:341–349.
6. Fischetti AJ, Kovak J. Imaging diagnosis: azygous continuation of the caudal vena cava with and without portocaval shunting. *Vet Radiol Ultrasound* 2008;49:573–576.
7. Kutara K, Seki M, Ishikawa C, et al. Triple-phase helical computed tomography in dogs with hepatic masses. *Vet Radiol Ultrasound* 2014;55:7–15.
8. Fukushima K, Kanemoto H, Ohno K, et al. CT characteristics of primary hepatic mass lesions in dogs. *Vet Radiol Ultrasound* 2012;53:252–257.
9. Mai W, Caceres AV. Dual-phase computed tomographic angiography in three dogs with pancreatic insulinoma. *Vet Radiol Ultrasound* 2008;49:141–148.
10. Oliver JH, Baron RL, Federle MP, et al. Detecting hepatocellular carcinoma: value of unenhanced or arterial phase CT imaging or both used in conjunction with conventional portal venous phase contrast-enhanced CT imaging. *AJR Am J Radiol* 1996;167:71–77.
11. Ohashi I, Hanafusa K, Yoshida T. Small hepatocellular carcinomas: two-phase dynamic incremental CT in detection and evaluation. *Radiology* 1993;189:851–855.
12. Baron RL. Understanding and optimizing use of contrast material for CT of the liver. *AJR Am J Radiol* 1994;163:323–331.
13. Honda H, Matsuura Y, Onitsuka H, et al. Differential diagnosis of hepatic tumors (hepatoma, hemangioma, and metastasis) with CT: value of two-phase incremental imaging. *AJR Am J Radiol* 1992;159:735–740.
14. Hollett MD, Jeffrey RB, Nino-Murcia M, et al. Dual-phase helical CT of the liver: value of arterial phase scans in the detection of small (≤ 1.5cm) malignant hepatic neoplasms. *AJR Am J Radiol* 1995;164:879–884.
15. Erturk SM, Ichikawa T, Sou H, et al. Effect of duration of contrast material injection on peak enhancement times and values of the aorta, main portal vein, and liver at dynamic MDCT with the dose of contrast medium tailored to patient weight. *Clin Radiol* 2008;63:263–271.
16. Awai K, Hori S. Effect of contrast injection protocol with dose tailored to patient weight and fixed injection duration on aortic and hepatic enhancement at multidetector-row helical CT. *Eur Radiol* 2003;13:2155–2160.
17. Bae KT. Intravenous contrast medium administration and scan timing at CT: considerations and approaches. *Radiology* 2010;256:32–61.
18. Bouma JL, Aronson LR, Keith DG, et al. Use of computed tomography renal angiography for screening feline renal transplant donors. *Vet Radiol Ultrasound* 2003;44:636–641.
19. Brown JC Jr, Chanoit G, Reeder J. Complex extrahepatic portocaval shunt with unusual caval features in a cat: computed tomographic characterisation. *J Small Anim Pract* 2010;51:227–230.
20. Bae KT, Heiken JP, Brink JA. Aortic and hepatic contrast medium enhancement at CT. Part I. Prediction with a computer model. *Radiology* 1998;207:647–655.
21. Awai K, Hiraishi K, Hori S. Effect of contrast material injection duration and rate on aortic peak time and peak enhancement at dynamic CT involving injection protocol with dose tailored to patient weight. *Radiology* 2004;230:142–150.
22. Makara M, Dennler M, Kuhn K, et al. Effect of contrast medium injection duration on peak enhancement and time to peak enhancement of canine pulmonary arteries. *Vet Radiol Ultrasound* 2011;52:605–610.
23. Bae KT, Heiken JP, Brink JA. Aortic and hepatic peak enhancement at CT: effect of contrast medium injection rate—pharmacokinetic analysis and experimental porcine model. *Radiology* 1998;206:455–464.
24. Bae KT, Tran HQ, Heiken JP. Multiphasic injection method for uniform prolonged vascular enhancement at CT angiography: pharmacokinetic analysis and experimental porcine model. *Radiology* 2000;216:872–880.
25. Mai W, Suran JN, Caceres AV, et al. Comparison between bolus tracking and timing-bolus techniques for renal computed tomographic angiography in normal cats. *Vet Radiol Ultrasound* 2013;54:343–350.

EFFECTS OF TWO CONTRAST INJECTION PROTOCOLS ON FELINE AORTIC AND HEPATIC ENHANCEMENT USING DYNAMIC COMPUTED TOMOGRAPHY

MARIANO MAKARA, JENNIFER CHAU, EVELYN HALL, HEIDE KLOEPPEL, JUAN PODADERA, VANESSA BARRS

This prospective study compared aortic and hepatic enhancement achieved using a contrast injection protocol with a fixed rate of 5 ml/s vs. that achieved using a protocol with fixed injection duration of 20 s in eight cats. Cats were assigned into two groups (Group 1, rate 5 ml/s; Group 2, duration 20 s). The dose of contrast was the same in both groups (740 mgI/kg). Regions of interest (ROI) were drawn in the aorta and liver for transverse scans acquired at the hepatic hilus. Time to peak aortic enhancement occurred significantly earlier in Group 1 (M = 11s, SD = 1.63) than in Group 2 (M = 25.5 s, SD = 2.51). Peak aortic enhancement was significantly higher in Group 1 (M = 1906.51 HU, SD = 368.64) than in Group 2 (M = 745.08 HU, SD = 201.84). Duration of aortic enhancement equal to or above 300 HU was statistically longer in Group 2 (M = 24.5 s, SD = 8.39) than in Group 1 (M = 10 s, SD = 1.63). There were no significant differences in time to peak liver enhancement, peak liver enhancement, or duration of hepatic arterial phase between groups. Findings supported the hypothesis that longer injection duration results in a broader bolus geometry with a longer time to peak and a lower peak aortic enhancement in cat. This strong influence of injection duration on timing of aortic enhancement may help future users optimize protocols for CT angiography of the aorta and multiphasic evaluation of the liver, pancreas, and small intestine.

Key words: aortic enhancement, fixed-injection-duration, injection-rate.

Introduction

DISEASES OF THE LIVER, pancreas, and small intestine are frequently encountered in cats.[1] In this species, inflammatory hepatobiliary disorders are regarded as the second most common hepatic disease.[2] These disorders are usually centered on the biliary tract with secondary involvement of the hepatic parenchyma and are classified into three distinct forms: neutrophilic, lymphocytic, and chronic cholangitis.[2] The neutrophilic form is frequently associated with pancreatitis and inflammatory bowel disease.[1] The association of these entities suggests a common underlying disease process. It has been speculated that the presence of inflammatory bowel disease may predispose to ascending infection through the pancreatic and bile ducts.[3] In turn, the unique ductal anatomy in which both the common bile duct and the pancreatic duct open onto the major duodenal papilla, may explain concurrent development of pancreatitis and neutrophilic cholangitis.[1] Due to its availability, low cost and lack of requirement for anesthesia, ultrasonography has been frequently used for the diagnosis of hepatobiliary, pancreatic, and small intestinal diseases in cats.[4–8] However, limitations related to its poor diagnostic accuracy, operator dependency, and incomplete assessment secondary to bowel gas interference have also been reported.[4,5,7–11] In human medicine, multiphasic CT has been described as the most clinically useful imaging modality for pancreatitis and small bowel disease.[12–14] Additionally, multiphasic CT is considered an alternative clinical tool for noninvasive evaluation of the biliary system.[15,16] The diagnostic accuracy of multiphasic CT studies largely relies upon image acquisition during different enhancement phases after the bolus administration of intravenous contrast medium.[17] As an example, CT findings in the mildest forms of pancreatitis are related to poor enhancement of the pancreatic parenchyma during the late arterial phase.[13] Similarly, CT signs of active inflammatory bowel disease in people, which include mural hyper enhancement, mural stratification, and engorged vasa recta, rely on scanning the small intestine during the late arterial or enteric phase.[18,19] Furthermore, one of the CT features of cholecystitis is hyper-enhancement of the liver parenchyma adjacent to the gallbladder, which can only be detected during the late arterial phase.[20]

From the Faculty of Veterinary Science, University of Sydney, NSW, 2006, Sydney, Australia.

Address correspondence and reprint requests to Mariano Makara, at the above address. E-mail: mariano.makara@sydney.edu.au

Received November 27, 2013; accepted for publication November 19, 2014.

doi: 10.1111/vru.12239

So far the application of CT in cats has been limited to single-phase studies of the pancreas and angiography of the renal vasculature in transplantation donors.[21–25] Limited information is available on the influence of injection technique on aortic enhancement for angiography or multiphasic studies of the liver, pancreas, and small intestine. Optimal protocols for these applications have not been defined. Evidence of this is the limited information regarding the injection technique provided in by some studies. As an example, information regarding injection rate, which is key parameter is most contrast injection protocol, has not been reported.[21–24] Other studies evaluating the renal vasculature in cats used an injection protocol with a dose of 2.2 ml/kg (240 mgI/ml) and a fixed rate of 5 ml/s.[26] The application of this injection technique to animals with a mean body weigh of 5 kg results in an injection duration of around 2 s. This short injection duration may have desirable and undesirable effects.[17] The desirable effects are related to the increased temporal separation between scan phases in multiphasic studies of the renal vasculature or liver. The undesirable effects of a very short injection duration are related to the narrow geometry of the first pass of contrast medium through the aorta.[17] A very short injection duration could result in a very high peak aortic enhancement occurring very early. This could potentially reduce the temporal window for CT scanning the aorta or the arterial phase in multiphasic studies of the liver, pancreas, and small intestine.

Before the accuracy of multiphasic CT studies could be tested in cats, the influence of contrast injection technique on aortic and hepatic enhancement should be studied. Accurate estimation of time to peak aortic enhancement has a key role in multiphasic evaluations of the liver, pancreas, and small intestine.[17,27,28] Therefore, the aim of this project was to compare the aortic and the hepatic enhancement achieved using a contrast injection protocol with a fixed rate of 5 ml/s with that achieved using a protocol with fixed injection duration of 20 s in a sample population of cats with no evidence of abdominal disease. We hypothesized that: (1) the injection protocol with a fixed duration of 20 s would produce a broader bolus geometry with a longer time to peak and a lower peak enhancement compared to the injection protocol with a fixed rate of 5 ml/s, that (2) the injection protocol with a fixed duration will result in a longer aortic enhancement equal to or above 300 HU, and that (3) the injection protocol with a fixed injection rate of 5 ml/s would result in better temporal separation between scan phases in multi phasic studies of the renal vasculature or liver compared to the injection protocol with a fixed rate of 5 ml/s.

Material and Methods

The experimental design for this prospective study was randomized block. The study was approved by the Ethics Committee of The University of Sydney. Eight cats referred for CT of a body region other than the abdomen were recruited. With informed client consent, a screening precontrast CT examination of the abdomen was performed and cats with evidence of intra-abdominal abnormalities were excluded.

For each included cat, an intravenous cannula was placed into the cephalic vein. Cats were premedicated with butorphanol (Butorgesic, Troy Laboratories Pty Ltd., Smithfield, NSW, Australia, 0.3 mg/kg) or buprenorphine (Temgesic, Reckitt Benchiser Helthcare (UK) Limited, Hull, UK, 0.01 mg/kg intravenously). Anesthesia was induced with alfaxalone (Alfaxan, Jurox Pty Ltd., Rutherford, NSW, Australia) intravenously to effect and the trachea of the cats was intubated. General anesthesia was maintained with isoflurane (Isoflo^{TM}, Abbott Australasia Pty Ltd., Botany, NSW, Australia) in 100% oxygen. Fluid therapy consisted of Hartmann's solution (Viaflex, Baxter Healthcare Pty Ltd., Toongabbie, NSW, Australia) administered during the procedure at 5 ml/kg/h. Heart rate, electrocardiography, respiratory rate, end-expiratory CO_2-concentration, peripheral oxygen saturation, noninvasive blood pressure, and body temperature data were monitored and recorded every 5 min during the procedure using a multiparameter monitor (Mindray PM 9000, Mindray Medical USA Corp., Redmond, WA).

Injection and Scan Protocol

Cats were randomly allocated into two groups of four cats each. In Group 1, a fixed rate injection of 5 ml/s was used. In Group 2, contrast medium was administered using a fixed injection duration of 20 s. In this group, the injection rate was adjusted individually to obtain the desired injection duration. Each cat received 740 mgI/kg of an isoosmolar iodinated contrast medium using a concentration of 370 mgI/ml at 2 ml/kg (Omnipaque^{TM}, GE Healthcare Australia Pty Ltd., Rydalmere NSW, Australia). Contrast medium was administered via an automatic injector (Empower CTA^{R}, E-Z-EM Inc., Westbury, NY) using a 20- or 22-gauge intravenous catheter inserted into a cephalic vein. Cats were positioned in sternal recumbency.

All CT scans were acquired using the same 16-slice multidetector CT scanner (Phillips 16 Slice, Brilliance^{TM} CT V2.3, Phillips Medical Systems Netherlands, Eindhoven, The Netherlands). Thirty, single-level, transverse CT scans were acquired at the level of the hepatic hilus with a 2-s interval. The dynamic scan started one second after the beginning of contrast medium injection. Scans were performed using the following parameters: 1-s rotation time, four data channels with a detector-row width of 0.75 mm (4 × 0.75 mm), 120 kV (peak kilovoltage), and 75 mA. Images were reconstructed with a slice thickness of 3 mm using a soft tissue algorithm. The single-level scans were followed by the routine postcontrast clinical examination.

Quantitative Analysis

A single observer (J.C.) who was unaware of cat group status performed all measurements using an image analysis workstation and software (Apple Thunderbolt Display, 1 Infinite Loop, Cupertino, CA; Mac Mini, 1 Infinite Loop, Cupertino, CA; Osirix v 5.7 64-bit, Pixmeo SARL, Bernex, Switzerland). Regions of interest (ROI) were drawn in the center of the aorta and within the liver parenchyma. The area of the ROI was maintained constant on all single-level CT images. For the liver, two ROI were obtained on every single-level scan. Values from these ROI were then averaged. All attenuation values were expressed as absolute enhancement. Absolute enhancement was calculated by subtracting the mean unenhanced values to the post-contrast values. Mean CT attenuation was measured and time-enhancement curves were created.

To compare the injection protocols, time to aortic arrival, peak aortic enhancement, time to peak aortic enhancement, duration of aortic enhancement equal to or above 300 HU, peak liver enhancement, time to peak liver enhancement and duration of hepatic arterial phase were calculated. Time to aortic arrival was defined as the time elapse from the beginning of the injection to the time when the attenuation of the aorta reached 100 HU. Peak enhancement of the aorta and liver were determined as the maximal enhancement of those structures obtained during the dynamic study. Time to peak enhancement of the aorta and liver was determined as the time period from the start of the injection to the maximum enhancement of the aorta and liver, respectively. The duration (in seconds) of aortic enhancement equal to or greater than 300 HU was calculated as 2 times the number of images in which the region of interest over the aorta had a CT number of 300 HU or more. An intravascular attenuation of at least 300 HU is a prerequisite for CT angiography.[29] Duration of hepatic arterial phase was defined as the period elapsed from the time to reach an enhancement of 100 HU in the aorta to the time to reach an enhancement of 140 HU in the liver parenchyma.[30]

Statistical Analysis

Statistical analyses were selected and performed by two of the authors (E.H. and M.M.). All calculations were performed using commercial software (IBM SPSS Statistics, version 20, International Business Machines Corp., Pyrmont, Australia). An independent samples *T*-test was run to determine if there were differences between Groups 1 and 2 on variables with normally distributed data. The Mann–Whitney test was used on data that was not normally distributed. Distribution of data for each variable was assessed by Shapiro–Wilke test. For all tests, a *P* value of 0.05 was considered to be significant.

Results

The median body weight of cats in Groups 1 and 2 was 4.4 kg (range 4.2 (EH and MM). All calculations were performed using commercial software (IBM SPSS Statistics, version 20, International Business Machines Corp.). An independent-samples T test was run to Mean age in Groups 1 and 2 was 10.8 years (SD 5.0) and 8.8 years (SD 4.9), respectively. Age data was normally distributed. The difference of age, 2.00, 95% CI [−4.91, 10.91], was not significant t (6) = 0.570, p = 0.59. Breeds in Group 1 included; Domestic Short Hair, Exotic, Cornish Rex, and Ragdoll. Breeds in Group 2 included; Domestic Short Hair, Ragdoll, and Burmese. There were 3 neutered males and 1 spayed females in Group 1 and 2 neutered males, 2 spayed females in Group 2.

Data on time to contrast arrival in the aorta, time to aortic peak, duration of aortic enhancement above 300 HU, time to liver enhancement above, time to peak liver enhancement, duration of hepatic arterial phase, peak aortic enhancement and peak hepatic enhancement were normally distributed. Values for these parameters for each animal are presented in Table 1. Comparison of means between groups for each of these parameters is presented in Table 2. Short injection durations (typically 2 s) as those in Group 1, resulted in time attenuation curves with a narrow geometry (Figure 1). Peak aortic enhancement was high and occurred very early. In contrast, longer injection durations (20 s) as those in Group 2 resulted in time attenuation curves with broader bolus geometry (Figure 1). Peak aortic enhancement was lower and occurred later. The different injection rates used in the present study did not result in significant differences in the duration of the hepatic arterial phase.

Discussion

Our results supported the hypothesis that contrast injection duration influences timing and magnitude of aortic enhancement in cats.[31] The effect of injection duration on time to peak aortic enhancement may be explained following a theoretical model that divides the time periods from the start of injection to the aortic peak enhancement in three phases.[32] The first phase comprises the injection process. During this phase contrast medium continually flows into the right heart. The right heart acts like a reservoir and as a second independent pump, which further pumps contrast to the aorta. During this first phase, there is a continuous increase in radiopacity of the aorta due to the large inflow and relatively small outflow of contrast to visceral organs. The second phase starts after the completion of the injection. During this phase, the radiopacity of the aorta continues to increase due to the inflow of the remaining contrast from the right heart to the aorta. The length of this

TABLE 1. Weight, Injection Rate, Injection Duration, Time to Aortic Arrival, Time to Peak, Aortic Enhancement, Duration of Aortic Enhancement Equal to or Above 300 Hounsfield Units, Time to Hepatic Enhancement, Time to Peak Hepatic Enhancement, Duration of Hepatic Arterial Phase, Peak Aortic Enhancement and Peak Hepatic Enhancement Values For Cats Within Group 1 and 2

	Weight (kg*)	Injection Rate (ml† /s‡)	Injection Duration (s)	Aortic Arrival (s)	Time to Aortic Peak Enhancement (s)	Duration Aortic Enhancement Above 300HU (s)	Time to Hepatic Enhancement 140 HU	Time to Peak Hepatic Enhancement (s)	Duration Hepatic Arterial Phase	Peak Aortic Enhancement (HU§)	Peak Hepatic Enhancement (HU§)
Group 1											
	7.3	5	3	9	13	12	25	39	16	2260.83	143.65
	4.4	5	2	9	11	10	29	39	20	1409.02	91.46
	4.5	5	2	9	11	10	13	43	4	2072.38	129.4
	4.2	5	2	7	9	8	21	49	14	1883.81	103.44
Group 2											
	4.8	0.5	20	9	25	36	25	41	16	598.62	129.91
	8.5	0.5	20	11	29	22	41	57	30	974.27	130.51
	5.1	0.5	20	11	23	24	27	43	16	860.6	205.47
	4.9	0.5	20	13	25	16	39	45	26	546.81	77.61

A Fixed rate of 5 ml/s was used in Group 1 while a protocol with a fixed injection duration of 20 s was used in Group 2.
*Kilograms.
†Milliliters.
‡Seconds.
§Hounsfield units.
§Hounsfield units.

TABLE 2. Comparison of Time to Aortic Arrival, Time to Peak Aortic Enhancement, Duration of Aortic Enhancement Equal to or Above 300 Hounsfield Units, Time to Liver Enhancement, Time to Peak Liver Enhancement, Duration of Hepatic Arterial Phase, Peak Aortic Enhancement, and Peak Hepatic Enhancement Means between Groups

	Group 1 Mean (Standard Deviation)	Group 2 Mean (Standard Deviation)	*t*	*p*	Mean Difference	95% Confidence Interval	
Time to aortic arrival (s)	8.5 (1)	11 (1.63)	2.61	0.40	2.5	0.16	4.84
Time to peak aortic enhancement (s)	11 (1.63)	25.5 (2.51)	9.67	0.00	14.5	10.83	18.17
Duration of aortic enhancement above 300 HU (s)	10 (1.63)	24.5 (8.39)	−3.39	0.02	−14.5	−24.95	−4.05
Time to liver enhancement 140 HU (s)	22 (6.83)	33 (8.16)	2.07	0.08	11	−2.28	24.02
Time to peak liver enhancement (s)	37.5 (5.97)	46.5 (7.19)	1.93	0.10	9	−2.43	20.43
Duration hepatic arterial phase (s)	13.5 (6.81)	22 (7.12)	1.73	0.13	8.5	− 3.55	20.55
Peak aortic enhancement (HU)	1906.51 (368.64)	745.08 (201.84)	−5.54	0.00	−1161.44	−1674.56	−648.31
Peak hepatic enhancement (HU)	116.99 (23.81)	135.88 (52.61)	0.65	0.54	18.89	−51.76	89.53

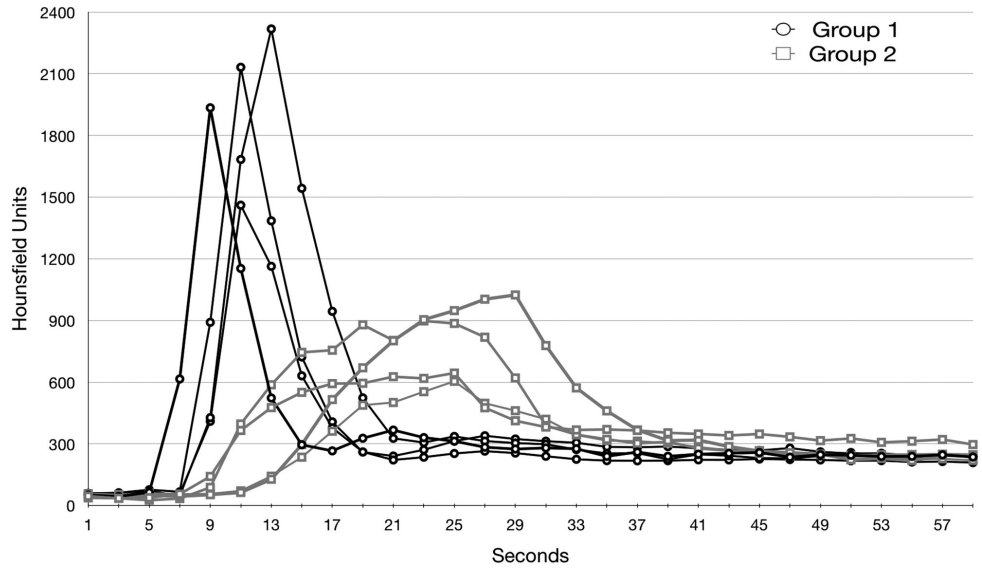

FIG. 1. Time attenuation curves of the aorta from cats in Groups A and B. In Group 1, an injection technique with an fixed rate of 5 ml/s was used. In Group 2, an injection protocol with a fixed injection duration of 20 seconds was used. Note the broader bolus geometry with a longer aortic time to peak and a lower aortic peak enhancement in Group 2 compared to Group 1.

phase depends on the cardiac output and is independent of the injection duration. This second phase represents the physiological mean transit time from the right heart to the aorta. During the third phase, the radiopacity of the aorta begins to decrease due to the absence of inflow and continuous outflow of contrast medium. Based on this model, longer injection durations prolong the first phase, which in turn results in a longer time to peak enhancement.

In contrast to what we hypothesized, the longer injection duration used in Group 2 did not result in overlapping of the arterial and portal phases. Theoretically, this overlap of phases could occur if the delivery of contrast is so slow that appropriate arterial enhancement is only reached after substantial enhancement of the liver parenchyma has occurred.[17] This enhancement of the liver parenchyma occurs as a result of recirculation of contrast through the portal system. This hypothetical slow injection rate may result in almost simultaneous enhancement of the hepatic arteries and the liver parenchyma. Even thought the injection rate used in Group 2 was 10 times slower than the one previously applied to cats,[26] it produced an early and strong enhancement of the aorta. This aortic enhancement resulted in good separation between the arterial and porta phases. Interestingly, this injection technique rather than that using an injection rate of 5 ml/s (Group 1) resulted in a bolus geometry similar to that obtained after the application of injection rate of 5 ml/s to people.[33] This could be explained by considering how injection rate, cardiac output, and blood volume relate to arterial enhancement.[34] Arterial enhancement is directly related to the rate of delivery of contrast medium, and inversely related to cardiac output and blood volume. This means that the application of the same injection rate to individuals with a great variability in cardiac output and blood volume may not result in similar arterial enhancement. The smaller cardiac output and blood volume of cats compared to people explains the extremely high peak enhancement value that resulted from the application of contrast with an injection rate of 5 ml/s. If the injection rate is adjusted to patient weight, which in turn correlates to cardiac output and blood volume, the injection technique used in Group 2 results in an injection rate of 0.1 ml/kg/s. The application of this injection rate to an individual with a body weight of 60 kg results in an injection rate of 6 ml/s. This may explain the similar enhancement between human studies using an injection rate of 5 ml/s and the enhancement values in Group 2.

Accurate estimation of time to peak aortic enhancement has a key role in multiphasic evaluations of the liver, pancreas, and small intestine.[17,27,28] In agreement with other studies in people, our study showed that the hepatic arterial phase corresponded to the time of maximum aortic

enhancement regardless of the contrast injection technique.[17] Similarly, studies in people have shown that depending on the injection duration and injection rate, time to aortic peak enhancement occurred immediately before the onset of the late arterial or pancreatic phase.[27] In case of small intestinal applications, the arterial phase occurred 14 s after peak aortic enhancement.[29] The strong influence of injection duration on time to peak aortic enhancement found in our study suggest that injection duration should be considered when estimating time to peak aortic enhancement. Studies in human medicine empirically estimate time to peak aortic enhancement as the sum of the injection duration plus time to contrast arrival to the target organ after the intravenous injection.[31] For injection durations of less than 15 s, time to peak aortic enhancement is mainly determined by time to arrival with a limited contribution of injection duration (time to aortic peak = time to arrival + injection duration/2).[17] For injection durations of more than 15 s, time to peak aortic enhancement is mainly determined by injection duration with a limited contribution of time to arrival (time to aortic peak = injection duration + time to arrival – 5).[17] Based on these formulas, the estimated mean time to aortic peak in Group 1 and Group 2 were 9.7 and 26.0 s, respectively. These estimated values are similar to the actual values of time to aortic peak in Group 1 and Group 2 with a mean of 11 and 25.5 s, respectively. The similar results between the estimated and actual values suggest that these formulas could also be used to estimate peak aortic enhancement in cats. Further work is needed to study the relationship between peak aortic enhancement, and peak pancreatic and small intestinal enhancement.

Our study supports estimating injection duration based on scanning conditions and the clinical objectives of the examination.[17] Authors recommend that the injection duration should be long enough to maintain adequate enhancement throughout image acquisition. A prematurely ended injection may result in poor contrast enhancement homogeneity along the scanned volume while an unnecessarily long injection, may translate into poor vascular and parenchymal enhancement. In Group 1, the mean duration over which aortic enhancement was equal to or above 300 HU was 10 s ($SD = 1.63$). This means that given the minimum built-in delay of 5 s present in most CT machines, the whole CT scan should be performed in around 5 s in order not to miss the arterial phase. On the other hand, the broader bolus geometry that resulted from using an injection protocol with fixed duration of 20 s could decrease the likelihood of missing the arterial phase. Evidence for this is the longer duration of aortic enhancement equal or above 300 HU in Group 2 ($M = 24.50$ s, $SD = 8.39$ s), which translates into a longer temporal window for optimal scan timing.

Our results may explain why, in a previous report, the peak enhancement of the renal arteries was missed when using a bolus tracking technique to measure time to contrast arrival.[26] Based on our data, the period between contrast arrival to the aorta and the time to peak aortic enhancement after the delivery of contrast using an injection rate of 5 ml/s ranged from 2 to 4 s. This very short temporal window of diagnostically adequate enhancement makes perfect synchronization between peak enhancement and CT scan impossible if the minimum built-in delay of 5 s present in most CT machines is considered. On the contrary, the longer temporal window of diagnostically adequate enhancement that results from a longer injection duration could be more easily synchronized with the CT scan. In other words, it seems reasonable to assume that the peak enhancement of the renal arteries was missed not because of a deficient technique to measure time to arterial contrast arrival but rather because of the very short temporal window of adequate enhancement that resulted from a very short injection duration.

For purposes of this study, we defined the arterial phase as the period elapsed from the time to reach an enhancement of 100 HU in the aorta to the time to reach an enhancement of 140 HU in the liver parenchyma. In case of the aorta, a threshold value of 100 HU has been routinely used to establish the arrival of contrast medium to this artery.[17] In case of the liver parenchyma, a threshold value of 140 HU was decided based on the percentage of enhancement that could be attributed to the delivery of contrast through the hepatic artery. Because this artery supplies approximately 30% of blood flow to the liver, it has been suggested that parenchymal enhancement greater than 30% of the hepatic peak value may indicate portal venous phase predominance.[30] In our study, 30% of peak liver enhancement corresponded to 61 HU. This value was obtained by calculating 30% percent of the mean peak liver enhancement in all cats. The mean precontrast attenuation value of the liver parenchyma for all cats was 77 HU. The threshold value of 140 HU was then obtained by adding the mean precontrast attenuation values (77 HU) to the calculated 30% (61 HU) of mean peak liver enhancement.

One of the limitations of this study was that our study population only included cats without abdominal disease. The application of the injection protocols used in our study to animals with abdominal disease may not yield the same results. Another limitation of this study was the small sample population.

In conclusion, findings from the current study supported the hypothesis that a longer injection duration results in a broader bolus geometry with a longer time to peak and a lower peak aortic enhancement in cats without abdominal disease. This broader bolus geometry may

translate into easier synchronization of the arterial phase with the CT scan. Findings may be helpful for use in future design injection strategies for CT evaluation of specific organs such as the CT angiography of the aorta and multi-phasic studies of the live, pancreas and small intestine.

REFERENCES

1. Weiss DJ, Gagne JM, Armstrong PJ. Relationship between inflammatory hepatic disease and inflammatory bowel disease, pancreatitis, and nephritis in cats. J Am Vet Med Assoc 1996;209:1114–116.
2. Cullen JM. Summary of the World Small Animal Veterinary Association standardization committee guide to classification of liver disease in dogs and cats. Vet Clin North Am Small Anim Pract 2009;39:395–418.
3. Brain P, Barrs V, Martin P, Baral R, White J, Beatty J. Feline cholecystitis and acute neutrophilic cholangitis: clinical findings, bacterial isolates and response to treatment in six cases. J Feline Med Surg 2006;8:91–98.
4. Saunders HM, VanWinkle TJ, Drobatz K, Kimmel SE, Washabau RJ. Ultrasonographic findings in cats with clinical, gross pathologic, and histologic evidence of acute pancreatic necrosis: 20 cases (1994–2001). J Am Vet Med Assoc 2002;221:1724–1730
5. Marolf AJ, Leach L, Gibbons DS, Bachand A, Twedt D. Ultrasonographic findings of feline cholangitis. J Am Anim Hosp Assoc 2012;48:36–48
6. Biller DS, Kantrowitz B, Miyabayashi T. Ultrasonography of diffuse liver disease: a review. J Vet Intern Med 1992;6:71–76.
7. Feeney DA, Anderson KL, Ziegler LE, Jessen CR, Daubs BM, Hardy RM. Statistical relevance of ultrasonographic criteria in the assessment of diffuse liver disease in dogs and cats. Am J Vet Res 2008;69:212–269.
8. Zwingenberger AL, Marks SL, Baker TW, Moore PF. Ultrasonographic evaluation of the *Muscularis propria* in cats with diffuse small intestinal lymphoma or inflammatory bowel disease. J Vet Intern Med 2010;24: 289–292.
9. Callahan Clark JE, Haddad JL, Brown DC, Morgan MJ, Van Winkle TJ, Rondeau MP. Feline cholangitis: a necropsy study of 44 cats (1986–2008). J Feline Med Surg 2011;8:570–576.
10. Swift NC, Marks SL, MacLachlan NJ, Norris CR. Evaluation of serum feline trypsin-like immunoreactivity for the diagnosis of pancreatitis in cats. J Am Vet Med Assoc 2000;217:37–42.
11. Ferreri JA, Hardam E, Kimmel SE, et al. Clinical differentiation of acute necrotizing from chronic nonsuppurative pancreatitis in cats: 63 cases (1996–2001). J Am Vet Med Assoc 2003;223:469–474.
12. Koo BC, Chinogureyi A, Shaw AS. Imaging acute pancreatitis. Br J Radiol 2010;83:104–112.
13. Balthazar EJ. Acute pancreatitis: assessment of severity with clinical and CT evaluation. Radiology 2002;223:603–613.
14. Paulsen SR, Huprich JE, Fletcher JG, et al. CT Enterography as a diagnostic tool in evaluating small bowel disorders: review of clinical experience with over 700 cases. Radiographics 2006;26:641–657.
15. Smith EA, Dillman JR, Elsayes KM, Menias CO, Bude RO. Cross-sectional imaging of acute and chronic gallbladder inflammatory disease. Am J Roentgenol 2009;192:188–196.
16. O'Connor OJ, Maher MM. Imaging of cholecystitis. Am J Roentgenol 2011;196:W367–W374.
17. Bae KT. Intravenous contrast medium administration and scan timing at CT: considerations and approaches. Radiology 2010;256:32–61.
18. Horton KM, Fishman EK. Volume-rendered 3D CT of the mesenteric vasculature: normal anatomy, anatomic variants, and pathologic conditions. Radiographics 2002;22:161–172.
19. Fishman EK. From the RSNA refresher courses: CT angiography: clinical applications in the abdomen. Radiographics 2001;21:S3–S16.
20. Yamashita K, Jin MJ, Hirose Y, et al. CT finding of transient focal increased attenuation of the liver adjacent to the gallbladder in acute cholecystitis. Am J Roentgenol 1995;164:343–346.
21. Head LL, Daniel GB, Becker TJ, Lidbetter DA. Use of computed tomography and radiolabeled leukocytes in a cat with pancreatitis. Vet Radiol Ultrasound 2005;46:263–266.
22. Forman MA, Marks SL, De Cock HEV, et al. Evaluation of serum feline pancreatic lipase immunoreactivity and helical computed tomography versus conventional testing for the diagnosis of feline pancreatitis. J Vet Intern Med 2004;18:807–815.
23. Caceres AV, Zwingenberger AL, Aronson LR, Mai W. Characterization of normal feline renal vascular anatomy with dual-phase CT angiography. Vet Radiol Ultrasound 2008;49:350–356.
24. Bouma JL, Aronson LR, Keith DG, Saunders HM. Use of computed tomography renal angiography for screening feline renal transplant donors. Vet Radiol Ultrasound 2003;44:636–641.
25. Gerhardt A, Steiner JM, Williams DA, et al. Comparison of the sensitivity of different diagnostic tests for pancreatitis in cats. J Vet Intern Med 2001;15:329–333.
26. Mai W, Suran JN, CJN, CJ AV, Reetz JA. Comparison between bolus tracking and timing-bolus techniques for renal computed tomographic angiography in normal cats. Vet Radiol Ultrasound 2013;54:343–350.
27. Kim T, Murakami T, Takahashi S, et al. Pancreatic CT imaging: effects of different injection rates and doses of contrast material. Radiology 1999;212:219–225.
28. Schindera ST, Nelson RC, DeLong DM, et al. Multi-detector row CT of the small bowel: peak enhancement temporal window–initial experience. Radiology 2007;243:438–444.
29. Prokop M. Multislice CT angiography. Eur J Radiol 2000;36:86–96.
30. Frederick MG, McElaney BL, Singer A, et al. Timing of parenchymal enhancement on dual-phase dynamic helical CT of the liver: how long does the hepatic arterial phase predominate? Am J Roentgenol 1996;166: 1305–1310.
31. Bae K, Heiken J, Brink J. Aortic and hepatic contrast medium enhancement at CT. Part I: Prediction with a computer model. Radiology 1998;207:647–655.
32. Erturk SM, Ichikawa T, Sou H, Tsukamoto T, Motosugi U, Araki T. Effect of duration of contrast material injection on peak enhancement times and values of the aorta, main portal vein, and liver at dynamic MDCT with the dose of contrast medium tailored to patient weight. Clin Radiol 2008;63:263–271.
33. Awai K, Hiraishi K, Hori S. Effect of contrast material injection duration and rate on aortic peak time and peak enhancement at dynamic CT involving injection protocol with dose tailored to patient weight. Radiology 2004;230:142–150.
34. Itoh S, Ikeda M, Achiwa M, Ota T, Satake H, Ishigaki T. Multiphase contrast-enhanced CT of the liver with a multislice CT scanner. Eur Radiol 2003;13:1085–1094.

SECTION 3 – Research Chapters (1-4)

Chapter 2. Developing a standardised protocol for multiphase abdominal CECT in dogs and comparison with other veterinary institutions.

Based on knowledge of experimental studies in animal models, and our research in Chapter 1 on modifying the contrast injection technique to better predict time to enhancement in the splanchnic vessels and liver in dogs and cats, we developed a new standardised protocol for multiphase CECT of the abdomen at the University Veterinary Teaching Hospital Sydney (UVTHS). The recommendations in this CT protocol were new and unfamiliar in the veterinary industry. The main components of a CT protocol can be divided into three elements: 1) Timed injection of contrast medium, 2) CT monitoring of contrast transit from the injection site to the cranial abdominal aorta 3) CT scan delays for multiphasic study (i.e. arterial phase and hepatic phase).

1. Timed injection of contrast medium

We recommend controlling the contrast injection duration. In our protocol, contrast medium is administered at a fixed injection duration of 20 seconds for all patients (canine and feline) regardless of patient body weight or size. This means that injection rate (ml/s) will vary depending on the total contrast volume, because the contrast dose is tailored to body weight (usually 2ml/kg). For example, a 5kg dog will need 10mls of contrast medium, administered at a fixed duration of 20 seconds, therefore the injection rate will be 0.5ml/s. This technique differs to commonly used techniques in veterinary and human imaging. The most common method for timing the contrast injection is through a fixed rate, ranging from 2-5mls in veterinary CT protocols. Invariably, this means that the injection duration changed between patients of different body weight. For example, a 5kg dog will need 10 mls of contrast medium, administered at a fixed rate of 5mls, therefore the injection duration will be 2 seconds. The injection duration is a by-product in other CT protocols, and not directly controlled.

2. CT monitoring of contrast transit from the injection site to the cranial abdominal aorta

The contrast transit time from the injection site to the aorta is mostly affected by the patient's unique hemodynamic condition. The patient's body size affects the length of the circulatory path. The heart rate, cardiac output and presence of cardiac disease will affect the inflow and outflow of the contrast medium through the right and left side of the heart, respectively. CT imaging in animals is mostly performed under general anesthesia, and the anesthetic drugs can alter the circulatory flow rate. We recommend monitoring the contrast transit time to the aorta, using CT bolus tracking software. This can be applied from the beginning of contrast injection. The bolus tracking software takes cyclical single slice CT images at the level of the patient's aorta every 1 second, and contrast arrival in the aorta can be directly visualised on CT images. Contrast arrival in the aorta is reached when the density threshold is

100-150 Hounsfield units. This is a familiar CT software tool that is used in other University veterinary institutions and private specialist hospitals. An alternative method for monitoring contrast transit time is the test bolus. A partial contrast dose is given to the patient intravenously (e.g. 25-50% of the full contrast dose) using the same injection rate as the full contrast dose that is given later. A dynamic CT scan is performed at the level of the patient's aorta from the beginning of contrast injection for 60 -120 seconds. A bolus geometry curve of the aorta is derived by measuring the degree of contrast enhancement in the aorta over time.

3. CT scan delays for multiphasic study

CT scan delay times are preset into the machine at the beginning of the patient's imaging study. They determine the time of initiation of the CT machine for the arterial and hepatic phases. Accurate CT scan delays are necessary to synchronise the arterial and hepatic phase scan with the peak of contrast flow in the splanchnic arteries and liver, respectively. From our research studies in dogs and cats in this thesis, we were able to predict the timing of peak contrast flow in the splanchnic arteries and liver. Our recommendations for CT scan delays in a new standardised protocol is based on knowledge of time to peak enhancement. The recommended CT scan delay for the arterial phase is 10 seconds post aortic arrival time, and the CT scan delay for the hepatic phase is 35 seconds post aortic arrival time. Our recommendation differed to other previously published CT protocols. Our recommended CT start time for the arterial phase is later compared to other published CT protocols. Other institutions recommend an earlier CT start time for the arterial phase, coinciding with the aortic arrival time (based on bolus tracking or test bolus). More broadly in the veterinary literature, the arterial and hepatic phase scan delay is not standardised.

We hypothesised that the new standardised CT protocol at UVTHS would accurately and consistently capture the arterial and hepatic phase in all dogs in the study population, regardless of body weight or size. A comparison study was performed to assess the quality of vascular enhancement in multiphasic CT studies acquired at three veterinary institutions using three different CT scanners.

Received: 10 November 2017 | Revised: 6 July 2018 | Accepted: 6 July 2018

DOI: 10.1111/vru.12679

ORIGINAL INVESTIGATION

WILEY

Vascular conspicuity differs among injection protocols and scanner types for canine multiphasic abdominal computed tomographic angiography

Florence Thierry[1] | Jennifer Chau[2] | Mariano Makara[2] | Swan Specchi[3] | Edoardo Auriemma[3] | Maurizio Longo[1] | Ian Handel[1] | Tobias Schwarz[1]

[1]The Royal (Dick) School of Veterinary Studies and Roslin Institute, The University of Edinburgh, Roslin, EH25 9RG, UK

[2]Faculty of Veterinary Science, University of Sydney, New South Wales, 2006, Australia

[3]Istituto Veterinario di Novara, Granozzo con Monticello, Novara, Italy

Correspondence
Dr. Tobias Schwarz, The Royal (Dick) School of Veterinary Studies and Roslin Institute, The University of Edinburgh, Roslin, EH25 9RG, UK.
Email: tobias.schwarz@ed.ac.uk

Abstract

Multiphasic multidetector computed tomographic angiography is a standard diagnostic test for canine abdominal vascular disorders. Three imaging protocols have been previously described. The test-bolus protocol allows precise timing but can be time consuming to perform. Bolus-tracking software is fast and easy to use but can be problematic for exact timing of vascular phases. A recently described fixed-injection-duration protocol is not influenced by body weight and provides a wider temporal window for arterial acquisitions. Objectives of this retrospective and prospective, multicentric, method comparison study were to determine which of the three multidetector computed tomographic angiography protocols allows best vascular conspicuity of the canine abdomen and to assess the influence of different multidetector computed tomography (CT) scanners on study quality. Triple-phase multidetector computed tomographic angiography canine abdominal studies from 30 dogs were retrospectively retrieved from three different institutions. Each institution performed one of the three computed tomographic angiography protocols (4-row and 16-row multidetector CT). Prospectively, the three protocols were also acquired with similar conditions on a 64-row MDCT in 21 dogs. Main abdominal vessels were scored by blinded readers for each phase. The fixed-injection-duration protocol had the best combined arterial and portal vascular conspicuity on scanners of limited speed, while the test-bolus protocol provided the best overall vascular conspicuity on 64-row multidetector CT scanner. The quality of arterial studies performed on 64-row MDCT scanner was improved compared to the ones performed on four- to 16-row multidetector CT scanners. Findings supported the fixed-injection-duration protocol as the best compromise between an ideal portal vascular enhancement and an easily reproducible protocol on scanners with low and high number of detector rows.

KEYWORDS

angiographic, arterial, dog, multidetector CT, portal

1 | INTRODUCTION

Multiphasic multidetector computed tomographic angiography is currently a standard diagnostic test for canine vascular disorders such as portosystemic shunts, arteriovenous fistulae, or vascular tumor invasion.[1–3] This method is also commonly used for characterizing parenchymal disease such as pancreatic insulinoma and may help characterizing benign and malignant lesions.[4–8] A major advantage of multiphasic multidetector computed tomographic angiography is the ability to separate the arterial from the portal and systemic venous phases in order to reach an optimal visualization of each vascular bed and to identify hypervascular or hypovascular parenchymal lesions.[9]

The test-bolus multidetector computed tomographic angiography protocol has been used for more than a decade in veterinary

Previous presentation: Portions of this study were presented at the Annual European Veterinary Diagnostic Imaging Meeting, August 30th–September 2nd 2017, Verona, Italy.

patients.[2,10,11] This protocol is based on the initial injection of a low dose of contrast medium, i.e., test bolus, to determine the peak of aortic and portal enhancement using time attenuations curves followed by a dynamic angiography with a full dose of contrast agent. This technique has the advantage of being specifically adapted to the patient, which is valuable in animals with impaired cardiovascular function. The bolus-tracking multidetector computed tomographic angiography protocol uses software tools to monitor the arrival of contrast medium into a vessel and triggers an automatic or manual start of the acquisition once the preset density threshold has been reached. This type of protocol provides an individualized timing of the arterial phase.[8,12,13] The fixed-injection-duration multidetector computed tomographic angiography protocol is another technique that has been recently described in cats and dogs using a fixed injection duration of 20 s and adjusted injection rate.[14–16] This new method triggers a later and lower peak of aortic enhancement with good separation between the arterial and portal phases. An advantage of this new technique is a more homogeneous pattern of vascular enhancement regardless of the body weight. Another advantage is a wider temporal window for acquiring the arterial phase.

A previous study compared bolus-tracking and test-bolus techniques for thoracic computed tomographic angiography in healthy beagles and did not identify differences in image quality, consistent with previously published data in human medicine.[17,18] An increasing number of publications have described multiphasic multidetector computed tomographic angiography protocols for investigations of parenchymal disorders.[5–7] However, the choice of a particular abdominal multidetector computed tomographic angiography protocol may possibly influence the parenchymal enhancement and have an impact on subsequent results. New multidetector computed tomography (CT) scanners have been recently introduced that have a higher number of detector rows and can therefore offer shorter acquisition times.[19] A detailed comparison of different multidetector computed tomographic angiography protocols was not found in the veterinary literature.

The aim of this study was to compare the conspicuity of vessels in the cranial abdomen using three different protocols of triple-phase multidetector computed tomographic angiography (test-bolus, bolus-tracking, and fixed-injection-duration protocols). We also aimed to determine which protocol allows the best vascular visualization and to assess the influence of the canine weight and different multidetector CT scanners on the quality of the studies. We hypothesized that there is a difference in vascular conspicuity between the three multidetector computed tomographic angiography protocols and that the quality of these studies depends on the number of detector rows used and body weight.

2 | MATERIALS AND METHODS

2.1 | Sample population

This retrospective and prospective, multicentric, method comparison study gathered triple-phase abdominal multidetector computed tomographic angiography studies performed on dogs under general anesthesia presented for clinical reasons unrelated to the abdominal vasculature. Decisions for study inclusion and exclusion were made by a final year small animal imaging resident (F.T.). Studies were included if the injection of contrast medium was performed via a cephalic vein and if the arterial, portal and late venous phases included the abdomen from the diaphragm to the caudalmost kidney margin. Dogs were excluded if any vascular impairment or malformation was present in the abdomen. Images were acquired in ventral recumbency under general anesthesia during apnea following hyperventilation in order to avoid motion artifacts. A precontrast study of the abdomen was acquired in all dogs. All contrast medium injections were performed with a power injector without the use of saline chaser. All late venous phases were performed within 5 min after contrast medium injection.

2.2 | Retrospective computed tomographic data

Canine abdominal multidetector computed tomographic angiography studies were retrospectively retrieved from three different institutions. The sample size for each institution group was matched and based on the maximal number of studies available at the University of Edinburgh that fitted the inclusion criteria. Each institution performed one of the three multidetector computed tomographic angiography protocols. As part of the inclusion criteria, the same test-bolus protocol was performed at the Royal (Dick) School of Veterinary Studies of the University of Edinburgh with the following protocol. First, a 0.5 mL/kg bolus of contrast medium (185 mg Iodine/kg) was injected. A dynamic acquisition in a single location at the porta hepatis was performed at the start of the contrast medium injection every 2 s during 40 s. Regions of interest were placed in the aorta and portal vein by an imaging resident or a board-certified veterinary radiologist. Time attenuation curves were used to establish optimal timings for the arterial and portal acquisitions. The arterial acquisition delay was set at the peak of aortic contrast enhancement. The minimum interscan delay was 4 s. The portal delay was initiated shortly before peak portal enhancement or following the minimum reset time between two phases. The full bolus of contrast medium (700–740 mg I/kg) was injected at 3 mL/s in dogs weighing less than 10 kg and at 5 mL/s if over 10 kg as per previous publication.[10] The arterial phase was performed in a caudo-cranial direction, the portal and late venous phase were scanned in a cranio-caudal direction.

The bolus-tracking protocol was performed at the Istituto Veterinario di Novara. As part of the inclusion criteria, the following protocol was used. A premonitoring transverse scan was set at the cranial aspect of the diaphragm, and designated as the start location of the arterial acquisition. A region of interest was placed in the aorta by an imaging resident, and the automated bolus-tracking set at 100 Hounsfield units (HU) with a cycle time of 3 s. The bolus of contrast medium (700 mg I/kg) was performed in all dogs at 3 mL/s. The arterial phase was run in a cranio-caudal direction, the portal phase scanned immediately after the minimum reset time in a caudo-cranial direction and the late venous phase in a cranio-caudal direction. The minimum interscan delay was 2 s.

The fixed-injection-duration protocol was performed at the University of Sydney. As part of the inclusion criteria, the following protocol

was followed. Bolus-tracking software and fixed delay times after contrast arrival were used for the arterial and portal scans. Contrast medium was injected over 20 s for all dogs and the injection rate was adjusted accordingly. A pre-monitoring transverse scan was set at the cranial aspect of the diaphragm. A region of interest was placed in the aorta by an imaging resident and the automated bolus-tracking set at 100 HU with a cycle time of 2 s. The time-to-aortic-arrival was defined as the time elapse from the beginning of the contrast medium injection to the time when the aortic attenuation reached 100 HU. The delay for arterial acquisition was similar for all dogs and equal to 10 s after time-to-aortic-arrival in order to scan during the arterial peak or immediately after. The minimum interscan delay was 2 s. The portal acquisition was automatically triggered 35 s after time-to-aortic-arrival. The arterial phase was run in a cranio-caudal direction, the portal phase scanned in a caudo-cranial direction, and the late venous phase in a cranio-caudal direction.

2.3 | Prospective computed tomographic data

Twenty-one canine abdominal computed tomographic angiography studies were prospectively acquired at the Royal (Dick) School of Veterinary Studies of the University of Edinburgh. The sample size was chosen based on a consensus opinion of the authors, one of whom was a statistician. The Veterinary Ethics and Welfare Committee of the Royal (Dick) School of Veterinary Studies of the University of Edinburgh granted approval for the prospective study prior to publication (Veterinary Ethics and Welfare Committee reference 106.17). The test-bolus, bolus-tracking, and fixed-injection-duration protocols were identical to the retrospective part of the study but performed on a 64-row multidetector CT scanner (Somatom® Definition AS Siemens, Erlangen, Germany). Injections of 700 mg I/kg of Iopamidol (Niopam 350®, Bracco UK Ltd) were performed with Empower CTA®+ Injector System (Bracco® injeneering S.A., Milan, Italy) set with a maximum pressure of 325 psi. Dogs were randomly allocated to a protocol according to their weight in order to achieve similar body weight distribution in each group of seven dogs. All acquisitions were performed by the same operator (F.T.). Scan settings included a collimator pitch of 1.4, tube potential of 100–120 kVp, reference tube current of 250–320 mA, slice thickness of 2 mm, matrix 512 × 512, and reconstruction with low frequency algorithms. Scan tube current was modulated by an automatic exposure control system (Care Dose 4D, Siemens Medical Solutions, International). The minimum interscan delay was 2 s.

2.4 | Computed tomographic data recorded

All retrospective multidetector computed tomographic angiography studies were randomized, reviewed by a board-certified veterinary radiologist (T.S.) and an imaging resident (F.T.), and scored by consensus. All studies were anonymized and reviewers were blinded to the angiographic protocol used. All assessments and measurements were performed using dedicated DICOM viewer software (OsiriX v5.8.5 64-bit, Geneva, Switzerland). A window width of 350 HU and a window level of 100 HU were used in order to allow optimal visualization of vascular streaming artifacts. The abdomen was divided into three regions of different vascular beds. During the arterial phase, each main abdominal vessel was subjectively scored using a binary grading system (+1 or −1). The same process was repeated for the portal phase. The most cranial abdominal region was established from the cranial aspect of the liver to the first hepatic vein ramification allowing scoring of the aorta and caudal vena cava. The mid-abdominal region extended from the first hepatic vein ramification to the gastroduodenal vein entrance into the portal vein, allowing scoring of the aorta, hepatic arteries, caudal vena cava, hepatic veins, intrahepatic portal branches, and extrahepatic portal vein. The caudal abdominal region included the portion of the abdomen between the gastroduodenal vein entrance into the portal vein and the jejunal veins, allowing scoring of the aorta, celiac and cranial mesenteric arteries, caudal vena cava, extrahepatic portal vein, gastroduodenal vein, and splenic vein. For example, to achieve a satisfactory score of +1 in the aorta during the arterial phase, the aorta had to present with a homogeneous strong vascular enhancement and absence of contrast streaming artifact. An ideal arterial phase of a computed tomographic angiography was defined as having strong contrast enhancement in the aorta, hepatic arteries, and celiac arteries but none in the systemic venous and portal vasculature (Figure 1). The portal phase was considered optimal if the entire portal vasculature, splenic vein included, presented strong contrast enhancement compared to the caudal vena cava and hepatic veins (Figure 2). During the arterial phase, the arterial index was equal to the summation of all vascular scores given for the three abdominal regions. The maximal arterial index was 15 and minimal arterial index −15. Similarly, the portal index resulted from the sum of all scores given for the abdominal vessels during the portal phase. The maximal portal index was 10 and minimal portal index −10. We summed both arterial and portal indices to create a combined vascular index. The same subjective scoring process was repeated for the prospective multidetector computed tomographic angiography studies.

A small animal imaging resident (F.T.) performed a quantitative scoring by placing a 10 mm^2 region of interest in the main abdominal vessels during the arterial and portal phases. A region of interest was placed as appropriate in the aorta, caudal vena cava, and portal vein in the three abdominal regions. The attenuation values were then averaged per dog and per phase for each vessel. Any vascular or extra-vascular artifact was recorded. The same quantitative scoring process was repeated for the prospective multidetector computed tomographic angiography studies.

2.5 | Data analyses

Statistical analysis was performed by a statistician (I.H.) using a free software (R Core Team 2017, R: A language and environment for statistical computing, R Foundation for Statistical Computing, Vienna, Austria). We investigated the relationship between weight, scan duration, scanner type, and protocol on index for the two phases separately and in combination using a linear regression model with index as the dependent variable. Although index is derived from ordinal scores the overall index was treated as a numerical variable. Models were assessed by inspection of histograms of their residuals. Summary estimates of the relationship between protocol and index

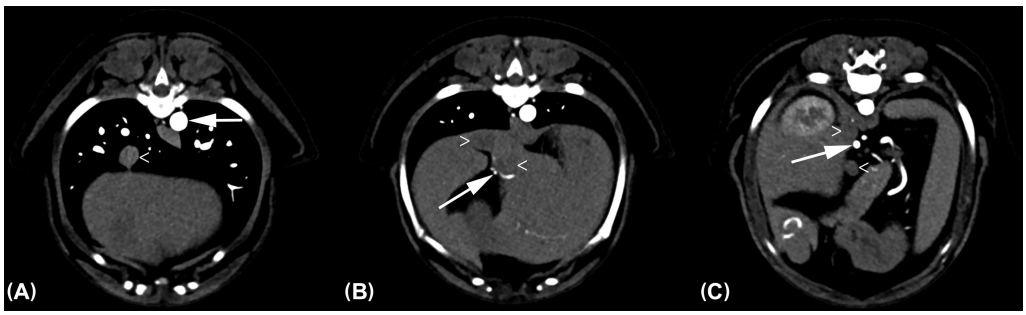

FIGURE 1 Optimal arterial phase illustrated by a transverse plane for each abdominal region (A–C) in a dog using the bolus-tracking protocol on 64-row multidetector computed tomography unit. Note the strong contrast enhancement in the aorta, celiac and hepatic arteries (arrows) but none in the portal and venous vasculature (arrowheads)

were estimated using the Least-Squares means (Lsmeans) R-package and reported as estimate and 95% confidence interval. In order to investigate any difference of scan duration between four- and 16-slice CT units, a Kruskal–Wallis test was performed. The significance level for statistical tests was set at 0.05.

3 | RESULTS

3.1 | Retrospective computed tomographic data

A total of 30 dogs were included in the sample (10 dogs from each institution). At the Royal (Dick) School of Veterinary Studies of the University of Edinburgh, computed tomographic images were acquired using the test-bolus protocol with a four-row multidetector CT unit (Somatom® Volume Zoom, Siemens, Germany) over a 6-year period. Scan settings included slice thickness 3 mm, pitch between 1 and 1.5, tube potential 120 kVp, tube current 120–150 mA, matrix 512 × 512. Injections of 350–370 mg I/mL Iopamidol (Niopam®, Bracco UK Ltd) were performed with Mark V power injector (Medrad®, PA, USA) set at 300 psi injection pressure.

At the Istituto Veterinario di Novara, computed tomographic images were acquired using the bolus-tracking protocol with a 16-row MDCT unit (Light Speed, GE Medical Systems, Milan, Italy) over a 8-month period. Scan settings included slice thickness between 1.25 and 2.5 mm, pitch 0.938, tube potential 100–120 kVp, tube current 180–200 mA, matrix 512 × 512. Injections of 350 mg I/mL of iohexol (Omnipaque®, GE Healthcare, Princeton, NJ) were performed with Medrad® envision CT injector (Medrad Italia, Cava Manara, Italy) set at 300 psi injection pressure.

At the University of Sydney, computed tomographic images were acquired using the fixed-injection-duration protocol with a 16-row MDCT unit (Phillips 16 Slice, Brilliance® CT V2.3, Phillips Medical Systems Netherlands, the Netherlands) over a 6-month period. Scan settings included slice thickness between 1 and 2 mm, pitch between 0.813 and 0.938, tube potential 120 kVp, tube current 100–250 mA, matrix 512 × 512. Injections of 350 mg I/mL of iohexol (Omnipaque®, GE Healthcare, Princeton, NJ) were performed with Empower CTA®

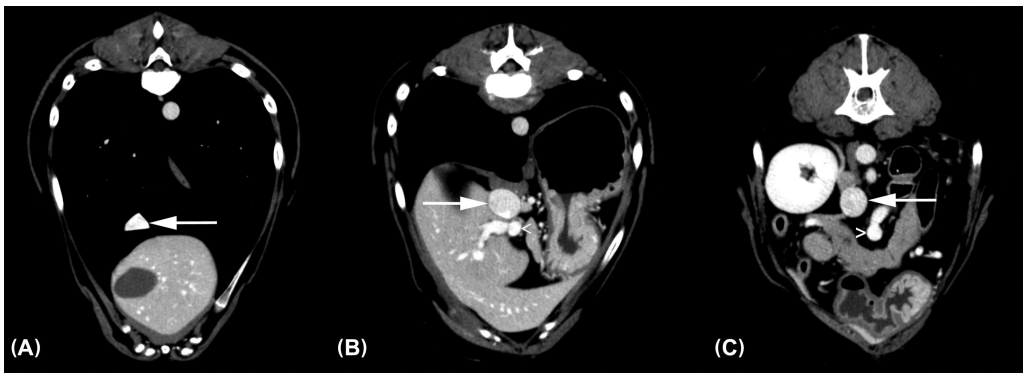

FIGURE 2 Optimal portal phase illustrated by a transverse plane for each abdominal region (A–C) in a dog using the fixed-injection-duration protocol on 16-row multidetector computed tomography unit. Note the strong contrast-enhancement in the portal vein (arrowhead) in comparison to the caudal vena cava (arrow)

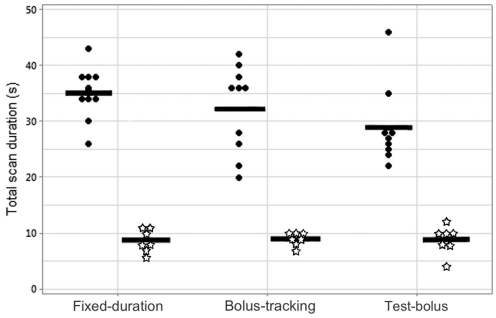

FIGURE 3 Dotplot representing the total scan duration (sum of arterial scan and portal scan duration in seconds) for each protocol and multidetector computed tomography scanner (●, four- and 16-row multidetector computed tomography scanners; ⋆, 64-row multidetector computed tomography scanner; —, mean)

power injector (E-Z-EM Inc., Westbury, New York) set at 300 psi injection pressure.

Various breeds were represented. The median weight of dogs was 12 kg (n = 10, range: 7–38 kg) in the test-bolus group, 26 kg (n = 10, range: 7–47 kg) in the bolus-tracking group, and 24 kg (n = 10, range: 7–43 kg) in the fixed-injection-duration group. The test-bolus group gathered seven female and three male dogs, the bolus-tracking group, five females and five males, and the fixed-injection-duration group, four female and six male dogs. The median age of dogs was 5 years (n = 10, range: 0.3–12 years) in the test-bolus group, 9 years (n = 10, range: 2–14 years) in the bolus-tracking group, and 5 years (n = 10, range: 2–11 years) in the fixed-injection-duration group. Among all groups, nine of 30 dogs had no significant abnormality and nine of 30 dogs had a final diagnosis of neoplasia. Other disorders included hepatopathy (3/30), thoracic or subcutaneous abscesses (2/30), nephropathy (2/30), lymphadenomegaly (2/30), ureteral ectopia (1/30), gastric foreign body (1/30), and pelvic fracture (1/30). In the test-bolus group, the portal acquisition was initiated following the minimum reset time between two phases in seven dogs. These seven dogs were small breed dogs weighing up to 15 kg. The median injection rate for the fixed-injection-duration protocol was 2.3 mL/s (n = 10, range: 0.7–4.3 mL/s). The median time-to-aortic-arrival of the contrast medium bolus was 9 s (n = 10, range: 2–14 s) for the test-bolus protocol, 15 s (n = 10, range: 4–19 s) for the bolus-tracking protocol, and 15 s (n = 10, range: 8–22 s) for the fixed-injection-duration protocol. The median time for initiation of the portal acquisition scan was 15 s after time-to-aortic-arrival (n = 10, range: 10–17 s) for the test-bolus protocol, 28 s after time-to-aortic-arrival (n = 10, range: 21–32 s) for the bolus-tracking technique, and 35 s after time-to-aortic-arrival (n = 10, range: 35–35 s) for the fixed-injection-duration protocol. Duration of the arterial and portal scans is summarized in Figure 3. The total scan duration was not significantly different between the four-slice CT scanner and both 16-slice CT units (n = 30, df = 2, χ^2 = 4.43, P = 0.109). These scanners were therefore grouped together in the following linear regression models.

The mean indices are summarized in Table 1. During the arterial phase, the fixed-injection-duration protocol had the narrowest dispersion of data. Quantitatively, the arterial phase of the test-bolus protocol had the highest mean arterial index compared to the other two protocols, while the portal phase of the fixed-injection-duration protocol offered the highest mean portal index. Overall, the fixed-injection-duration protocol has the highest mean combined vascular index and narrowest dispersion of data.

On the arterial phase of the fixed-injection-duration protocol, contrast enhancement was visible in the portal vein at the porta hepatis in nine of 10 dogs consistent with a late arterial acquisition. In the test-bolus group during the portal phase, contrast streaming artifact was reported in the portal vein in four dogs and in the caudal vena cava in six dogs. This artifact was less commonly noted in the bolus-tracking group (2/10 dogs) and the fixed-injection-duration group (4/10 dogs) during the portal phase.

During the arterial phase, the mean aortic attenuation was quantitatively higher for the test-bolus protocol compared to the bolus-tracking and fixed-injection-duration protocols (Table 2). These two last protocols nevertheless achieved acceptable aortic enhancement. During the portal phase, the mean aortic attenuation was lower for the fixed-injection-duration protocol compared to the test-bolus and bolus-tracking protocols.

3.2 | Prospective computed tomographic data

Various breeds were represented among which Retrievers (7/21) and collie (3/21) breeds were common. The median weight of dogs was 25 kg (n = 7, range: 5–37 kg) in the test-bolus group, 25 kg (N = 7, range: 6.5-36 kg) in the bolus-tracking group and 19 kg (N = 7, range: 9-36 kg) in the fixed-injection-duration group. Each group gathered 3 female and 4 male dogs. The median age of dogs was 8 years (N = 7, range: 2-10 years) in the test-bolus group, 11 years (N = 7, range: 6-16 years) in the bolus-tracking group and 10 years (N = 7, range: 0.6–11 years) in the fixed-injection-duration group.

Among all groups, 15/21 dogs had a final diagnosis of neoplasia while one of 21 dogs had no significant abnormality. Other disorders included pulmonary disease (2/21), sialadenitis (1/21), brachycephalic obstructive airway syndrome (1/21), and retrobulbar abscess (1/21). The median injection rate for the fixed-injection-duration protocol was 2.0 mL/s (n = 7, range: 0.9–3.6 mL/s). The median time-to-aortic-arrival of the contrast medium bolus was 10 s (n = 7, range: 9–14 s) for the test-bolus protocol, 11 s (n = 7 range: 5–15 s) for the bolus-tracking protocol and 10 s (n = 7, range: 7–12 s) for the fixed-injection-duration protocol. The median time for initiation of the portal acquisition scan was 11 s after time-to-aortic-arrival (n = 7, range: 7–18 s) for the test-bolus protocol, 8 s after time-to-aortic-arrival (n = 7, range: 7–14 s) for the bolus-tracking technique and 35 s after time-to-aortic-arrival (n = 7, range: 35–35 s) for the fixed-injection-duration protocol. Duration of the arterial and portal scans is summarized in Figure 3.

The mean indices are summarized in Table 1. The arterial phase of the bolus-tracking protocol had the highest mean arterial index and narrowest dispersion of data compared to the other two protocols. The portal phase of the fixed-injection-duration protocol offered the highest mean portal index and narrowest dispersion of data. The

TABLE 1 Arterial, portal, and combined indices for each protocol and multidetector computed tomography scanner

		Test-bolus protocol	Bolus-tracking protocol	Fixed-injection-duration protocol
4 and 16 MDCT ($n = 3$)	Mean arterial index	7.9 (SD 7.1)	2.4 (SD 6.2)	3.1 (SD 3.4)
	Mean portal index	1 (SD 5.3)	6.2 (SD 3.6)	7.2 (SD 3.9)
	Mean combined arterial and portal index	8.9 (SD 10.4)	8.6 (SD 8.2)	10.3 (SD 6.1)
64-row MDCT ($n = 2$)	Mean arterial index	11.3 (SD 4.4)	15 (SD 0)	4 (SD 2.8)
	Mean portal index	2.9 (SD 5.0)	−1.1 (SD 3.2)	8 (SD 2)
	Mean combined arterial and portal index	14.1 (SD 4.7)	13.9 (SD 3.2)	12 (SD 4.5)

Abbreviation: MDCT, multiphasic multidetector computed tomography; SD, standard deviation.

mean bolus-tracking portal index, on the other hand, was lower than the two other protocols due to a very premature acquisition. Overall, the test-bolus protocol had the highest mean combined vascular index.

On the arterial phase of the fixed-injection-duration protocol, contrast enhancement was visible in the portal vein at the porta hepatis in five of dogs consistent with a late arterial acquisition. In the bolus-tracking group during the portal phase, contrast streaming artifact was present in the portal vein in all seven dogs and in the caudal vena cava in five dogs (Figure 4). This artifact remained common in the test-bolus group (4/7 dogs) but was never present in the studies of the fixed-injection-duration group during the portal phase.

During the arterial phase, the mean attenuation in the portal vein and caudal vena cava was quantitatively higher for the fixed-injection-duration protocol compared to the other two protocols, consistent with a late arterial acquisition (Table 2). During the portal phase, the mean aortic attenuation was quantitatively lower for the fixed-injection-duration protocol compared to the test-bolus and bolus-tracking protocols.

3.3 | Linear regression model for combined vascular index

The factor scan duration was found to be non-significant and strongly correlated to the scanner type ($\rho = 0.836$). This factor was dropped from initial model, which was then re-estimated.

The variable weight (estimate ± standard error = −0.043 ± 0.043, $t = 0.991$, $P = 0.324$) and scanner type (estimate ± standard error = −2.130 ± 1.195, $t = -1.783$, $P = 0.078$) had no significant effect on the combined index. This combined index for the fixed-injection-duration protocol was not significantly different from the test-bolus (estimate ± standard error = 0.073 ± 1.436, $t = 0.051$, $P = 0.959$) or from the bolus-tracking protocol (estimate ± standard error = −0.380 ± 1.460, $t = -0.260$, $P = 0.795$) (Figure 5).

3.4 | Separated linear regression models for arterial and portal phases

Similarly, the factor scan duration was found to be non-significant and strongly correlated to the scanner type ($\rho = 0.815$ for the arterial phase

TABLE 2 Vascular contrast attenuation in Hounsfield units during the arterial and portal phase for each protocol and multidetector computed tomography scanner

			Test-bolus protocol	Bolus-tracking protocol	Fixed-injection-duration protocol
4- and 16-row MDCT ($n = 30$)	Arterial phase	Mean aortic attenuation	760 (SD 438)	433 (SD 132)	556 (SD 159)
		Mean portal attenuation	86 (SD 62)	114 (SD 42)	123 (SD 60)
		Mean caudal vena cava attenuation	119 (SD 81)	158 (SD 43)	179 (SD 72)
	Portal phase	Mean aortic attenuation	314 (SD 93)	250 (SD 49)	207 (SD 69)
		Mean portal attenuation	268 (SD 79)	249 (SD 59)	236 (SD 66)
		Mean caudal vena cava attenuation	240 (SD 77)	218 (SD 48)	205 (SD 56)
64-row MDCT ($n = 21$)	Arterial phase	Mean aortic attenuation	713 (SD 132)	757 (SD 351)	604 (SD 104)
		Mean portal attenuation	99 (SD 46)	52 (SD 29)	145 (SD 71)
		Mean caudal vena cava attenuation	120 (SD 55)	49 (SD 16)	168 (SD 55)
	Portal phase	Mean aortic attenuation	370 (SD 101)	363 (SD 227)	244 (SD 36)
		Mean portal attenuation	246 (SD 47)	226 (SD 100)	263 (SD 45)
		Mean caudal vena cava attenuation	262 (SD 91)	216 (SD 86)	228 (SD 41)

Abbreviation: MDCT; multiphasic multidetector computed tomography, SD; standard deviation.

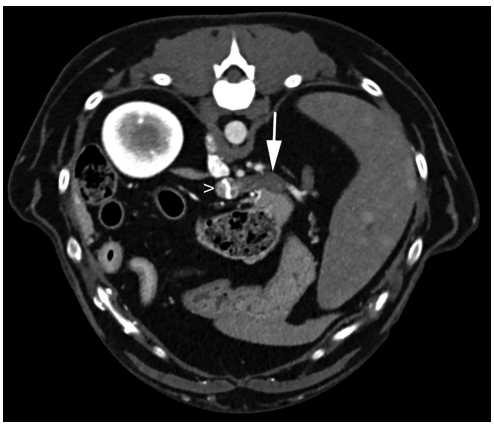

FIGURE 4 Portal phase in a dog using the bolus-tracking protocol on a 64-row multidetector computed tomography unit. Note the contrast streaming artifact in the portal vein (arrowhead) due to arrival of unenhanced blood from the splenic vein (arrow)

and $\rho = 0.857$ for the portal phase). This factor was dropped from initial models, which were then re-estimated.

The variable weight had no significant effect on the arterial index (estimate ± standard error = 0.105 ± 0.054, t = 1.930, P = 0.060). The scanner type (four- to 16-row unit vs. 64-row unit) had a significant effect on the arterial index (estimate ± standard error = −5.866 ± 1.502, t = −3.905, P = 0.0003). Indeed the arterial studies performed on the 64-row scanner had significantly higher arterial indices. The arterial index of the fixed-injection-duration was significantly lower and different from the test-bolus protocol (estimate ± standard error = 5.931 ± 1.805, t = 3.285, P = 0.002) but not different from the bolus-tracking protocol (estimate ± SE = 3.474 ± 1.835, t = 1.893, P = 0.065) (Figure 6A).

For the portal phase, the variable weight (estimate ± standard error = −0.019 ± 0.047, t = −0.411, P = 0.683) and scanner type (estimate ± standard error = 1.605 ± 1.295, t = 1.240, P = 0.221) had no significant effect on the portal index. The portal index of the fixed-injection-duration was significantly higher and different from the test-bolus protocol (estimate ± standard error = −5.784 ± 1.556, t = −3.717, P = 0.0005) and from the bolus-tracking protocol (estimate ± standard error = −4.235 ± 1.582, t = −2.677, P = 0.010) (Figure 6B).

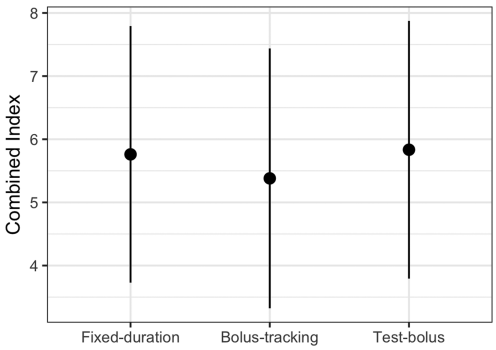

FIGURE 5 Dotplot representing the corrected mean (lsmean) combined index with 95% confidence intervals for each protocol on all four-, 16-, and 64-row multidetector computed tomography scanners

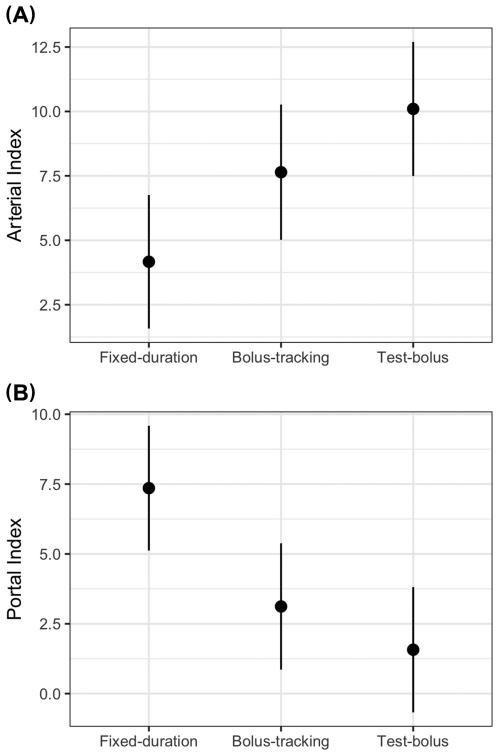

FIGURE 6 Dotplot representing the corrected mean (lsmean) arterial index (A) and portal index (B) with 95% confidence intervals for each protocol on all four-, 16-, and 64-row multidetector computed tomography scanners

4 | DISCUSSION

Findings from this study support our primary hypothesis in that there was a difference of vascular conspicuity between protocols during the arterial and portal phase in the separated linear regression model. The quality of arterial studies performed on the 64-row multidetector CT scanner was improved compared to the ones performed on four- to 16-row multidetector CT scanners. This effect was not demonstrated during the portal phase. Contrary to our last hypothesis, body weight had no effect on image quality.

The lack of difference in overall vascular conspicuity between the different protocols in the combined linear regression model does not

fully reflect the more detailed results for each vascular phase. In fact, the test-bolus and bolus-tracking protocols provided arterial studies of better quality than the fixed-injection-duration protocol while it was the contrary during the portal phase, and these effects cancelled each other out. In order to interpret the specificity of each protocol during each phase, we chose to focus the rest of our discussion based on the separated linear regression model.

The choice of protocol had an effect on the quality of studies. The test-bolus protocol offered the best arterial conspicuity on a four-row multidetector CT scanner, while the bolus-tracking protocol exceeded this quality on a 64-row multidetector CT scanner. This finding highlights that an automated scan trigger associated with a fast scanning time produces the best arterial result. Indeed, the use of bolus-tracking software also allows individual variations such as cardiac output and triggers the acquisition sooner if the bolus of contrast medium has an early arrival. The fixed-injection-duration protocol offered the best portal vascular conspicuity of multidetector computed tomographic angiography studies performed on slow and fast multidetector CT units. This result confirms that a slow and fixed injection duration yields homogeneous and strong portal enhancement due to its wide bolus geometry.

On 64-row multidetector CT unit, the fixed-injection-duration protocol scoring results suffered because the arterial phase was often scanned too late. To optimize the arterial phase of the fixed-injection-duration protocol, we have since the cessation of the study shortened the arterial scan delay after time-to-aortic-arrival from 10 s to 7 s with good empirical results. This avoids streaming artifacts in veins, which can be confused with arterial flow. By using a shorter arterial delay on a 64-row multidetector CT unit, the overall arterial conspicuity is expected to reach similar excellent quality as the bolus-tracking protocol on such a fast scanner.

Our hypothesis that image quality depends on the number of detector rows of a CT scanner was confirmed for the arterial phase but not for the portal phase. The arterial phase was of higher quality on a 64-row MDCT scanner. Indeed, a low number of detector rows represents a limitation to the scanner speed. By increasing detector row numbers in multidetector CT, scanning time is reduced, and thus, the image quality is more homogeneous for each vascular phase.[19] On fast CT units, bolus-tracking software is optimal to trigger an arterial phase of excellent quality as shown in this study. In practice, on MDCT scanners with a low number of detector rows, the portal phase of the bolus-tracking protocol can be run immediately after the arterial phase and result in a study of acceptable quality. Unfortunately, if the exact same protocol is run on a fast multidetector CT unit, like in the prospective part of this study, it will trigger a very premature portal phase. The absence of optimal portal timings explains the overall low quality of the portal phase using the bolus-tracking protocol on 64-row multidetector CT scanner. Previous publications have established optimal delays using bolus-tracking technique for the pancreas and liver, although the need for organ-specific delays is not practical for daily use.[8,13] Weight is another variable that has to be taken into account for the bolus-tracking protocol since the time-to-arterial peak is influenced by body weight when the injection rate is fixed.[14] The bolus-tracking protocol needs to be adapted for fast multidetector CT scanners with a high number of detector rows by establishing longer delays between the arterial and portal phases.

Depending on the protocol and the multidetector CT scanner used, studies had wide to narrow variation of quality. Overall, the fixed-injection-duration and the bolus-tracking protocol presented the narrowest data dispersion for all phases combined. These two protocols are therefore better reproducible compared to the test-bolus technique. This finding may be related to human errors. Indeed, for the test-bolus protocol, the operator has to select the optimal timings on the time-attenuation curves of the test bolus, which is often done by observing a graph, rather than using displayed time figures. The retrospective studies of the test-bolus protocol highlighted an unexpected wide variation of quality. The low number of detector rows and long scan duration are likely responsible for this qualitative variation during the arterial phase. The variation in portal phase imaging is more difficult to explain. The time-attenuation curve of the portal phase is supposed to be the shape of a plateau,[10,11] however, in reality it is often more shaped like a wedge, with a steep rise and slow decline. Operators had no instructions which time point to choose from the portal attenuation curve, which likely introduced variability in vascular conspicuity. If the phase of the test-bolus protocol is, for example, acquired at the beginning of the portal plateau, as performed for some of the data of this study, it will likely result in poorer quality of the portal enhancement with contrast streaming artifact arising from the non-enhanced splenic vein. Establishing the optimal portal timing on time-attenuation curves was considered by the authors as the main source of variability of the portal phase and limitation to the test-bolus protocol. Another possible reason explaining the poor quality of some test-bolus studies is the potential discrepancy between timings established via a small test bolus of contrast medium and the real timings after a full bolus of contrast medium. Indeed, a test bolus has a different volume and dose in relation to body weight compared to the full bolus of contrast medium causing different bolus geometry.[12,17,20] Its optimal arterial and portal timings may not be representative of the optimal delays of a full bolus.

The fixed-injection-duration protocol was designed to suppress the variability of vascular enhancement due to weight and to have a wide temporal window to acquire the arterial phase.[14] A slow injection of contrast medium over 20 s triggers a later and lower aortic peak enhancement due its wider bolus geometry.[14–16,21] On four- and 16-row multidetector CT scanners, the aortic attenuation during the arterial phase was indeed lower compared to the test-bolus protocol but higher than the bolus-tracking protocol. On 64-row multidetector CT scanner, the three protocols had similar aortic attenuation during the arterial phase. The bolus-tracking protocol had nevertheless a wide distribution of data for the aortic attenuation. For a fixed injection rate, the time to arterial peak is influenced by body weight.[14] A short acquisition time thus increases the variability of aortic attenuations between dogs of different body weights. Overall, the choice of protocol for the arterial phase appears to have little impact on the aortic contrast enhancement. During the portal phase, however, the aortic contrast enhancement was lower with the fixed-injection-duration protocol. This is most likely due to a later portal acquisition compared to the other two protocols.

Surprisingly, the scan duration had no effect on vascular conspicuity in this study. It has been suggested that contrast medium injection rate should be increased with fast CT acquisition in order to match the fast scanning duration.[16,19] The disadvantage of decreasing the injection duration is the narrowing of the temporal window for the arterial scan. Given the good quality of the portal phase of the fixed-injection-duration protocol, we therefore recommend to keep a long injection duration of 20 s for this protocol.

Contrast streaming artifact was commonly reported in early-performed portal studies. Non-contrast enhanced blood of the splenic vein mixes with contrast-enhanced blood in the portal vein and causes this artifact when the portal phase is performed too early. In the caudal vena cava, contrast streaming artifact is visible when early renal contrast-enhancing venous flow mixes with non-enhancing caval blood. In the authors' opinion, streaming artifact in the caudal vena cava or portal vein can be considered as a good marker of a premature portal phase. In the test-bolus group, 11/17 studies demonstrated this vascular artifact during the portal phase while it was rarely noted in the fixed-injection-duration group. On a 64-row multidetector CT unit, the portal phases of the bolus-tracking group were all performed too early, which was confirmed by the low portal index and commonly reported contrast streaming artifact.

Due to the multicentric nature of the study, different MDCT scanners have been used by different operators, which may have influenced the quality of the acquisitions. Several anesthetic protocols have been performed, which may have triggered different cardiovascular response and affected the timings of vascular enhancement. Indeed, it has been demonstrated that peak and time to peak of aortic contrast-enhancements increase when the cardiac output is reduced due to an increased circulation time.[20,22] It does however reflect the reality of daily practice. Having larger groups of dogs might have yielded further meaningful statistics. Due to the retrospective nature of part of the study, the median weight of dogs in the test-bolus group was smaller compared to the other groups, which may have affected the vascular conspicuity.

In conclusion, the three multidetector computed tomographic angiography protocols yielded different abdominal vascular conspicuity. The fixed-injection-duration protocol performed by multiple operators had the best vascular conspicuity on scanners of limited speed, while the test-bolus protocol performed by a single operator provided the best vascular conspicuity on fast MDCT scanner. The number of detector rows influenced the quality of the arterial phase due to scanner speed limitation but it did not affect the quality of the portal phase. In the authors' opinion, the main disadvantages of the test-bolus protocol were the increased dose of contrast medium required, and being operator dependent. Authors propose that the fixed-injection-duration protocol offers a good compromise between an ideal vascular enhancement during the portal phase and an easily reproducible protocol on scanners with low and high number of detector rows. For the arterial acquisition of this protocol, we recommend improving it by using a fixed delay of 7 s after time-to-aortic-arrival and keeping the delay of 35 s after time-to-aortic-arrival for the portal acquisition.

LIST OF AUTHOR CONTRIBUTIONS

Category 1

(a) Conception and Design: Thierry F, Chau J, Makara M, Specchi S, Auriemma E, Longo M, Handel I, Schwarz T

(b) Acquisition of Data: Thierry F, Chau J, Makara M, Specchi S, Auriemma E, Longo M, Handel I, Schwarz T

(c) Analysis and Interpretation of Data: Thierry F, Handel I

Category 2

(a) Drafting the Article: Thierry F

(b) Revising Article for Intellectual Content: Thierry F, Chau J, Makara M, Specchi S, Auriemma E, Longo M, Handel I, Schwarz T

Category 3

(a) Final Approval of the Completed Article: Thierry, Chau J, Makara M, Specchi S, Auriemma E, Longo M, Handel I, Schwarz T

ORCID

Florence Thierry http://orcid.org/0000-0003-4175-4397
Maurizio Longo http://orcid.org/0000-0002-6838-8430
Ian Handel http://orcid.org/0000-0001-6407-4963
Tobias Schwarz http://orcid.org/0000-0001-8412-573X

REFERENCES

1. Zwingenberger AL, Schwarz T, Saunders M. Helical computed tomographic angiography of canine portosystemic shunts. *Vet Radiol Ultrasound*. 2005;1:27–32.
2. Frank P, Mahaffey M, Egger C, Cornell KK. Helical computed tomographic portography in ten normal dogs and ten dogs with a portosystemic shunt. *Vet Radiol Ultrasound*. 2003;4:392–400.
3. Zwingenberger AL, McLear RC, Weisse C. Diagnosis of arterioportal fistulae in four dogs using computed tomographic angiography. *Vet Radiol Ultrasound*. 2005;46:472–477.
4. Caceres AV, Zwingenberger AL, Hardam E, Lucena JM, Schwarz T. Helical computed tomographic angiography of the normal canine pancreas. *Vet Radiol Ultrasound*. 2006;3:270–278.
5. Mai W, Caceres AV. Dual-phase computed tomographic angiography in three dogs with pancreatic insulinoma. *Vet Radiol Ultrasound*. 2008;49:141–148.
6. Kutara K, Seki M, Ishikawa C, Sakai M, Kagawa Y, Lida G, et al. Triple-phase helical computed tomography in dogs with hepatic masses. *Vet Radiol Ultrasound*. 2014;55:7–15.
7. Jones ID, Lamb CR, Drees R, Priestnall SL, Mantis P. Associations between dual-phase computed tomography features and histopathologic diagnoses in 52 dogs with hepatic or splenic masses. *Vet Radiol Ultrasound*. 2016;57:144–153.
8. Choi SY, Lee I, Seo JW, Park HY, Choi HJ, Lee YW. Optimal scan delay depending on contrast material injection duration in abdominal

multi-phase computed tomography of pancreas and liver in normal Beagle dogs. *J Vet Sci*. 2016;17:555–561.

9. Bae KT. Intravenous contrast medium administration and scan timing at CT: Considerations and approaches. *Radiology*. 2010;256:32–61.
10. Zwingenberger AL, Schwarz T. Dual-phase CT angiography of the normal canine portal and hepatic vasculature. *Vet Radiol Ultrasound*. 2004;2:117–124.
11. Winter MD, Kinney LM, Kleine LJ. Three-dimensional helical computed tomographic angiography of the liver in five dogs. *Vet Radiol Ultrasound*. 2005;*6*:494–499.
12. Mehnert F, Pereira PL, Trübenbach J, Kopp AF, Claussen CD. Biphasic spiral CT of the liver: automatic bolus tracking or time delay? *Eur Radiol*. 2001;11:427–431.
13. Choi S-Y, Choi H-J, Lee K-J, Lee Y-W. Establishment of optimal scan delay for multi-phase computed tomography using bolus-tracking technique in canine pancreas. *J Vet Med Sci*. 2015;77:1049–1054.
14. Makara M, Dennler M, Kühn K, Kalchofner K, Kircher P. Effect of contrast medium injection duration on peak enhancement and time to peak enhancement of canine pulmonary arteries. *Vet Radiol Ultrasound*. 2011;52:605–610.
15. Makara M, Chau J, Hall E, Kloeppel H, Podadera J, Barrs V. Effects of two contrast injection protocols on feline aortic and hepatic enhancement using dynamic computed tomography. *Vet Radiol Ultrasound*. 2015;56:367–373.
16. Chau J, Young AC, Dhand N, Makara MA. Estimation of time to peak contrast enhancement of the aorta and liver for dual-phase computed tomography on the basis of contrast medium arrival time, injection duration, and injection technique in dogs. *Am J Vet Res*. 2016;77:1093–1100.
17. Cassel N, Carstens A, Becker P. The comparison of bolus tracking and test bolus techniques for computed tomography thoracic angiography in healthy beagles. *JSAVA*. 2013;84:930–939.
18. Kerl JM, Lehnert T, Schell B, Bodelle B, Beeres M, Jacobi V, et al. Intravenous contrast material administration at high-pitch dual-source CT pulmonary angiography: Test bolus versus bolus-tracking technique. *Eur J Radiol*. 2012;81:2887–2891.
19. Hallett RL, Fleischmann D. Tools of the trade for CTA: MDCT scanners and contrast medium injection protocols. *Tech Vasc Interv Radiol*. 2006;9:134–142.
20. Bosch B, Alef M, Ludewig E, Hause A, Oechtering G, Kiefer I. Multiphasic contrast-enhanced CT: correlation of the peak attenuation in the aorta abdominalis and portal vein with easily detectable clinical parameters. *TierarztI Prax*. 2013;41:23–30.
21. Lee SK, Lee D, Kim D, Cha A, Choi J. Effect of catheter size and injection rate of contrast agent on enhancement and image quality for triple-phase helical computed tomography of the liver in small dogs. *Vet Radiol Ultrasound*. 2017;58:664–670.
22. Bae KT, Heiken JP, Brink JA. Aortic and hepatic contrast medium enhancement at CT. Part II. Effect of reduced cardiac output in a porcine model. *Radiology*. 1998;207:657–662.

How to cite this article: Thierry F, Chau J, Makara M, et al. Vascular conspicuity differs among injection protocols and scanner types for canine multiphasic abdominal computed tomographic angiography. *Vet Radiol Ultrasound*. 2018;59:677–686. https://doi.org/10.1111/vru.12679

SECTION 3 – Research Chapters (1-4)

Chapter 3. Refining contrast CT imaging in cats: Identify the Ideal Dose of Iohexol

Introduction:

The current intravenous dose rate for iodinated contrast used in multiphase CECT of the abdomen in dogs and cats has derived from early radiographic contrast studies including urogams and non-selective angiograms (Feeney et al, 1982; Wise, 1982). The recommended dose is 600-880mgI/kg with variation in the volume depending on the concentration of the formulation (average 2ml/kg) (Schwarz and Saunders, 2011). Reduced dose rates have been reported for iohexol clearance studies using dynamic CT to calculate glomerular filtration rates in cats. Dose rates of 0.25ml to 1.5ml/kg for iodinated contrast was reported and sufficient enhancement of the kidneys was achieved. However, evaluation of the remainder of the abdomen using these reduced doses is lacking.

The authors have observed a difference in the intensity of vascular and parenchymal enhancement between the dogs and cats during multiphasic contrast CT of the abdomen. At the same contrast dose tailored to body weight (2ml/kg), cats showed a much higher and markedly intense enhancement of the arteries and liver. The intense enhancement of the liver had undesirable effects with poor conspicuity between the liver parenchyma and intrahepatic vessels. The objective degree of enhancement of the aorta was excessive in cats. This was observed in our feline research study (Chapter 1) assessing the influence of contrast injection technique on bolus geometry of the aorta and liver. Particularly in the feline group that received contrast through a rapid injection rate, there was excessive aortic enhancement with a median value of 1900HU. The feline group that received contrast through a slower, fixed injection duration also had excessive aortic enhancement with a median value of 780HU. The optimal aortic enhancement value is 180-300HU for CT angiography (Hsieh et al, 2021).

There is a clinical preference towards using reduced contrast dose rates to avoid exacerbating renal dysfunction, particularly in the feline population due to a high incidence of pre-existing renal disease. Radiographic contrast is listed as a known drug related cause for acute renal failure (Ross, 2011). There are multiple patient related risk factors that predispose to renal injury such as age, hypotension (e.g. anesthesia related), hypertension, endocrine disease, pancreatitis or vasculitis. The reported incidence of acute renal failure in animals is low, mainly associated with ionic forms of iodinated contrast. The incidence is much higher in human patients with contrast induced nephropathy as one of the leading causes of acute renal failure in hospitalised patients (Stokes and Bartges, 2006). A recent study of feline renal function post administration of iodinated and gadolinium based contrast, overall showed no significant changes in renal parameters with the exception of proteinuria in 11% of cases (Prullage et al, 2022). Despite the low incidence of reported renal side effects, veterinary clinicians remain cautious and prefer to avoid intravenous contrast or request a reduced dose rate when considering contrast enhanced CT studies for elderly feline patients with pre-existing renal disease.

There is a strong drive to reduce contrast dose while simultaneously optimising contrast enhanced CT imaging in human diagnostic radiology. Due to the high risk of contrast induced nephropathy in elderly humans or azotemic patients, contrast doses were reduced and a compensatory decrease in radiation exposure was used to maximise CT attenuation of the contrast (Wintersperger et al, 2005, Szucs 2009, Bolmquist, 2006, Ippolito 2015). Decreased radiation energy levels at lower x-ray tube voltages have been associated with higher CT attenuation levels from iodinated contrast. Multiple human clinical studies have been performed using a lowered radiation exposure energy (80kVp) coupled with a reduced contrast dose, compared to regular radiation exposure energy (120kVp) coupled with a full contrast dose. The studies showed that a similar degree of CT contrast enhancement could be reached in both patient groups. There was no significant difference in image noise or signal to noise ratio and reducing contrast did not interfere with vascular conspicuity or diagnostic confidence.

We propose reducing the intravenous contrast dose for CT imaging in cats. We wanted to explore the limit of dose reduction before a deterioration in contrast enhancement and image quality would be observed. The value of using lowered kVp levels in CT scans of cats given reduced contrast doses would be assessed. We hypothesised that reduced contrast dose would improve vascular conspicuity within abdominal organs, and lower radiation exposures would improve CT attenuation of contrast.

Materials and Methods

Quantitative analysis of image noise

Circular regions of interest (ROIs, area of 10mm^2) were placed in multiple vascular and parenchymal structures during the arterial portovenous and delayed venous phases (performed by a radiologist, JC). A single ROI was placed in the following vessels: aorta, caudal vena cava, portal vein at the level of the porta hepatis. The average of two ROIs in the spleen, pancreas (left limb and right limb/body region) and renal cortex (left and right) was measured. In each parenchymal structure, efforts were made to place the ROI in as homogeneous an area as possible, such as away from vasculature. The standard deviation of the mean attenuation in the ROI served as an **objective measure of image noise.** The signal-to-noise ratio (SNR) of each ROI was calculated by dividing the mean HU by its standard deviation.

Qualitative evaluation
Images were scored by board certified veterinary radiologist at standardised window level of 40 and window width of 350 (standard viewing window for the abdomen on Osirix software viewer).

Scoring table for vascular conspicuity

Score	Description
0	No to insufficient enhancement of the vessels and parenchyma
1	Mild enhancement of vessels
2	Adequate enhancement of vessels but poor distinction between vessels and parenchyma
3	Adequate enhancement of vessels and good distinction between vessels and parenchyma

Scoring table for renal corticomedullary differentiation:

Score	Description
1	No distinction
2	Poor or subtle distinction.
3	Adequate distinction.

Scoring table for image noise

Score	Description
0	Poor quality (severely grainy image)
1	Satisfactory (moderately grainy but sufficient for diagnosis)
2	Good quality (mildly grainy)
3	Excellent quality (no appreciable mottle)

Statistical analysis:
All statistical analyses were conducted in Genstat v22 (VSN International, 2022) and a p value <0.05 was considered significant. Data were separated into three datasets: arterial phase, hepatic phase and delayed phase for analysis. Within each group, linear models were used to assess the effect of Group (1-4) on each of the outcome variables. Outcome variables included 7 locations (aorta, caudal vena cava, portal vein, liver, spleen, pancreas and renal cortex), for each of which data was obtained for 3 measures; HU of location itself, the standard deviation (SD) and signal to noise ratio (SNR). Outcome variables were assessed for normality prior to analysis and post-hoc pairwise Tukey tests were conducted to determine pairwise significance. The effect of group on score data (vascular conspicuity, renal corticomedullary contrast and image noise) was assessed using logistic regression. Scores were reduced to either >2 or <2 for analysis.

Results

Reduced xray energy
There was no significant difference between the cats that received standard xray energy (120kVp in Group 1) and reduced xray energy (90kVp in Group 2) for all of the objective measurements (Tables 1, 2 and 3). These two groups received the same standard contrast dose, and reducing the xray energy did not significantly

affect the objective mean attenuation values or the signal to noise ratio for the arterial, venous and delayed phases. Despite not reaching statistical significance, the highest mean attenuation values were obtained in Group 2 (Tables 1, 2 and 3). There was an increase in the mean attenuation value in Group 2 for all structures measured in the delayed phase, and an increase in the mean attenuation value for all structures in the hepatic phase (with the exception of the spleen). Group 2 also had increased mean attenuation values for the aorta and portal vein in the arterial phase. The subjective visual scores showed no significant deterioration in image quality due to image noise in any of the three phases (p value 0.115).

Lowered contrast dose

In the arterial phase, the mean aortic enhancement in Group 3 (1.5ml/kg) was significantly lower than Group 2 (2ml/kg), however it was not significantly different to Group 1 (2ml/kg, high xray energy). Other vascular and parenchymal structures measured in Group 3 on the arterial phase had no significant differences to other groups. Group 3 had the best visual scores for vascular conspicuity (100% > score 2) and renal corticomedullary differentiation (100% > score 2) on the arterial phase.

In the venous and delayed phases, Group 3 (1.5ml/kg) had significantly lower mean attenuation values compared to Group 2 (2ml/kg) for almost all vascular/parenchymal structures measured (except aorta in the hepatic phase). However, there was no significant difference in the mean attenuation values between Group 3 and Group 1 (despite Group 1 having the same contrast dose as Group 2 at 2ml/kg). Despite statistically significant differences in mean attenuation between Groups 3 and 2, the mean attenuation levels in Group 3 remained >230HU in the hepatic phase for all vascular and parenchymal structures measured. The mean aortic attenuation for Group 3 in the arterial phase was 560HU.
The signal to noise ratio in Group 3 was significantly lower than Group 1 for the portal vein, spleen, pancreas and renal cortex measured in the venous phase. Group 3 used a lower xray energy (90kVp) compared to Group 1 (120kVp). Signal to noise ratios were similar between Groups 3 and 2 (both lower xray energy) except for the caudal vena cava in the venous and delayed phase.

All HU measurements in Group 4 (1ml/kg) were significantly lower than the standard contrast dose groups (2ml/kg), in the venous and delayed phases (Tables 2 and 3). The attenuation values were also significantly lower for Group 4 in the arterial phase for all structures except the caudal vena cava (Table 1). The differences in the arterial phase were more pronounced between Groups 4 and 2, than compared to Group 4 and 1. The signal to noise ratios in Group 4 were significantly lower in all delayed phase measurements, and multiple hepatic phase measurements (portal vein and all organs measured). However, vascular conscpiuity scores were the highest for Group 4 in the hepatic phase (82% > score 2).

The visual scores for vascular conspicuity was only significantly different between Groups in the delayed phase. The post hoc analysis indicated that vascular conspicuity score for group 4 is significantly less likely to be 3 compared to Groups 1,2 & 3. However, there is no significant difference between Groups 1 & 2, Groups 2& 3 and Groups 1&3. There was no significant difference in vascular conspicuity between groups in the arterial and venous phases. Likewise, renal corticomedullary differentiation was not significantly different between groups in all three phases.

However, the visual scores for renal corticomedullary differentiation tended to perform better in the low contrast dose groups (3 and 4) for all three phases.

Figure 1. Example of post contrast CT images of the liver from a patient in Group 1 (top row A), Group 3 (middle row B) and Group 4 (bottom row C). Images on the left were taken during the arterial phase, and images on the right were taken during the hepatic phase. Images from top row A using a standard contrast dose of 2ml/kg show excessive enhancement of the liver parenchyma with effacement of intraparenchymal vessel at the standard soft tissue window level and width. Images from B and C using reduced contrast dose of 1.5ml/kg and 1ml/kg, respectively, show improved vascular conspicuity of the intrahepatic vessels.

A.

B.

C.

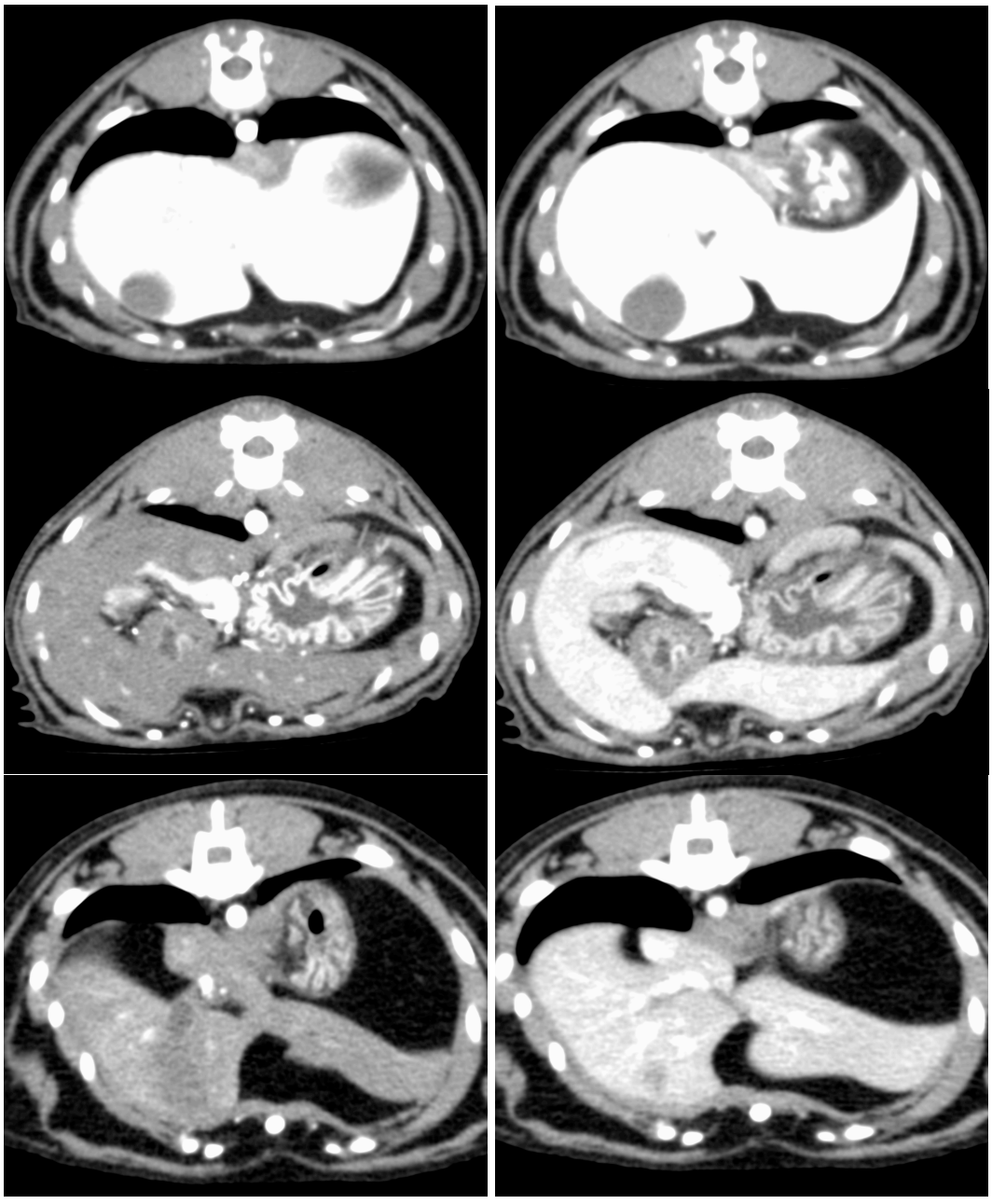

The present study had some limitations. Cats with abdominal abnormalities were included as well as normal abdomens. This was justified by the fact that multi- phase CT evaluations are often indicated for diseased patients. We therefore chose a study population that we believed represented the target clinical population. We cannot rule out the possibility that the abdominal disease could have affected portovenous pressure and affected the flow of contrast medium and intensity of contrast enhancement. Additional studies may be needed to evaluate the effect of gross liver disease on contrast enhancement. Only two levels of xray energy was trialled in this study (standard 120kVp and reduced level at 90kVp) because this is limited by the CT machine presets.

Table 1. Arterial phase: Results of mean attenuation measurements (HU) with variation in radiation exposure and contrast dose. SNR = signal to noise ratio, Ao = aorta, CVC = caudal vena cava, PV = portal vein, panc = pancreas and RC = renal cortex

Outcome variable	**P value**	**Group 1. HU (2ml/kg, 120kVp)**	**Group 2. HU (2ml/kg, 90kVp)**	**Group 3. HU (1.5ml/kg/ 90kVp)**	**Group 4. HU (1ml/kg, 90kVp)**
Aorta	**<0.001**	706.27	1064.22	561.16	387.61
Ao SNR	0.056	22.42	33.78	20.91	16.44
CVC	0.2594	175.91	139.77	134.29	115.58
CVC SNR	0.8849	9.45	8.39	9.24	5.84
PV	**0.026**	336.97	347.23	228.15	192.48
PV SNR	0.2955	11.37	9.21	7.23	9.00
Liver	**0.02**	259.82	257.24	188.67	156.02
Liver SNR	0.4747	10.25	8.88	7.69	8.30
Spleen	**0.02**	298.87	301.87	210.61	175.91
Spleen SNR	0.3793	10.82	9.04	7.41	8.51
Panc	**0.02**	278.66	278.66	198.34	165.67
Panc SNR	0.412	10.54	8.96	7.54	8.38
Renal Cortex	**0.015**	290.03	292.95	204.38	164.02
RC SNR	0.3734	10.68	9.00	7.47	8.16

Table 2. Hepatic phase: Results of mean attenuation measurements with variation in radiation exposure and contrast dose.

Outcome variable	**P value**	**Group 1. HU (2ml/kg, 120kVp)**	**Group 2. HU (2ml/kg, 90kVp)**	**Group 3. HU (1.5ml/kg/ 90kVp)**	**Group 4. HU (1ml/kg, 90kVp)**
Aorta	**<0.001**	295.10	337.20	260.20	195.80
Ao SNR	0.171	21.90	20.30	20.20	13.60
CVC	<0.001	281.40	318.50	234.70	180.40
CVC SNR	0.179	16.80	17.40	16.80	13.20
PV	**<0.001**	314.80	369.70	282.00	211.90
PV SNR	<0.001	30.60	24.70	17.50	14.00
Liver	**<0.001**	298.10	344.10	258.30	196.10
Liver SNR	<0.001	21.40	20.30	16.80	12.90
Spleen	**<0.001**	306.40	256.90	270.20	204.00
Spleen SNR	<0.001	25.00	22.20	17.10	13.30
Panc	**<0.001**	302.20	350.50	264.30	200.10
Panc SNR	<0.001	23.00	21.20	16.90	13.10
Renal Cortex	**<0.001**	304.30	353.70	267.20	198.50
RC SNR	<0.001	24.00	21.70	17.00	12.60

Table 3. Delayed phase Results of mean attenuation measurements with variation in radiation exposure and contrast dose.

Outcome variable	**P value**	**Group 1. HU (2ml/kg, 120kVp)**	**Group 2. HU (2ml/kg, 90kVp)**	**Group 3. HU (1.5ml/kg/ 90kVp)**	**Group 4. HU (1ml/kg, 90kVp)**
Aorta	**<0.001**	200.00	227.80	168.30	133.60
Ao SNR	0.001	18.90	16.40	13.00	10.20
CVC	<0.001	193.90	212.60	154.90	125.30
CVC SNR	<0.001	20.30	19.50	13.00	10.30
PV	**<0.001**	209.40	234.00	178.30	144.50
PV SNR	0.024	21.00	17.20	15.30	11.60
Liver	**<0.001**	201.60	223.30	166.60	134.90
Liver SNR	<0.001	20.00	17.90	13.80	10.90
Spleen	**<0.001**	205.50	228.60	172.50	139.70
Spleen SNR	0.004	20.30	17.40	14.40	11.20
Panc	**<0.001**	206.70	226.00	169.50	137.30
Panc SNR	0.002	20.00	17.60	14.10	11.00
Renal Cortex	**<0.001**	206.00	227.30	171.00	138.50
RC SNR	0.01	18.90	17.50	14.20	11.10

Figure 2. Visual scores for vascular conspicuity in the arterial phase (A), hepatic phase (B) and delayed phase (C) between treatment groups. Percentage of scores >2 (Grade 0-3) are compared between Group 1 (standard contrast dose 2ml/kg at 120kVp), Group 2 (standard contrast dose 2ml/s at 90kVp), Group 3 (reduced contrast dose 1.5ml/kg at 90kVp) and Group 4 (reduced contrast dose 1ml/kg at 90kVp). For the arterial phase, the scores were highest for Groups 3 followed by Group 4. For the hepatic phase, the scores were highest for Group 4 followed closely by Groups 2 and 3. For the delayed phase, the scores were highest for Group 2.

A.

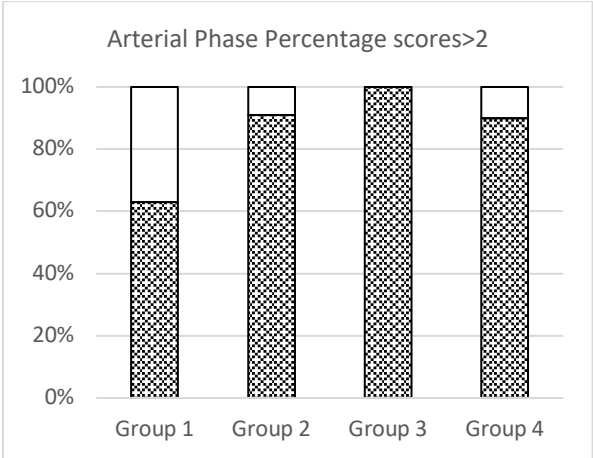

B.

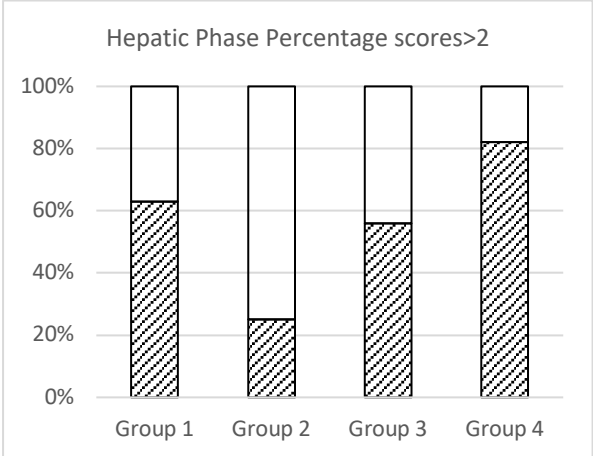

C.

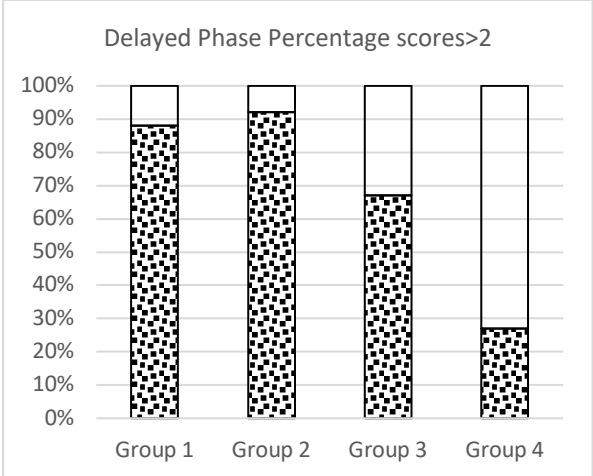

Discussion

Reducing x-ray energy can increase CT density measurement. There was no statistically significant difference between the high x-ray dose group (1) and lower x-ray dose group (2) when using the same contrast dose (2ml/kg) for any of the measurements. Despite not reaching statistical significance, the mean attenuation value of the aorta and portal were highest in Group 2 for the arterial phase. The mean attenuation value of the organs was also the highest in Group 2 for the hepatic phase (except spleen) and delayed phase. The step up in attenuation seen in Group 2 when using a reduced x-ray energy, became statistically apparent when comparing Group 3 (1.5ml kg and 1ml/kg) with Group 1 and 2 (both 2ml/kg). The mean attenuation values in Group 3 were significantly different from Group 2 for all structures in the hepatic phase (except aorta) and delayed phase. However, these measurements were not significantly different between Groups 3 and 1. Therefore, using reduced x-ray energy (90kVp) was able to elevate the attenuation characteristics of iodinated contrast which is compatible with experimental studies in humans (Wintersperger, 2005, Szucs et al, 2009). It is very likely that the use of reduced x-ray energy in Group 3 also helped to increase mean attenuation values that would have otherwise been further reduced in this group given a lowered contrast dose. However, comparison of 1.5ml/kg contrast dose in a high x-ray energy group versus lower x-ray energy group was not performed in this study.

Commonly applied settings for x-ray tube kilovoltage during CT studies are in the range of 120-140kVp. This results in a mean photon energy level of approximately 66–72 keV (some variation depending on the applied ray filtering) (Huda et al, 2000). This is a lot higher than the K edge of iodine which is at 33.2 keV. The K-edge is the sudden increase in absorption of x-ray photons by a target atom when the applied x-ray energy is just above the binding energy of the inner shell electron. In the context of this research study, the target atom is iodinated contrast medium, and approximating the K edge of iodine is desirable to increase the intensity of of x-ray absorption and photoelectric effect. This type of x-ray interaction with matter contributes to the attenuation of the x-ray beam. This will in turn improve contrast resolution in CT imaging. Huda et al. [11] reported a mean photon energy level of 60 keV at 100 kVp, leading to an increase in the attenuation level of iodine of ~27% when compared to 120 kVp. We used a 90kVp setting which increased aortic enhancement in the arterial phase by 34%, and increased enhancement in the portal vein, liver, pancreas and renal cortex in the hepatic phase by 13-15%.

Generally lower signal to noise ratio in Group 2 compared to Group 1 in the arterial phase (except aorta) and hepatic/delayed phases (except caudal vena cava) but this was not statistically significant. in the venous phase. The lower SNR despite the increase in mean attenuation indicates that the image noise objectively increased. However, this was not appreciable on the visual scoring system.

A lowered dose of iohexol (1.5ml/kg) was feasible and the mean attenuation levels met radiological requirements; vascular enhancement >250HU and liver enhancement >60HU above precontrast levels (Gbande et al, 2022). The aortic enhancement values in the arterial phase using 1.5mls/kg ranged from 245-1169HU. Liver enhancement values in the hepatic phase ranged from 158-330HU in this group. The mean attenuation values of the vascular structures in Group 4 during the

hepatic phase did not meet minimum radiological criteria (<250HU). Visual scores were highest in Groups 3 in the for the arterial phase (100% > score 2) and Group 4 for the hepatic phase (82% > score 2), compared to 63% > score 2 in the standard contrast dose group (2ml/kg). In the hepatic phase, vascular conspicuity scores was superior in Group 4 (1ml/kg) with 82% > score 2. Vascular conspicuity was worse using a 2ml/kg compared to lower doses in the arterial and hepatic phases due to excessive parenchymal enhancement (predominantly observed in the liver) leading to effacement of intraparenchymal vessels at standard window width/level settings (Figure 1). The mean attenuation of the liver in the venous phase for cats that received 2ml/kg was on average 321HU, which exceeded the average aortic enhancement (316HU) and approached the average portal vein attenuation (342HU). In comparison, cats that received 1.5ml/kg had improved differential enhancement of vessels and liver, with a mean liver attenuation of 258HU. Excessive liver enhancement was not previously observed in canine studies on multiphase CECT using the same or different contrast injection technique and scan timing (Chapter 1 and 2). The excessive liver enhancement seen with using 2mls/kg of contrast can be compensated for using CT post processing (window width) to broaden the grey scale. However, excessive enhancement can be avoided by reduced contrast dose and has the added benefit of reduced load on the kidneys, which is desirable in geriatric cats that often have degenerative nephropathy.

This variation between dogs and cats could be due to differences in liver weight as a percentage of body weight and circulating blood volume. The feline adult liver (female and male combined) has a mean percent body weight of 2.46% (Latimer, 1967). Whereas the canine adult liver has a mean percent body weight of 2.3-3.9% as evaluated in Beagle dogs aged between 8-38months of age (Latimer, 1967). Therefore, the feline adult liver is at the low end of the canine liver mean percent body weight. In dogs, the circulating blood volume is 79mls/kg compared to cats which is lower at approximately 65mls/kg (Courtice, 1943). Therefore, the contrast dose (mls/kg) required to achieve the same degree of vascular enhancement will differ between cats and dogs. Based on results on this research study, we recommend using lower contrast dose in cats (1.5ml/kg) at a lower kVp setting (90kVp) which provided adequate vascular and parenchymal enhancement, particularly in the arterial and hepatic phases. Deterioration in vascular conspicuity occurred in the delayed phase for Groups 3 (67%) and Group 4 (27%), whereas Groups 1 or 2 performed well in the delayed phase (88% and 92% respectively). Therefore, a standard contrast dose of 2ml/kg performed better in the delayed phase only. This may be suitable for slow CT scanners with long interscan delays that would require prolonged enhancement during the delayed phase. Otherwise, a lower contrast dose of 1.5ml/kg was sufficient for the arterial and hepatic phases.

In conclusion, findings from the current study support the hypothesis that reduced contrast dose improved vascular conspicuity within abdominal organs (particularly the liver) and a dose of 1.5mls/kg performed better than the standard dose in the arterial and hepatic phases. Lower radiation exposures (90kVp) improved mean CT attenuation values of contrast for the aorta in the arterial phase, and all vascular and parenchymal structures measured in the hepatic phase (except spleen) and delayed phase. The combination of lower radiation exposure and reduced contrast dose can be used in cats for multiphase CECT.

SECTION 3 – Research Chapters (1-4)

Chapter 4. Developing a protocol for CECT of the biliary tract using a novel gadolinium based contrast agent.

Veterinary patients presenting with jaundice, abdominal pain, vomiting, elevated liver parameters or abdominal effusion prompts evaluation of the hepatobiliary tract. Biliary imaging in canine and feline patients is mostly based on ultrasound with minimal use of cross-sectional modalities. In a small proportion of cases, cross sectional imaging is preferred when ultrasound cannot adequately visualise the biliary tract due to factors such as large canine body size affecting ultrasound penetration or reverberation artifacts from bowel gas or peritonitis. In terms of cross-sectional imaging, MRI has superior soft tissue resolution compared to CT and the use of fluid sensitive sequences would allow direct visualisation of the biliary tree. However, at this stage abdominal MRI remains uncommon due to limited accessibility and the need for respiratory gated technology. Non-contrast CT of the biliary tract provides limited information except for the identification of mineral calculi.

There are limited options for CECT of the biliary tract. Contrast agents that excrete into the biliary system are uncommon. The only iodinated intravenous cholangiographic agent currently available in Australia is Biliscopin (meglumine iotroxate). Early studies describing the use of iotroxate in cats for cholangiography reported side effects in 50% of cases, including vomiting, defecation and increased liver enzymes (Fujita 1994). Recent studies have reported iotroxate use in dogs and cats as a slow intravenous infusion, providing contrast enhancement of the biliary tree after 60 minutes (Hayakawa et al, 2018; Tanaka et al, 2018). At the time our research study on cholangiography, iotroxate was temporarily unavailable in Australia.

Intravenous contrast agents used for CT imaging are mostly iodine based, with the option of using gadolinium for CT under certain circumstances (Schwarz and Saunders, 2011). Gadoxetic acid is a gadolinium based intravenous contrast agent (also known as gadoxetate disodium). It undergoes approximately 50% excretion through the hepatobiliary system after administration, with sufficient accumulation in the biliary tract 20 minutes after injection to allow for robust imaging (Lee et al, 2009). Results of preclinical safety trials in healthy dogs and a clinical trial involving diseased dogs indicate no clinically relevant adverse effects. We explore the feasibility of using gadoxetic acid as a novel contrast agent in dogs and cats for CT cholangiography.

Use of gadoxetic acid for computed tomographic cholangiography in healthy dogs

Jennifer Chau BVSc
Juan M. Podadera Dr Med Vet
Alex C. Young BVSc
Mariano A. Makara Dr Med Vet

Received April 27, 2016.
Accepted September 19, 2016.

From the Faculty of Veterinary Science, University of Sydney, Sydney, NSW 2006, Australia.

Address correspondence to Dr. Chau (jennifer.chau@sydney.edu.au).

OBJECTIVE
To evaluate the effect of gadoxetic acid (contrast) dose on biliary tract enhancement, determine the optimal time after contrast injection for CT image acquisition, and assess the feasibility of CT cholangiography in sedated dogs.

ANIMALS
8 healthy dogs.

PROCEDURES
The study had 2 parts. In part 1, 4 dogs were anesthetized and underwent CT cholangiography twice. Gadoxetic acid was administered IV at a low dose (0.025 mmol/kg) for the first procedure and high dose (0.3 mmol/kg) for the second procedure. Serial CT scans were obtained at predetermined times after contrast injection. In part 2, 4 dogs were sedated and underwent CT angiography 85 minutes after IV administration of the high contrast dose. Contrast enhancement of the biliary tract on all scans was objectively assessed by measurement of CT attenuation and qualitatively assessed by use of a subjective 4-point scoring system by 3 independent reviewers. All measurements were compared over time and between contrast doses for the dogs of part 1. Subjective measurements were compared between the sedated dogs of part 2 and anesthetized dogs of part 1.

RESULTS
Enhancement of the biliary tract was positively associated with contrast dose and time after contrast injection. Optimal enhancement was achieved 65 minutes after contrast injection. Subjective visualization of most biliary structures did not differ significantly between sedated and anesthetized dogs.

CONCLUSIONS AND CLINICAL RELEVANCE
Results indicated CT cholangiography with gadoxetic acid was feasible in sedated dogs. The high contrast dose provided better visualization of biliary structures than the low dose; CT scans should be obtained 65 minutes after contrast injection. (*Am J Vet Res* 2017;78:828–839)

Cholangiography is an important imaging technique for evaluating the integrity and patency of the biliary tract in patients with various disease processes. The integrity of the biliary tract may be compromised in patients with abdominal trauma; however, the clinical signs of such can be insidious at onset, and the acute stage may be masked by other concurrent problems such as fractures or abdominal hemorrhage.[1] Bile duct leakage is the most common and serious complication secondary to cholecystectomy in human patients.[2] The prognosis for patients with bile-induced peritonitis is often guarded, and careful radiologic assessment early in the course of the disease is recommended.[1] The patency of the biliary tract should also be evaluated in patients with icterus, abdominal pain, and vomiting. Ultrasonography is a sensitive imaging tool for the diagnosis of extrahepatic biliary obstruction in cats and is specific for the diagnosis of calculi-induced bile duct obstruction; however, it cannot accurately differentiate between bile duct obstructions caused by inflammatory disease and neoplasia.[3] The presence of ductal dilation alone may not correlate with obstructive disease in patients that have recovered from a previous obstructive episode, and ductal dilation may be absent in patients with cirrhosis.[4] Patients with liver or pancreatic masses can suffer from secondary obstruction or abnormalities of the biliary tract and may benefit from presurgical evaluation of biliary structures.

Several techniques for cholangiography have been described but are not commonly used because of various limitations.[5–8] Magnetic resonance cholangiopancreatography with fast acquisition and high-resolution sequencing has been described in cats and provides consistent visualization of the bile ducts.[8] Unfortunately, that technique requires a high-field magnet that is not widely available in veterinary medicine, and acquisition of the MRI sequences requires

ABBREVIATIONS

HU	Hounsfield units
ROI	Region of interest

suspending ventilation for up to 2 minutes, which is not feasible in all patients.[9] Endoscopic retrograde cholangiopancreatography has been described in dogs and cats, but its success is dependent on operator experience, and the procedure is technically difficult in dogs < 10 kg and cats because the small diameter of the duodenum in those animals limits maneuverability of the endoscope.[10–12] Cholangiography following oral, percutaneous, or IV administration of iodinated contrast medium has been experimentally performed in dogs and cats, but various problems associated with efficacy and adverse effects of the contrast medium have been reported.[1,6,7,12–14,a] Oral administration of cholangiographic media such as ipodate calcium and ipodate sodium allowed radiographic visualization of the gallbladder but failed to result in opacification of the intrahepatic bile ducts and provided only variable enhancement of the extrahepatic bile ducts.[6,7] Radiographic evaluation of the ductal system following oral administration of cholangiographic medium is also inhibited by superimposition of contrast medium retained in the bowel. Additionally, the optimal time for the acquisition of radiographs following oral administration of cholangiographic medium is 12 to 14 hours,[6,7] which is less than ideal for patients with biliary disease that require laparotomy. Percutaneous injection of iodinated contrast medium into the gallbladder occasionally results in leakage of medium from the injection site into the peritoneal cavity.[13,14] Intravenous injection of an iodinated contrast medium such as iodipamide in dogs and cats has yielded variable results. In 1 study,[1] IV administration of iodinated contrast medium to dogs resulted in no enhancement of the biliary tract on radiographs obtained 3 hours after injection. In other radiographic studies,[6,14] IV administration of iodinated contrast medium resulted in ill-defined enhancement of the gallbladder, and the extrahepatic biliary passages, including the common bile duct, were not always visible. However, in another study,[a] IV administration of iodipamide and use of CT provided adequate visualization of the biliary tract. Frequently reported adverse effects associated with IV administration of iodinated contrast media include licking, vomiting, defecation, and abnormally increased liver enzyme activities.[7,15]

A newer hepatobiliary-specific contrast agent, gadoxetic acid (also known as gadoxetate disodium) undergoes approximately 50% excretion through the hepatobiliary system after IV administration, with sufficient accumulation in the biliary tract 20 minutes after injection to allow for robust imaging.[2] Results of preclinical safety trials[16,17] in healthy dogs and a clinical trial[18] involving diseased dogs indicate no clinically relevant adverse effects associated with IV administration of gadoxetic acid. Gadolinium in gadoxetic acid has paramagnetic properties that make it widely useful for hepatobiliary MRI in human patients. Gadolinium is also an effective absorber of x-rays because of its high atomic number (64), and its k-edge value approximates x-ray energies used in clinical tube currents. The CT attenuation of gadolinium is 40% higher than that of iodine, and results of experimental studies[19–21] indicate that gadolinium contrast medium can be visualized in the liver and biliary tract on CT images, although the gallbladder was only partially filled with the contrast medium.

Computed tomography is becoming widely available in private veterinary practice. As a cross-sectional imaging modality, CT allows rapid acquisition of high-resolution, thin-slice topographic images of the body that overcome superimposition artifact. The ability to acquire images rapidly enables the use of CT for evaluation of dogs and cats with acute thoracic and abdominal disease without the aid of anesthesia.[22,b] Therefore, we hypothesized that CT cholangiography with gadoxetic acid will provide adequate visualization of the biliary tract and is a feasible imaging technique in sedated dogs. The purpose of the study reported here was to determine the effects of dose of gadoxetic acid contrast medium, timing of image acquisition, and chemical restraint on contrast enhancement and visualization of the biliary tract in healthy dogs. An additional aim was to evaluate the effect of body position on the redistribution of contrast medium in the gallbladder. On the basis of results of other experimental studies,[19–21] we hypothesized that contrast medium would accumulate in the nondependent regions of the biliary tract.

Materials and Methods

Animals

All study procedures were reviewed and approved by the Animal Ethics Committee of the University of Sydney. The prospective clinical study was divided into 2 parts and involved healthy dogs recruited from a privately owned research colony. Each dog was determined to be healthy on the basis of its clinical history and findings of a physical examination, biochemical analysis of liver-associated variables (alkaline phosphatase and alanine transferase activities and total protein, urea, creatinine, glucose, and total bilirubin concentrations), and ultrasonographic examination of the liver and gallbladder.

Part 1

During part 1 of the study, each of 4 dogs was anesthetized on 2 separate occasions for CT cholangiography following IV administration of gadoxetic acid. Each dog was administered a low dose (0.025 mmol/kg; low-dose treatment) of gadoxetic acid contrast medium[c] for the first cholangiographic examination and a high dose (0.3 mmol/kg; high-dose treatment) of contrast for the second cholangiographic examination. The low dose was chosen on the basis of the current recommended dose of gadoxetic acid contrast medium for MRI, and the high dose was selected on the basis of the dose used in another experimental study[19] that involved dogs. The contrast was administered IV by manual injection.

Prior to each cholangiographic examination, dogs were premedicated with butorphanol tartrate[d] (0.2 mg/kg, IM). Anesthesia was induced with alfaxalone[e] (1 to 2 mg/kg, IV) via a cephalic vein. Dogs were intubated, and anesthesia was maintained with isoflurane[f] and oxygen under spontaneous ventilation. Intravenous administration of Hartmann solution[g] (5 mL/kg/h) was initiated immediately following anesthesia induction and maintained for the duration of anesthesia. Cardiopulmonary variables monitored throughout each procedure included noninvasive blood pressure, heart rate, respiratory rate, end-tidal CO_2, and oxygen saturation as measured by pulse oximetry.

All scans were performed with a 16-slice multidetector CT scanner[h] with the dogs positioned in sternal recumbency. Tube settings were standardized for all scans and included a beam collimation of 16 data channels with a detector row width of 0.75 mm (ie, 16 X 0.75 mm), a tube potential of 120 kVp, and a tube current of 90 mA. Prior to injection of the contrast during each procedure, a precontrast helical scan of the abdomen from the cranial aspect of the diaphragm to the pubis was performed. Initiation of contrast injection was defined as time 0 (baseline). Serial CT scans of the abdomen were acquired at baseline and 5, 25, 45, 65, and 85 minutes after injection of the contrast. Then each dog was repositioned into dorsal recumbency, and another postcontrast CT scan of the abdomen was performed to assess redistribution of the contrast in the gallbladder.

Part 2

Four different dogs from those used in part 1 were used for part 2. During part 2, each dog underwent CT cholangiography only once, and dogs were sedated instead of anesthetized for the procedure. Each dog was sedated with butorphanol[d] (0.2 mg/kg, IM), and a 23-gauge catheter was aseptically placed in a cephalic vein for administration of gadoxetic acid contrast medium[c] (0.3 mmol/kg, IV; high-dose treatment with sedation), after which each dog was monitored for adverse effects. Eighty-five minutes after contrast injection, each dog was administered a sedation dose of alfaxalone[e] (0.5 mg/kg, IV), and a single postcontrast CT scan of the abdomen was performed with the dog in sternal recumbency and the same tube settings used in part 1. Then each dog was repositioned into dorsal recumbency, and another postcontrast CT scan of the abdomen was performed as described for the dogs of part 1.

Image analysis

Transverse CT images were transferred to a designated DICOM workstation and reviewed with DICOM imaging software.[i] Contrast enhancement of the biliary tract was objectively assessed by measurement of CT attenuation (measured in HU) and qualitatively assessed by use of a subjective 4-point scoring system by 3 independent reviewers. For all dogs in parts 1 and 2 of the study, objective measurements were performed in all postcontrast CT scans. Briefly, a standardized 0.5-cm^2 ROI was designated in the gallbladder neck region where contrast medium preferentially accumulated, and a point of interest was marked in the common bile duct. Objective measurement of CT attenuation could not be reliably obtained for the cystic or hepatic ducts owing to their small size. Data from the ROI and point of interest were exported to a spreadsheet.[j] For the dogs of part 1 that had multiple postcontrast CT scans performed, time-attenuation curves were generated to determine the time of optimal enhancement. Contrast enhancement of the liver was also measured in a standardized 0.5-cm^2 ROI in the hepatic parenchyma that was void of blood vessels. Precontrast attenuation and mean maximum postcontrast attenuation of the liver were measured. Additionally, the diameter of the bile duct was measured on all scans for each dog of part 1, and the mean maximum diameter and duration to maximum diameter of the bile ducts following contrast injection were compared between the low-dose and high-dose treatments. All measurements were performed by 1 investigator (JC) to minimize variability.

For subjective visual assessment of the biliary tract, 3 board-certified veterinary radiologists (JMP, ACY, and MAM) independently reviewed all scans obtained 85 minutes after contrast administration from each dog (low-dose and high-dose treatments [part 1] and high-dose treatment with sedation [part 2]). All scans were anonymized and reviewed in a randomized order. Each observer was asked to identify the gallbladder and extrahepatic bile passages on the basis of information provided in 2 anatomic references.[23,24] Briefly, in those references,[23,24] the extrahepatic bile passages were defined to consist of the hepatic ducts, cystic duct, and common bile duct. The cystic duct connects the gallbladder to the point of insertion of the first or second hepatic duct. From that point on, the bile passage is called the common bile duct, which enters the duodenum at the major duodenal papilla **(Figure 1)**. The intrahepatic (interlobular and intralobular) bile passages were not assessed. Extrahepatic bile passages were distinguished from intrahepatic bile passages on the basis of their central location and fusion with the cystic or common bile duct.

Observers were asked to assign a subjective score for visualization of the gallbladder and the extrahepatic bile passages in each CT scan. The visual scoring system was on a scale of 0 to 3, where 0 = no contrast medium evident in the biliary tract, 1 = poor visualization of the biliary tract (structures have faint contrast enhancement and poorly defined margins), 2 = good visualization of the biliary tract (structures have moderate contrast enhancement; however, the structure margins are ill defined in the region of enhancement), and 3 = excellent visualization of the biliary tract (structures have strong contrast enhancement and well-defined margins in the region of enhancement; **Figure 2**).

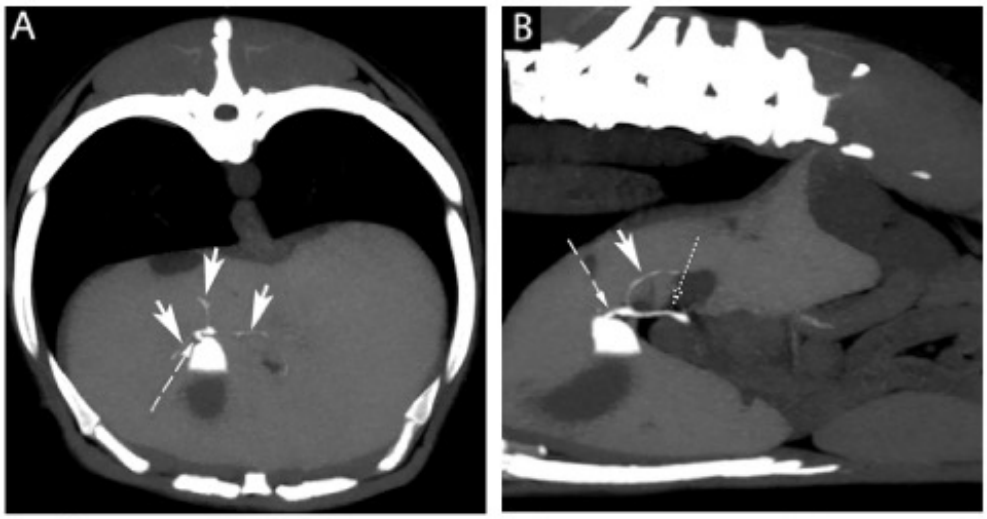

Figure 1—Representative reformatted CT cholangiographic images (maximum intensity projection, 2 to 3 mm slice thickness) obtained in the transverse (A) and sagittal (B) planes by use of a soft tissue algorithm for a healthy dog. Images were obtained 85 minutes after IV administration of gadoxetic acid contrast medium (0.3 mmol/kg; contrast) with the dog positioned in sternal recumbency. A—Contrast medium is filling the nondependent region of the gallbladder, neck of the gallbladder, cystic duct (dashed arrow), and multiple hepatic ducts (solid arrows). The cystic duct was defined as the continuation of the gallbladder neck to the first or second hepatic duct. Extrahepatic bile passages were distinguished from intrahepatic bile passages on the basis of their central location and fusion with the cystic or common bile duct. B—Contrast medium is filling the gallbladder, cystic duct (dashed arrow), a single hepatic duct (solid arrow), and common bile duct (dotted arrow). The common bile duct was defined as the continuation of the cystic duct (after joining of the first or second hepatic duct) to the duodenal papilla.

A score of 3 was assigned only when contrast was visualized along the entire length of the bile ducts. Additionally, the presence of motion artifact was recorded for each scan by use of a previously described 4-point scoring system,[22] where 0 = no motion artifact, 1 = mild motion artifact, 2 = noticeable motion artifact, and 3 = easily noticeable motion artifact. Visual scores from all 3 observers were combined and compared between the low-dose and high-dose treatments to evaluate the effect of contrast dose and between the high-dose treatments of parts 1 and 2 to evaluate the effect of anesthesia versus sedation.

Statistical analysis

All statistical analyses were performed with a commercially available statistical software program.[k] The effects of contrast dose and time after contrast injection on the magnitude of CT attenuation of the gallbladder and common bile duct were evaluated with a restricted maximum likelihood method. Subjective scores for each biliary structure (gallbladder, bile duct, cystic duct, and hepatic duct) were analyzed with an ordinal logistic regression model that included fixed effects for contrast dose (0.025 or 0.3 mmol/kg), chemical restraint used (anesthesia or sedation), and observer; all possible interactions between the fixed effects were also assessed. For all analyses, values of $P \leq 0.05$ were considered significant.

Results

Part 1

Dogs used in part 1 of the study included 2 sexually intact female Beagles and 2 sexually intact female Pug crossbreds with ages ranging from 5 to 7 years and body weights ranging from 10 to 14.5 kg. The volume of contrast administered ranged from 1.0 to 4.0 mL during the low-dose treatment and from 10 to 18 mL during the high-dose treatment. No adverse effects associated with the contrast were observed in any of the dogs immediately after injection; however, 2 dogs developed transient diarrhea during anesthesia recovery from the low-dose treatment.

Contrast dose administered (dose) and time after contrast injection (time) were significantly ($P < 0.001$ for all effects) associated with the CT attenuation in both the gallbladder and common bile duct; however, the interaction between dose and time was not significantly associated with the attenuation for either the gallbladder ($P = 0.38$) or common bile duct ($P = 0.56$). The mean attenuation of the gallbladder at 65 minutes after contrast injection was significantly greater than that at 0 (contrast injection; baseline), 5, 25, and 45 minutes after contrast injection. Although the mean maximum attenuation of the gallbladder was recorded at 85 minutes after contrast injection, the mean attenuation at 85 minutes after contrast injection did not differ significantly from that at 65 min-

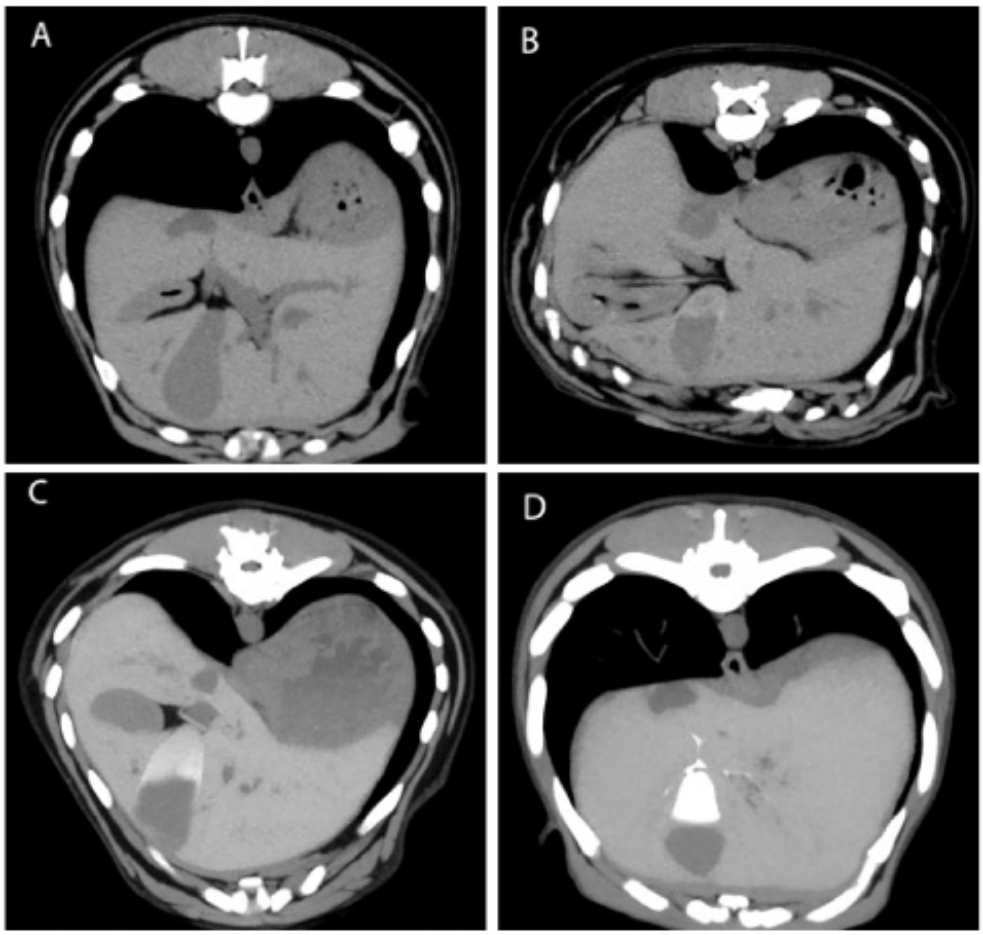

Figure 2—Representative reformatted CT cholangiographic images (maximum intensity projection, 2 to 3 mm in a soft tissue algorithm) obtained in the transverse plane for healthy dogs presented as examples of each grade of the subjective 4-point scoring system used to visually assess the biliary tract following IV administration of gadoxetic acid. A—Score 0; no contrast medium evident in the biliary tract. B—Score 1; poor visualization of the biliary tract (structures have faint contrast enhancement and poorly defined margins). C—Score 2; good visualization of the biliary tract (structures have moderate contrast enhancement; however, the structure margins are ill defined in the region of enhancement). D—Score 3; excellent visualization of the biliary tract (structures have strong contrast enhancement and well-defined margins in the region of enhancement) with complete filling of the bile ducts with contrast medium.

utes after contrast injection. The mean attenuation of the common bile duct at 45 minutes after contrast injection was significantly greater than that at 0, 5, and 25 minutes after contrast injection but did not differ significantly from the mean attenuation at 65 and 85 minutes after contrast injection. Similar to the gallbladder, the mean maximum attenuation of the common bile duct was recorded at 85 minutes after contrast injection **(Figure 3)**.

The mean maximum attenuation of both the gallbladder and common bile duct for the high-dose treatment was significantly ($P < 0.001$) greater than that for the low-dose treatment at all times after contrast injection (Figure 3).

The scores for the CT scans in part 1 (4 CT scans in the low-dose treatment and 4 CT scans in the high-dose treatment) were used to evaluate the effect of contrast dose (24 scores). The effect of chemical restraint was evaluated by comparison of visualization scores from dogs in part 1 and part 2 (4 CT scans in the high-dose treatment and 4 CT scans in high-dose treatment with sedation [24 scores]). The subjective visual scores for

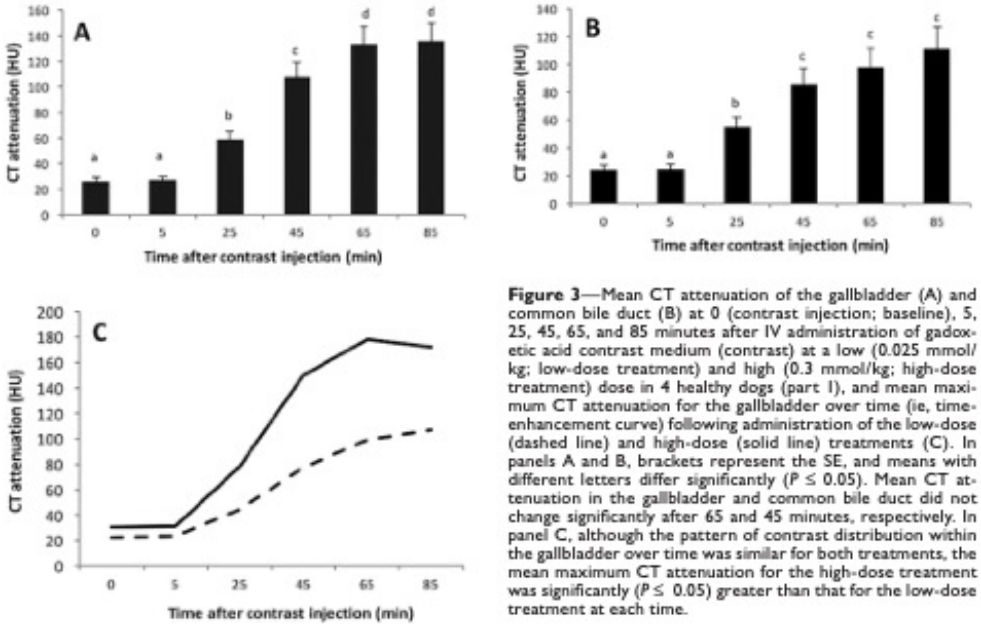

Figure 3—Mean CT attenuation of the gallbladder (A) and common bile duct (B) at 0 (contrast injection; baseline), 5, 25, 45, 65, and 85 minutes after IV administration of gadoxetic acid contrast medium (contrast) at a low (0.025 mmol/kg; low-dose treatment) and high (0.3 mmol/kg; high-dose treatment) dose in 4 healthy dogs (part 1), and mean maximum CT attenuation for the gallbladder over time (ie, time-enhancement curve) following administration of the low-dose (dashed line) and high-dose (solid line) treatments (C). In panels A and B, brackets represent the SE, and means with different letters differ significantly ($P \leq 0.05$). Mean CT attenuation in the gallbladder and common bile duct did not change significantly after 65 and 45 minutes, respectively. In panel C, although the pattern of contrast distribution within the gallbladder over time was similar for both treatments, the mean maximum CT attenuation for the high-dose treatment was significantly ($P \leq 0.05$) greater than that for the low-dose treatment at each time.

the gallbladder in the high-dose treatment were significantly ($P = 0.03$) greater than those for the low-dose treatment. The probability that the gallbladder would be assigned a subjective score of 3 was 40% for the low-dose treatment and 84% for the high-dose treatment **(Figure 4)**. In fact, scores for dogs in the high-dose treatment were 16.1 times (95% confidence interval, 1.62 to 160.3) as likely to be higher as were the scores for the dogs in the low-dose treatment.

For visualization of the common bile duct, the probability of a subjective score of 3 was only 20% for the low-dose treatment, compared with 45% for the high-dose treatment. Higher scores were 4 times as likely in the high-dose treatment, compared with scores in the low-dose treatment (95% confidence interval, 0.8 to 19.6). However, the distributions of subjective scores for the common bile duct did not differ significantly ($P = 0.122$) between the low-dose and high-dose treatments. Likewise, the subjective scores did not differ significantly between the low- and high-dose groups for the cystic duct ($P = 0.179$) and hepatic duct ($P = 0.518$). Visualization of the hepatic ducts was least reliable of all the biliary structures on CT scans. In fact, for both treatments, the probability of no contrast enhancement of the hepatic ducts (subjective score of 0) was up to 43%.

Following contrast injection, the duration required to achieve maximum duct diameter (time to maximum diameter) was similar between the low-dose and high-dose treatments. The time to maximum diameter was 45 minutes for the cystic duct and 25 minutes for the hepatic ducts regardless of contrast dose. For the common bile duct, the time to maximum diameter was 65 minutes for the low-dose treatment and 25 minutes for the high-dose treatment. The mean maximum diameters of the cystic duct (2.1 mm for the low-dose treatment and 2.2 mm for the high-dose treatment), common bile duct (2.3 mm for both treatments), and hepatic duct (1.3 mm for both treatments) did not differ significantly between the low-dose and high-dose treatments.

The mean ± SD maximum liver attenuation was 76 ± 5.8 HU for the low-dose treatment and 109 ± 7.7 HU for the high-dose treatment. The mean ± SD difference between baseline and maximum liver attenuation was 5 ± 3 HU for the low-dose treatment and 37 ± 9 HU for the high-dose treatment.

Part 2

Dogs used for part 2 (high-dose treatment with sedation) of the study included a spayed female Jack Russell Terrier, spayed female Maltese crossbred, neutered male German Shepherd Dog, and spayed female Kelpie crossbred with ages ranging from 2 to 9 years and body weights ranging from 3.4 to 18.4 kg. The volume of contrast administered ranged from 4 to 22 mL, and injection of the contrast was not associated with any signs of irritation or adverse effects in the sedated dogs. One dog developed transient and self-limiting diarrhea following contrast administration.

The motion artifact scores did not differ significantly ($P = 0.358$) between sedated (part 2) and anes-

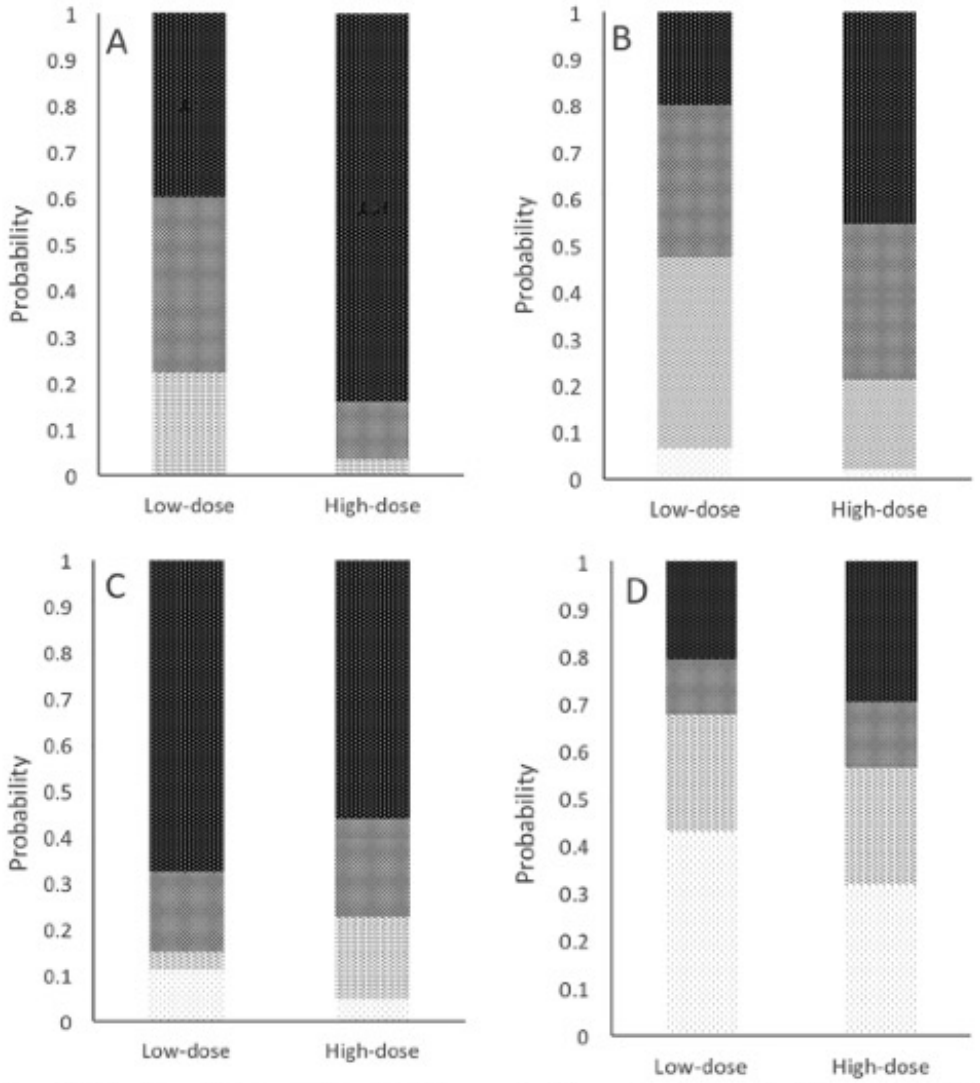

Figure 4—Cumulative probability of subjective visualization scores (0 = light gray, 1 = medium gray, 2 = dark gray, 3 = black) for the gallbladder (A), common bile duct (B), cystic duct (C), and hepatic duct (D) independently assigned by each of 3 radiologists to CT cholangiographic scans obtained for the dogs of Figure 3 at 85 minutes following administration of the low-dose and high-dose treatments. After dogs were given the high dose, the cumulative probability of receiving a score of 3 for the gallbladder and common bile duct doubled in comparison with the probability after they were given the low dose. The cumulative probability of each score was similar for the cystic duct and hepatic duct between treatment groups. ***See*** Figures 2 and 3 for remainder of key.

thetized (high-dose treatment of part 1) dogs. Likewise, the distributions of the subjective scores for visualization of the gallbladder ($P = 0.07$), common bile duct ($P = 0.18$), and hepatic duct ($P = 0.25$) did not differ significantly between sedated and anesthetized dogs. When the interaction between observer and chemical restraint was included in the model, the subjective scores for visualization of the cystic duct differed significantly ($P = 0.04$) between sedated and anesthetized dogs. However, the fixed effect for

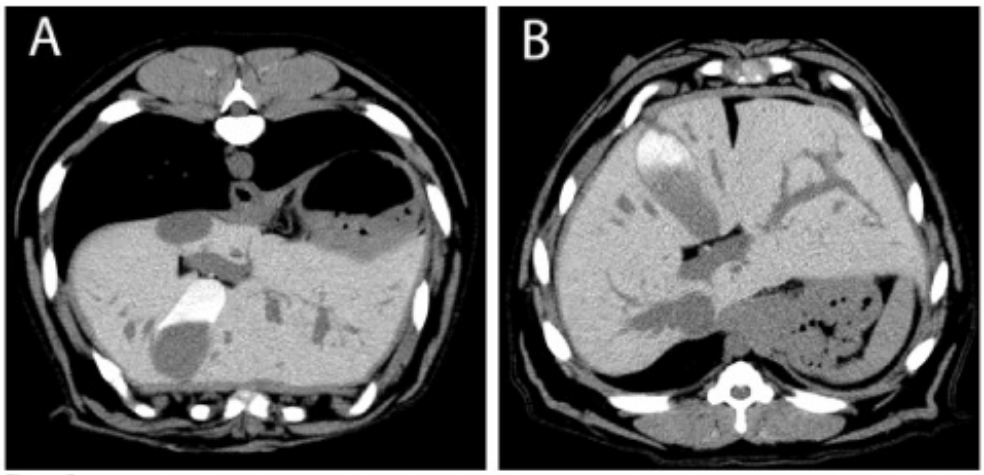

Figure 5—Representative CT cholangiographic images obtained in a transverse plane with a soft tissue algorithm for a sedated dog 85 minutes after IV administration of gadoxetic acid (0.3 mmol/kg; part 2) when it was positioned in sternal (A) and dorsal (B) recumbency. Notice that changing the position of the dog resulted in redistribution of the gadoxetic acid (contrast) to the nondependent region of the gallbladder.

chemical restraint was not significant ($P = 0.08$) in that model, which suggested that there was significant interobserver variability in the subjective scores for the cystic duct when sedated and anesthetized dogs were compared. When dogs were repositioned from sternal to dorsal recumbency, the contrast redistributed to the nondependent region of the gallbladder in all dogs **(Figure 5)**.

Discussion

To our knowledge, the present study was the first to describe the use of gadoxetic acid contrast medium for CT cholangiography in any veterinary species. The objectives of this study were to evaluate the effect of contrast dose on biliary tract enhancement, determine the optimal time after contrast injection for CT image acquisition, and assess the feasibility of CT cholangiography in sedated dogs. Results indicated that the duration between contrast injection and biliary tract enhancement was fairly uniform for the study dogs regardless of the dose of contrast administered. For all 4 dogs of part 1, CT attenuation (contrast enhancement) of the biliary tract was significantly increased from precontrast (baseline) attenuation beginning 25 minutes after contrast injection. For most dogs, although maximum attenuation for individual biliary tract structures was recorded for the last scan that was obtained 85 minutes after contrast injection, the magnitude of attenuation for the gallbladder did not differ significantly between scans obtained 65 and 85 minutes after contrast injection, and the magnitude of attenuation for the common bile duct did not differ significantly among scans obtained 45, 65, and 85 minutes after contrast injection. This was most likely because 90% of maximum contrast enhancement in the gallbladder was achieved by 65 minutes after contrast injection and approximately 80% of maximum contrast enhancement in the common bile duct was achieved by 45 minutes after contrast injection. Consequently, the time-enhancement curve for gadoxetic acid in the biliary tract was characterized by a gradual increase in attenuation followed by a plateau at maximum attenuation, which is advantageous in a clinical setting because it offers a wide temporal window for obtaining CT scans after contrast administration. Given that the maximum attenuation for both the gallbladder and common bile duct plateaued at 65 minutes after contrast injection, we recommend delaying CT image acquisition for at least 65 minutes after contrast injection to allow for optimal biliary enhancement.

In part 1 of the present study, contrast dose was significantly associated with biliary tract enhancement, and use of the high-dose treatment (0.3 mmol of contrast/kg) resulted in significantly greater enhancement of the biliary tract than use of the low-dose treatment (0.025 mmol of contrast/kg). As the dose of contrast administered increases, the amount of gadoxetic acid available for hepatic uptake also increases, as does the amount of gadoxetic acid that is subsequently excreted unchanged into bile. Gadoxetic acid is selectively absorbed by hepatocyte anion polypeptides and excreted into bile canaliculi via ATP-dependent multidrug resistance–associated protein 2.[25] Saturation of those hepatocyte and biliary transport proteins may explain the characteristic plateau observed at maximum contrast enhance-

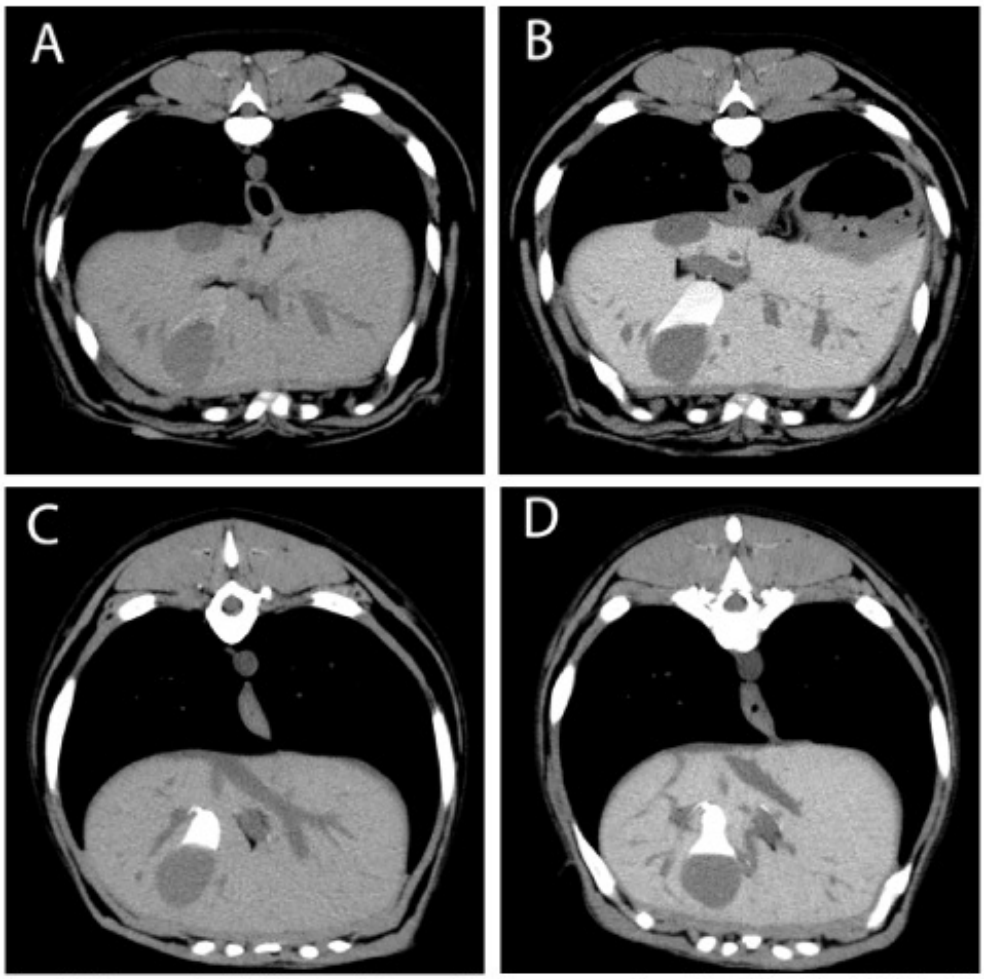

Figure 6—Representative CT cholangiographic images obtained in a transverse plane with a soft tissue algorithm for 2 of the 4 dogs described in Figure 3 following administration of the low-dose (A and C) and high-dose (B and D) treatments presented as an example of how enhancement and visualization of the biliary tract (as determined by independent review of CT scans by 3 board-certified veterinary radiologists and use of the subjective 4-point scoring system described in Figure 2) varied among dogs despite administration of the same contrast dose. One dog was assigned a subjective visualization score of 1 or 2 when administered the low-dose treatment (A) and 2 or 3 when administered the high-dose treatment (B). The other dog was assigned a subjective visualization score of 3 following administration of both the low-dose (C) and high-dose (D) treatments. ***See*** Figures 2 and 3 for remainder of key.

ment. The magnitude of contrast enhancement varied among dogs that received the same contrast dose **(Figure 6)**. Some dogs that had poor enhancement of the biliary tract when given the low-dose treatment had improved enhancement of the biliary tract when administered the high-dose treatment, but the magnitude of that enhancement remained fairly low, compared with that for the other study dogs. Other dogs had strong contrast enhancement of the biliary tract even when administered the low-dose treatment. That finding suggested that the number and type of hepatocyte and biliary transport proteins varies among dogs, and those inherent differences can affect total biliary excretion and the magnitude of contrast enhancement.[21,25] Hepatocytes also have other types of multidrug resistance–associated protein receptors that facilitate bidirectional transport, which may result in reflux of gadoxetic acid back into

the hepatic sinusoids and a decrease in excretion of contrast into the biliary tract. Other factors that can delay biliary excretion of contrast in clinical patients include hepatic dysfunction or biliary obstruction.[2,26] In human patients, following contrast injection for cholangiography, imaging is repeated until the contrast agent appears in the biliary tree or, for patients with high-grade biliary obstruction or hepatic dysfunction, no contrast excretion into the biliary tract is observed.[26]

When the dogs of part 1 were administered the high-dose treatment, contrast enhancement of the gallbladder, common bile duct, and cystic duct was considered moderate to excellent (subjective score ≥ 2) approximately 80% of the time, although the subjective scores for the gallbladder were generally greater than those for the other biliary structures. That was an expected finding because the properties of gadoxetic acid enable efficient absorption of x-rays. Results of another experimental study[19] involving phantoms containing either gadolinium or another contrast medium such as iodine indicate that x-ray attenuation was 40% better for gadolinium, compared with the other contrast agents at clinical x-ray currents (120 kVp). The k-edge of gadolinium (50 keV) is greater than that of iodine (33 keV); therefore, as a result of photoelectric effect, x-rays undergo k-edge interactions with gadolinium more readily than with iodine. This is a fundamental radiologic principle for consideration in the selection of contrast agents for maximum resolution. In clinical patients with conditions such as biliary rupture for which cholangiography may be indicated, peritoneal detail is often poor, and contrast resolution for assessment of biliary tract integrity is imperative for maximizing diagnostic sensitivity.

The subjective visualization scores for the hepatic duct indicated that the probability of no contrast enhancement of the hepatic ducts (subjective score 0) was 43% and that increasing the contrast dose did not improve visualization of the hepatic ducts. This finding reflects a limitation of the use of gadoxetic acid for CT cholangiography. Hepatic ducts are difficult to visualize because of their small size and border effacement with adjacent liver lobes. The mean maximum diameter of the hepatic duct was only 1.3 mm for both the low-dose and high-dose treatments of part 1. Moreover, compared with baseline, attenuation of the liver parenchyma was diffusely increased following contrast injection, particularly with the high-dose treatment. The mean maximum attenuation of the liver was 76 and 109 HU for the low-dose and high-dose treatments, respectively, which may have contributed to poor visualization of the hepatic ducts owing to border effacement.

The subjective visualization scores and artifact scores for the gallbladder, common bile duct, and hepatic ducts did not differ between sedated and anesthetized dogs in the present study. Additionally, contrast injection was well tolerated by sedated dogs. Therefore, CT cholangiography with gadoxetic acid is a feasible technique for use in sedated dogs. The ability to perform CT cholangiography in dogs without anesthesia reduces client costs and avoids the risks associated with anesthesia for patients. In clinical settings, CT cholangiography may be indicated for patients with acute abdominal trauma, jaundice, or other extensive disease localized to the cranial portion of the abdomen that requires surgical planning. Such patients are often systemically compromised and less-than-ideal candidates for anesthesia. However, further research is necessary to assess the use of CT cholangiography with gadoxetic acid in clinically diseased animals.

In the present study, there was significant interobserver variability in the subjective scores for the cystic duct between sedated and anesthetized dogs. That finding was likely a reflection of the inherent difficulty associated with isolation of the cystic duct from the surrounding structures in the hilar region. The cystic duct is short and tortuous, which makes its visualization challenging, even with CT reformatting. Thus, interobserver variability is not unexpected, and a small amount of motion artifact can substantially affect visualization of the cystic duct. Regardless, despite interobserver variability, most of the subjective scores for visualization of the cystic duct were ≥ 2 (ie, moderate to excellent visualization).

When the dogs of the present study were repositioned from sternal recumbency to dorsal recumbency, the contrast redistributed to the nondependent region of the gallbladder. This was because the physical density of gadoxetic acid (1.08 g/mL) is less than that of bile (1.2 g/mL).[27] Given that the gallbladder was only partially filled with contrast in the dogs of the present study, changing the position of patients between serial CT scans may be beneficial for assessment of gallbladder wall integrity when clinically warranted.

Transient diarrhea was observed in 3 dogs of the present study. It is unlikely that the diarrhea in those dogs was an adverse effect of gadoxetic acid because diarrhea was not associated with gadoxetic acid administration in dogs involved in preclinical safety trials.[16,17] Other possible causes of the transient diarrhea observed in the dogs of this study include changes in husbandry and diet, sedation, and anesthesia.

Various types of contrast media have been used for cholangiography with variable success. In the present study, we evaluated IV administration of a new hepatobiliary-specific contrast medium containing gadoxetic acid for CT cholangiography in anesthetized and sedated dogs. Other types of IV contrast agents used for cholangiography in dogs and cats include iodipamide and iotroxate.[1,6,7,14,a] Historically, radiography was the imaging modality most frequently used for cholangiography; however, CT is being used more frequently as that technology becomes more widely available. The

use of radiography with iodipamide to perform cholangiography resulted in consistent contrast enhancement and visualization of the gallbladder but not the extrahepatic ducts.[6] Conversely, iodipamide did allow visualization of all extrahepatic biliary tract structures when cholangiography was performed with CT instead of radiography.[a] In that study,[a] the dogs were anesthetized, and no adverse effects associated with administration of the contrast medium were reported. However, in cats, IV administration of iodipamide or iotroxate consistently results in immediate adverse effects such as vomiting, diarrhea, and restlessness.[7,15] Immediate adverse effects were not observed following gadoxetic acid administration to the dogs of the present study, and results of preclinical safety trials[16,17] in dogs indicate that gadoxetic acid has a wide safety range. Other biliary-specific contrast agents investigated include ipodate calcium and ipodate sodium[6,7]; however those agents can only be administered orally. Although adverse effects have not been reported following oral administration of ipodate calcium or ipodate sodium, disadvantages associated with the use of those agents include a long delay (10 to 13 hours) between contrast administration and enhancement, variable enhancement of the extrahepatic biliary ducts, and artifacts from the presence of contrast in the bowel.[6,7]

A limitation of the present study was that serial CT scans were performed up to only 85 minutes after contrast injection, which was not sufficient for identification of the point of decline in the time-enhancement curve. It is uncertain whether the maximum enhancement values obtained in this study represent the true maximum values; however, results of another experimental study[19] indicate that liver attenuation did not progressively increase on CT scans of dogs at 160 or 200 minutes after administration of gadoxetic acid. Moreover, the elimination half-life of gadoxetic acid is 60 minutes; therefore, it was considered unlikely that any significant increase in biliary enhancement would develop beyond the last measurement at 85 minutes after contrast injection. We chose to not obtain any CT scans > 85 minutes after contrast injection to avoid prolonged anesthesia for the dogs of part 1.

The high dose (0.3 mmol/kg) of gadoxetic acid contrast medium used in the present study was well below the upper dose limit that is safe for dogs.[17] Given that there was a significant association between dose and biliary tract enhancement, it is likely that increasing the dose of gadoxetic acid administered would further increase visualization of the biliary tract. Higher doses of gadoxetic acid contrast medium were not evaluated in this study because the volume that would be required for medium-size and large dogs at those doses would be cost prohibitive for clinical use.

The use of IV administration of gadoxetic acid for CT cholangiography in clinical patients with bile-induced peritonitis warrants further research. The effect of induced gallbladder emptying (eg, administration of cholecystokinin or feeding the patient a meal) after contrast injection on bile duct enhancement and visualization of the duodenal papilla also merits additional investigation.

Results of the present study indicated that CT cholangiography following IV administration of a high dose (0.3 mmol/kg) of gadoxetic acid to healthy dogs provided adequate enhancement and visualization of the biliary tract and is a feasible imaging technique for use in sedated dogs. Contrast enhancement of the biliary tract was significantly associated with contrast dose and time after contrast injection. Enhancement and visualization of the biliary tract increased as contrast dose increased, and our results suggested that CT scans should be obtained at 65 minutes after contrast injection to allow for adequate enhancement of the biliary tract. No adverse effects were observed when the contrast was administered to sedated dogs, and visualization of all biliary tract structures except the cystic duct did not differ significantly between sedated and anesthetized dogs, which indicated that anesthesia was not necessary for the procedure. Use of this technique in dogs with clinical disease warrants further investigation, particularly in dogs with bile-induced peritonitis or in those that are likely surgical candidates with masses in the cranial aspect of the abdomen in close proximity to the bile ducts.

Acknowledgments

Presented at the Radiology Chapter of the Australian and New Zealand Science Week Conference, Gold Coast, QLD, Australia, July 2016.

The authors thank Dr. Alastair Mair, Dr. Evelyn Hall, and Helen Laurendet for technical assistance.

Footnotes

a. Miller JW, Brinkman-Ferguson EL, Mackin AJ, et al. Cholangiography using 64 multidetector computed tomography in normal dogs (abstr). *Vet Radiol Ultrasound* 2013;54:683.
b. de Oliveira CR. *Computed tomography of cats without general anesthesia: feasibility, protocol development and assessment of cats with thoracic disease.* MS thesis, Department of Veterinary Clinical Medicine, College of Veterinary Medicine, University of Illinois, Urbana, Ill, 2011.
c. Primovist, Bayer Australia Ltd, Pymble, NSW, Australia.
d. Butorgesic, Troy Laboratories Pty Ltd, Smithfield, NSW, Australia.
e. Alfaxan, Jurox Pty Ltd, Rutherford, NSW, Australia.
f. Isoflo, Abbott Australasia Pty Ltd, Botany, NSW, Australia.
g. Baxter Healthcare Pty Ltd, Toongabbie, NSW, Australia.
h. BrillianceTM 16-slice CT scanner, version 2.3, Phillips Medical Systems, Eindhoven, The Netherlands.
i. OsiriX, version 4.1.2, Pixmea, Geneva, Switzerland.
j. Excel for Mac, version 15.17, Microsoft Corp, Redmond, Wash.
k. Genstat, Discovery 3 Edition 2007, VSNi, Hemel Hempstead, Hertfordshire, England.

References

1. Suter PF, Olsson SE. The diagnosis of injuries to the intestines, gallbladder and bile ducts in the dog. *J Small Anim Pract* 1970;11:575–584.

2. Lee NK, Kim S, Lee JW, et al. Biliary MR imaging with Gd-EOB-DTPA and its clinical applications. *Radiographics* 2009;29:1707–1724.
3. Gaillot HA, Penninck DG, Webster CR, et al. Ultrasonographic features of extrahepatic biliary obstruction in 30 cats. *Vet Radiol Ultrasound* 2007;48:439–447.
4. Finn ST, Park RD, Twedt DC, et al. Ultrasonographic assessment of sincalide-induced canine gallbladder emptying: an aid to the diagnosis of biliary obstruction. *Vet Radiol Ultrasound* 1991;32:269–276.
5. Gaschen L. Update on hepatobiliary imaging. *Vet Clin North Am Small Anim Pract* 2009;39:439–467.
6. Allan GS, Dixon RT. Cholecystography in the dog: the choice of contrast media and optimum dose rates. *Vet Radiol Ultrasound* 1975;16:98–104.
7. Carlisle CH. A comparison of techniques for cholecystography in the cat. *Vet Radiol Ultrasound* 1977;18:173–176.
8. Marolf AJ, Stewart JA, Dunphy TR, et al. Hepatic and pancreaticobiliary MRI and MR cholangiopancreatography with and without secretin stimulation in normal cats. *Vet Radiol Ultrasound* 2011;52:415–421.
9. Marolf AJ, Kraft SL, Dunphy TR, et al. Magnetic resonance (MR) imaging and MR cholangiopancreatography findings in cats with cholangitis and pancreatitis. *J Feline Med Surg* 2013;15:285–294.
10. Spillmann T, Happonen I, Kähkönen T, et al. Endoscopic retrograde cholangio-pancreatography in healthy Beagles. *Vet Radiol Ultrasound* 2005;46:97–104.
11. Spillmann T, Schnell-Kretschmer H, Dick M, et al. Endoscopic retrograde cholangio-pancreatography in dogs with chronic gastrointestinal problems. *Vet Radiol Ultrasound* 2005;46:293–299.
12. Spillmann T, Willard MD, Ruhnke I, et al. Feasibility of endoscopic retrograde cholangiopancreatography in healthy cats. *Vet Radiol Ultrasound* 2013;55:85–91.
13. Wrigley RH, Reuter RE. Percutaneous cholecystography in normal dogs. *Vet Radiol Ultrasound* 1982;23:239–242.
14. Maiti SK, Ajith P, Dutta A, et al. Laparoscopic-assisted cholecystocentesis and cholecystocholangiography in canines. *J Appl Anim Res* 2011;39:29–32.
15. Fujita M, Orima H. Effect and safety of meglumine iotroxate for cholangiocystography in normal cats. *Vet Radiol Ultrasound* 1994;35:79–82.
16. Marks AL, Hecht S, Stokes JE, et al. Effects of gadoxetate disodium (Eovist) contrast on magnetic resonance imaging characteristics of the liver in clinically healthy dogs. *Vet Radiol Ultrasound* 2013;55:286–291.
17. Döhr O, Hofmeister R, Treher M, et al. Preclinical safety evaluation of Gd-EOB-DTPA (Primovist). *Invest Radiol* 2007;42:830–841.
18. Yonetomi D, Kadosawa T, Miyoshi K, et al. Contrast agent Gd-EOB-DTPA (EOB-Primovist) for low-field magnetic resonance imaging of canine focal liver lesions. *Vet Radiol Ultrasound* 2012;53:371–380.
19. Schmitz SA, Wagner S, Schuhmann-Giampieri G, et al. A prototype liver-specific contrast medium for CT: preclinical evaluation of gadoxetic acid disodium, or Gd-EOB-DTPA. *Radiology* 1997;202:407–412.
20. Schmitz SA, Häberle JH, Balzer T, et al. Detection of focal liver lesions: CT of the hepatobiliary system with gadoxetic acid disodium, or Gd-EOB-DTPA. *Radiology* 1997;202:399–405.
21. Schmitz SA, Wagner S, Schuhmann-Giampieri G, et al. Gd-EOB-DTPA and Yb-EOB-DTPA: two prototypic contrast media for CT detection of liver lesions in dogs. *Radiology* 1997;205:361–366.
22. Shanaman MM, Hartman SK, O'Brien RT. Feasibility for using dual-phase contrast-enhanced multi-detector helical computed tomography to evaluate awake and sedated dogs with acute abdominal signs. *Vet Radiol Ultrasound* 2012;53:605–612.
23. Evans HE, de Lahunta A. Bile and gallbladder. In: *Miller's anatomy of the dog*. 4th ed. St Louis: Elsevier Saunders, 2013;331–332.
24. d'Anjou MA. Liver. In: Penninck DA, d'Anjou MA, eds. *Atlas of small animal ultrasonography*. Ames, Iowa: Blackwell Publishing, 2008;217–262.
25. Van Beers BE, Pastor CM, Hussain HK. Primovist, Eovist: what to expect? *J Hepatol* 2012;57:421–429.
26. Seale MK, Catalano OA, Saini S, et al. Hepatobiliary-specific MR contrast agents: role in imaging the liver and biliary tree. *Radiographics* 2009;29:1725–1748.
27. Cabral DJ, Small DM. Physical chemistry of bile. *Comprr Physiol* 2011;suppl 18:621–662.

Hepatic computed tomography and cholangiography by use of gadoxetic acid in healthy cats

Joanna L. Pilton BVSc
Jennifer Chau BVSc
Timothy S. Foo BVMS
Evelyn J. Hall BSc(Agr), PhD
Fernando Martinez-Taboada LV
Juan M. Podadera Dr Med Vet
Mariano A. Makara Dr Med Vet

Received June 4, 2018.
Accepted September 4, 2018.

From the Units of Diagnostic Imaging (Pilton, Chau, Foo, Podadera, Makara) and Anaesthesia (Martinez-Taboada), School of Veterinary Science, Faculty of Science, and School of Life and Environmental Sciences (Hall), Faculty of Science, University of Sydney, Sydney, NSW 2006, Australia.

Address correspondence to Dr. Pilton (joanna.pilton@sydney.edu.au).

OBJECTIVE
To evaluate 3 doses of gadoxetic acid (Gd-EOB-DPTA) for hepatic CT and cholangiography in cats and to determine optimal timing for hepatobiliary image acquisition and evaluation of the contrast-enhanced hepatobiliary anatomy.

ANIMALS
6 healthy cats.

PROCEDURES
Cats were anesthetized; sequential CT scans were performed 0, 5, 25, 45, 65, and 85 minutes after IV administration of Gd-EOB-DTPA at low (0.0125 mmol/kg), medium (0.1 mmol/kg), and high (0.3 mmol/kg) doses. Hepatobiliary enhancement for each dose was objectively assessed over time and by use of a subjective semiquantitative visual assessment score.

RESULTS
No contrast-related adverse effects were detected. Each increase in dose of contrast medium resulted in a significant increase in HU across the hepatobilliary system. The liver had a significantly higher number of HU at 45 minutes, with homogenous enhancement at all doses of contrast medium. Contrast-enhanced cystic and bile duct HU were significantly higher and maximal at 65 minutes. Contrast-enhanced gallbladder HU did not plateau by 85 minutes. At a high dose of contrast medium, 12 of 60 (20%) biliary tract scores indicated no enhancement, 34 (57%) indicated poor enhancement, and 14 (23%) indicated moderate enhancement. No cat had excellent enhancement of the biliary tract at any dose.

CONCLUSIONS AND CLINICAL RELEVANCE
Gd-EOB-DTPA–enhanced hepatic CT and cholangiography in cats were safely performed and provided good hepatic enhancement but poor to moderate enhancement of the biliary tract. This technique may be useful for assessing the liver parenchyma in cats, but its value for assessing the biliary tract is questionable. (*Am J Vet Res* 2019;80:385–395)

Hepatobiliary disease is common in cats because of their unique anatomy in which the bile duct and pancreatic duct frequently open concomitantly onto the major duodenal papilla.[1–4] Inflammatory hepatobiliary disease (cholangitis or cholangiohepatitis) is commonly centered on the biliary tract with possible secondary involvement of the hepatic parenchyma.[5,6] It can be evident as neutrophilic, lymphocytic, or chronic cholangitis (associated with liver flukes), with neutrophilic cholangitis often occurring with concurrent pathological conditions such as pancreatitis and inflammatory bowel disease.[7,8] Other pathological conditions of the intrahepatic hepatobiliary system include hepatic lipidosis, primary or metastatic neoplasia, and hepatic cirrhosis.[2,9] Additionally, extrahepatic hepatobiliary pathological conditions including gallbladder mucocele; congenital malformations such as choledochal cysts; disorders of the sphincter of Oddi; and extrahepatic biliary obstruction caused by stricture, malformations, parasites, choledocholiths or sludge, foreign bodies, pancreatitis, abscesses, or nonhepatobiliary neoplasia have also been described.[2,10–16] Regardless of the underlying cause of hepatobiliary disease, cats often have nonspecific clinical signs and biochemical changes that do not reflect the prognosis or functional reserve of the hepatobiliary system.[16–18]

A number of imaging modalities including ultrasonography, radiography, cholecystography, cholangiography, CT, ERCP, MRI, MRCP, and nuclear scintigraphy have been used to evaluate the hepatobiliary system in cats.[2,16–30] These techniques provide information on gross morphological or functional abnormalities of the liver and biliary tract, although findings are generally not disease specific. Other limitations of these techniques include poor sensitivity,

ABBREVIATIONS

ERCP	Endoscopic retrograde cholangiopancreatography
Gd-EOB-DTPA	Gadoxetic acid
MRCP	Magnetic resonance cholangiopancreatography
ROI	Region of interest

reliance on good patient compliance or operator skill (or both), poor visibility of anatomic structures owing to interference from bowel gas, high costs, limited availability, invasiveness, the need for patients to be anesthetized, and a lack of inherent contrast resolution.[1,19,24,26,29] In addition, there are various adverse effects after IV administration of iodinated cholangiographic contrast agents in cats.[21]

The criterion-referenced standard for evaluation of the biliary tract in human medicine is endoscopic retrograde cholangiography, which allows for delineation of the biliary tract with high spatial resolution.[31] The advantage of endoscopic retrograde cholangiography and ERCP is the option for concurrent treatment and collection of biopsy specimens, if required.[26,31–33] Disadvantages include the risk of acute pancreatitis, cholangitis, perforation, and hemorrhage attributable to its invasiveness.[1,26] Although these complications were not reported in a study[26] that involved the use of ERCP in cats, the risks of ERCP appear to outweigh the advantages in cats owing to the fact that their small size makes this technique diagnostically challenging, particularly because choledocholiths and neoplasia seem to be less common in cats than in humans. In other studies,[1,33] it was reported that MRCP was as accurate as ERCP for visual evaluation of the biliary anatomy of humans without being invasive or relying on ionizing radiation or operator skill. Additionally, MRCP enables concurrent assessment of the liver and pancreas as well as the biliary and pancreatic ducts proximal to an obstruction, particularly when combined with standard T1- and T2-weighted sequences.[1,34] When concurrent diagnostic and interventional procedures are not expected, MRCP is the preferred method. In addition, MRCP can be used with hepatocyte-specific contrast agents (eg, Gd-EOB-DTPA). This hepatocyte-specific contrast agent has improved the ability of investigators to visually examine and characterize focal liver lesions and provide both morphological and functional information on the biliary tract of humans,[35–38] dogs,[39–43] rats,[36] and rabbits.[42] Gadoxetic acid enters hepatocytes via an organic ion transport system and is excreted into the biliary system via ATP-dependent glutathione S-transferase.[35] Given the hepatocyte specificity of Gd-EOB-DTPA, use of this contrast agent has resulted in improvements in tumor detection and the ability to distinguish between benign and malignant lesions of hepatocellular or nonhepatocellular origin in the delayed phase, independent of the vascularity of a lesion during early dynamic phase imaging.[36,37] For example, lesions with altered hepatocyte function (eg, hepatic adenoma, nodular hyperplasia, and hepatocellular carcinoma) have variable contrast enhancement, compared with results for normal hepatic parenchyma.[37,39–41] Similarly, metastatic lesions that lack hepatocytes have no contrast enhancement.[37] Additionally, Gd-EOB-DTPA–enhanced MRI can potentially provide quantitative assessment of liver perfusion and hepatocyte function in diffuse liver disease.[37,41] The excretion properties of Gd-EOB-DTPA have also been used in the functional assessment of biliary anatomy with MRI, including bile duct injury, obstruction or stricture; sphincter of Oddi dysfunction; differentiation of biliary from extrabiliary lesions (including bilomas); identification of biliary-enteric anastomoses; and diagnosis of cholecystitis in people.[35]

Because of their paramagnetic properties, gadolinium-based contrast agents typically have been used in combination with MRI. The MRI procedures require only a 5% to 20% molar dose of a metal, compared with the dose needed for CT, to provide diagnostically useful tissue contrast.[42] However, biliary MRI requires a high-field magnet (1.5 T) that is not routinely used at veterinary clinics because of the high cost and limited availability. An alternative imaging modality is CT, which is now widespread at veterinary clinics and has a faster image acquisition time, fewer artifacts, and improved image resolution and reconstruction techniques and may be performed in sedated animals (rather than anesthetized animals).[27,33,41,44,45] Computed tomography frequently is used in human medicine to diagnose pathological biliary conditions.[45] The high atomic number of gadolinium also makes it a good contrast medium for CT.[42] Previous CT evaluations of the abdomen of dogs[41] and humans[38] after administration of gadolinium-based contrast agents revealed adequate visual examination of the liver and biliary tract.

To the author's knowledge, there has been no reported use of Gd-EOB-DTPA in cats. Therefore, the objectives of the study reported here were to determine a dose of Gd-EOB-DTPA that could be safely administered to healthy cats, identify any adverse effects, determine the optimal CT scan time for Gd-EOB-DTPA in the liver and biliary tract, and determine whether Gd-EOB-DTPA could improve visual assessment of the hepatobiliary anatomy via CT in healthy cats. We hypothesized that Gd-EOB-DTPA would be a contrast agent that could be safely used with CT to improve conspicuity of the hepatobiliary system in healthy cats.

Materials and Methods

Animals

Five healthy cats were recruited from a privately owned research facility.[a] All procedures were performed at the veterinary teaching hospital at the University of Sydney. Cats were included in the study when no abnormalities were detected during physical examination, there were no hepatic or renal abnormalities on biochemical analysis and urinalysis, and there were no major changes for a CBC. Ultrasonographic examination[b] of the hepatobiliary system was performed on each cat prior to initial noncontrast CT to rule out preexisting diseases. Cats were excluded from the study when hepatobiliary ultra-

sonography or the initial noncontrast CT revealed abnormalities. The study was approved by the Animal Ethics Committee of the University of Sydney.

Experimental procedures

Three phases of contrast-enhanced CT examinations were conducted for each cat; there was a washout period of at least 1 week between phases. Each phase involved IV administration of a dose of Gd-EOB-DTPA.[c] The first phase involved a low dose of contrast agent (0.0125 mmol/kg); that dose was based on half the recommended clinical dose for humans.[46] The second phase involved a medium dose of contrast agent (0.1 mmol/kg), and the third phase involved a high dose of contrast agent (0.3 mmol/kg).

Before each CT scan was performed, the cats were anesthetized and positioned in sternal recumbency. Alfaxalone[d] (0.2 mg/kg, IM) and butorphanol tartrate[e] (0.2 mg/kg, IM) were administered as preanesthetic medications. Alfaxalone (1 to 2 mg/kg) was administered IV for anesthetic induction to enable tracheal intubation, and anesthesia was maintained with isofluorane[f] in oxygen. During the procedure, a crystalloid solution[g] was administered (5 mL/h, IV), and physiologic variables (heart rate, respiratory rate, noninvasively measured blood pressure, end-tidal carbon dioxide concentration, and oxygen saturation) of cats were monitored continuously.

Apnea was induced by hyperventilation prior to each scan to avoid motion artifact. Each CT scan was conducted in accordance with the same CT protocol. A 16-slice multidetector CT scanner[h] was used. An air calibration was performed every other day, and a quality control scan was performed monthly with an ROI phantom. A helical precontrast scan (0 minutes) and 5 postcontrast scans (5, 25, 45, 65, and 85 minutes after administration of contrast agent) were acquired. Contrast agent was delivered via rapid manual injection, which was followed immediately by rapid administration of a bolus of saline (0.9% NaCl) solution[i] (3 mL, IV). At 90 minutes after injection of the contrast agent, cats were repositioned in dorsal recumbency to assess the distribution of contrast agent within the gallbladder and to subjectively visually assess the bile duct after the change in body position. No objective measurements were obtained while cats were positioned in dorsal recumbency, and these data were not included in the statistical analysis.

The abdomen CT protocol for both sternal and dorsal recumbency involved use of a detector row arrangement of 16 data channels with a detector width of 0.75 mm (16 × 0.75 mm), tube current of 90 mA, and tube potential of 120 kV (peak). The display field of view was determined for each cat; it included the diaphragm cranially and pubis caudally. Images were reconstructed with a slice thickness of 1.5 mm with a soft tissue kernel.

A CBC, biochemical analysis, and urinalysis were performed for each cat 48 hours after each dose of contrast agent. Vital parameters were monitored every 8 hours for 3 to 5 days after injection of the contrast agent. Two weeks after each phase of the study, the cats were examined at the research facility to assess general health.

Image analysis

Objective analysis—One investigator (JLP) objectively measured the number of HU of the hepatobiliary system for various anatomic structures, including the liver, gallbladder, cystic duct, and bile duct. The cystic duct is dorsally directed and was defined as the region from the neck of the gallbladder to the insertion of the hepatic ducts in the region of the porta hepatis.[5] The hepatic ducts were defined as the ducts that drained each lobe of the liver.[3] The hepatic ducts may join to form a common hepatic duct before entering the cystic duct.[5] The bile duct was defined as the portion of the duct distal to the union of the cystic duct and hepatic ducts to its opening onto the major duodenal papilla.[3] The HU of the hepatic ducts were not measured because of the inconsistent ability to visually evaluate the structures.

Standardized ROIs or points of interest were drawn on transverse CT images of each structure on a DICOM workstation and reviewed by use of software.[j] Data for ROIs or points of interest were exported to a spreadsheet,[k] and time-attenuation curves were generated for each part of the biliary tract and liver. When the liver was evaluated, a similar anatomic location was obtained for each ROI (0.5 cm^2), and care was used to not include vessels in the ROIs. For the gallbladder, each ROI (0.5 cm^2) was measured at the dorsal aspect of the gallbladder (neck of the gallbladder) where contrast was visible. In the cystic duct and bile duct, a single point of interest was used to measure enhancement at a location where structures were clearly visible.

Visual analysis—Two board-certified veterinary radiologists (MAM and JMP) and a veterinarian in the third year of a radiology residency program (TSF) separately assessed the CT images of each cat obtained at 65 minutes after injection of each of the 3 doses of contrast agent. Investigators were not aware of the dose administered to each cat, and images were anonymous and randomized. Investigators used a visual assessment scoring system to determine a score for the gallbladder, cystic duct, bile duct, and hepatic ducts (where they were visible from the porta hepatis to the insertion onto the bile duct) and comment on the ability to visually detect contrast agent in the duodenum (yes or no) and whether there was motion artifact (yes or no). Visual detection of contrast agent within these structures was graded on a scale of 0 to 3 (0 = absent, 1 = poor contrast enhancement with ill-defined borders, 2 = moderate contrast enhancement with incomplete delineation of borders, and 3 = excellent contrast enhancement along the length of the duct with well-defined borders throughout the entire length of the duct). This visual assessment

scoring system has been used for evaluation of the biliary system.[41]

Statistical analysis

Statistical analysis was performed with a commercially available software program.[1] For all analyses, significance was set at values of $P \leq 0.05$. Data for the liver, gallbladder, cystic duct, and bile duct were analyzed by use of a restricted maximum likelihood model to assess the timing and effect of the dose of contrast agent on enhancement. The objectively determined enhancement values (number of HU) were square root transformed to ensure normality of the data. Fixed effects included age, body weight, timing, anatomic structure, and dose of contrast agent.

Visual assessment scores of the investigators for each biliary structure (gallbladder, cystic duct, bile duct, and hepatic ducts) were analyzed by use of ordinal logistic regression. Fixed effects included the dose of contrast agent and investigator. Both of the fixed effects and the interaction between the fixed effects were evaluated.

Results

Animals

None of the cats was excluded on the basis of results of the ultrasonographic examination or initial noncontrast CT examination. One cat was excluded during the first phase of the study because it developed pneumomediastinum immediately after intubation and prior to administration of the contrast agent. The pneumomediastinum resolved without any complications. Another cat was recruited to replace this cat for the second and third phases of the study.

One cat developed diarrhea during hospitalization after the first phase; however, this was suspected to be transient or related to the diet because the diarrhea resolved immediately after the cat's diet was changed to a commercially available prescription gastrointestinal diet. This cat was fed the same commercially available prescription gastrointestinal diet during the subsequent phases of the study and had no further episodes of diarrhea.

Evaluation of safety

Gadoxetic acid was safely used in the 4 healthy cats during the first phase (0.0125 mmol/kg, IV) and the 5 healthy cats during the second (0.1 mmol/kg, IV) and third (0.3 mmol/kg, IV) phases. There were no immediate contrast-related reactions and no hematologic, biochemical, or urinary abnormalities at 48 hours after administration of the contrast agent for all of the cats at each dose of contrast agent. There were no physical examination abnormalities at any time after the administration of contrast agent to all cats at each dose.

Objective measurements

Age ($P = 0.21$) and body weight ($P = 0.92$) of cats did not significantly influence objective measurements of the biliary tract. There was a significant ($P < 0.001$) effect of dose of contrast agent on enhancement of all hepatobiliary structures because each increase in dose of contrast agent resulted in a significant increase in the mean number of HU **(Figure 1)**.

For each anatomic structure (liver, gallbladder, cystic duct, and bile duct) and each time point of contrast enhancement, the liver had homogenous contrast enhancement at all doses and had a significantly higher number of HU at 45 minutes, compared with the number of HU at 0, 5, and 25 minutes; however, there was no significant change in the number of HU in the liver after 45 minutes **(Table 1)**. Furthermore, the liver had a significantly higher number of HU than all other anatomic structures (gallbladder, cystic duct, and bile duct) at each time point (0, 5, 25, 45, 65, and 85 minutes; Figure 1). Mean ± SD maximum liver enhancement was 70 ± 6 HU at 0.0125 mmol/kg, 72 ± 15 HU at 0.1 mmol/kg, and 82 ± 17 HU at 0.3 mmol/kg. Mean difference between liver attenuation at time 0 and maximum liver attenuation was 2 ± 3 HU at 0.0125 mmol/kg, 15 ± 2 HU at 0.1 mmol/kg, and 19 ± 5 HU at 0.3 mmol/kg. Number of HU for the gallbladder differed significantly at each time point and did not reach maximum enhancement by 85 minutes after injection of contrast agent. In comparison, the number of HU in the cystic duct and bile duct was significantly higher at 65 minutes than at 0, 5, 25, and 45 minutes **(Figure 2)**. Maximum number of HU in both the cystic duct and bile duct was detected at 65 minutes, and there was no significant difference between the number of HU at 65 minutes and the number of HU at 85 minutes.

In all cats, the contrast agent distributed nonhomogenously in the gallbladder and was concentrated in the nondependent portion of the gallbladder when the position was changed from sternal to dorsal recumbency, similar to results for dogs[41] and people[42] **(Figure 3)**. The ability to visually assess the bile duct while cats were positioned in dorsal recumbency, as determined subjectively by an investigator, was not affected by the change in body position.

Visual assessment scoring of the biliary tract

Visual assessment scoring was conducted 65 minutes after injection of the contrast agent because there was not a significant difference in enhancement of the liver and biliary tract after that time. A total of 48 scores was obtained for the low dose of contrast agent (4 anatomic structures for each of 3 investigators for each of 4 cats), and 60 scores were obtained for the medium and high doses of contrast dose agent (4 anatomic structures for each of 3 investigators for each of 5 cats). There was no significant difference among scores of the 3 investigators for any anatomic structure (gallbladder, $P = 0.27$; cystic duct, $P = 0.47$; bile duct, $P = 0.20$; and hepatic ducts, $P = 0.59$). Motion artifact was not recorded by any investigator during any phase of the study. Contrast agent was not observed in the duodenum in any cat at any dose of the contrast medium.

Total visual assessment scores for all anatomic structures in the biliary tract at 65 minutes were evaluated **(Figure 4)**. For the low dose of contrast agent, 36 of 48 (75%) biliary tract scores indicated absent contrast enhancement, 12 (25%) scores indicated poor contrast enhancement with ill-defined borders, and 0 (0%) scores indicated moderate or excellent contrast enhancement. For the medium dose of contrast agent, 15 of 60 (25%) biliary tract scores indicated absent contrast enhancement, 32 (53%) indicated poor contrast enhancement, and 13 (22%) indicated moderate contrast enhancement with incomplete delineation of the borders. For the high dose of contrast agent, 12 of 60 (20%) biliary tract scores indicated absent contrast enhancement, 34 (57%) indicated poor contrast enhancement, and 14 (23%) indicated moderate contrast enhancement. None of the cats had excellent enhancement in any of the biliary structures at any dose of contrast agent.

Accordingly, there was a consistently significant effect of the dose of contrast agent for each

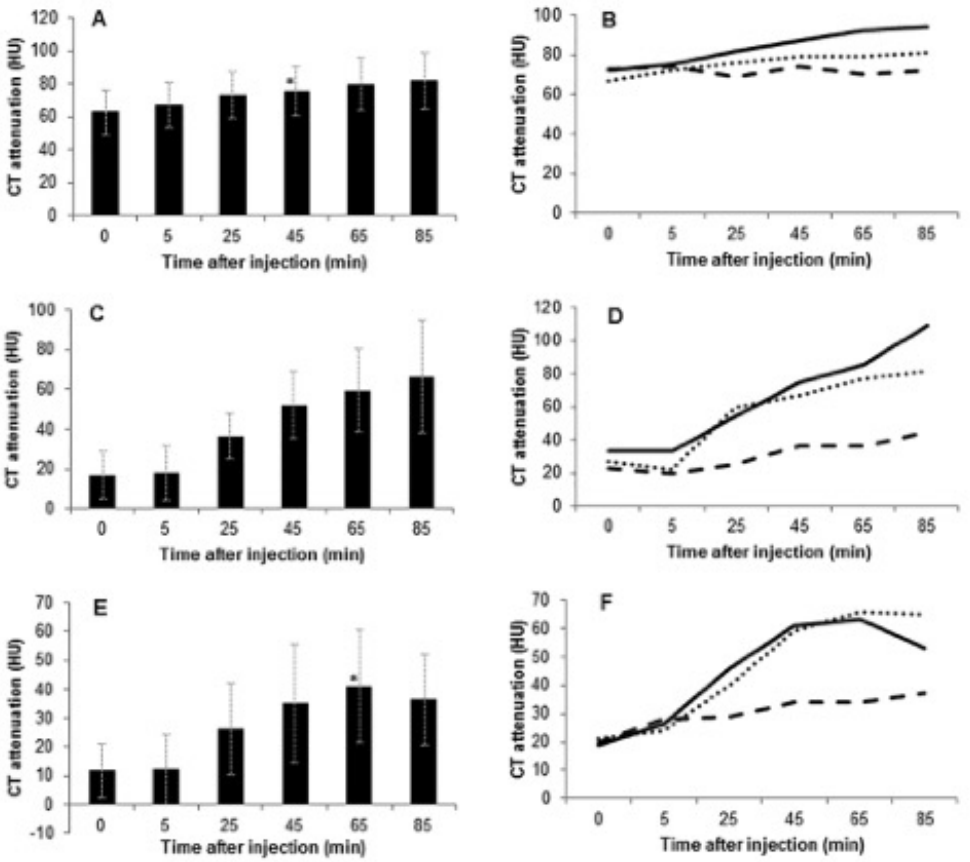

Figure 1—Mean ± SD (A, C, and E) and maximum (B, D, and F) values for CT attenuation of the liver (A and B), gallbladder (C and D), and bile duct (E and F) at the time of IV injection of contrast medium (time 0) and 5, 25, 45, 65, and 85 minutes after injection. For panels A, C, and E, results represent data after injection of the high dose of Gd-EOB-DTPA (0.3 mmol/kg; n = 14), whereas for panels B, D, and F, results represent data after injection of the low (0.0125 mmol/kg; dashed line [4]), medium (0.1 mmol/kg; dotted line [5]), or high (0.3 mmol/kg; solid line [5]) dose of Gd-EOB-DTPA. The mean CT attenuation of the hepatobiliary system has a similar pattern of increasing contrast enhancement over time, although the liver (A) has a significantly ($P \leq 0.05$) higher number of HU at each time point, compared with values for the gallbladder (C) and bile duct (E). Contrast enhancement reached a value (asterisk) that differed significantly ($P \leq 0.05$) from the value at time 0 (in the liver at 45 minutes after injection and in the bile duct at 65 minutes after injection); however, contrast enhancement did not reach a maximum value in the gallbladder by 85 minutes after injection of contrast agent. For panels B, D, and F, the mean maximum CT attenuation similarly was increased over time with increases in enhancement and increasing doses of contrast agent. Notice that the scale on the *y*-axis differs among panels.

Table 1—Mean CT enhancement (number of HU) of anatomic structures of the hepatobiliary system before (time 0) and at various times after IV injection of Gd-EOB-DTPA at a low (0.0125 mmol/kg; n = 4), medium (0.1 mmol/kg; 5), and high (0.3 mmol/kg; 5) dose.

		Time after injection (min)					
Hepatobiliary structure	**Dose**	**0**	**5**	**25**	**45**	**65**	**85**
Liver	Low	68.5	68.0	65.0	67.8	66.5	66.0
	Medium	56.6	63.0	66.0	69.2	70.8	70.2
	High	62.8	67.2	73.0	75.8	79.6	81.8
Gallbladder	Low	19.8	16.2	22.8	31.5	32.5	38.0
	Medium	16.8	14.2	29.4	42.0	49.0	55.2
	High	16.8	18.0	36.4	52.4	59.6	66.6
Cystic duct	Low	18.8	20.0	31.8	30.5	34.3	36.8
	Medium	19.0	17.4	33.2	48.8	49.6	49.4
	High	17.0	20.0	34.0	49.4	56.0	53.4
Bile duct	Low	16.5	21.3	23.8	28.3	28.8	31.8
	Medium	13.8	18.0	18.4	34.2	39.8	38.2
	High	11.8	12.2	26.4	35.2	41.0	36.4

A 0.5-cm^2 ROI was measured in the liver; care was used so that vessels were not included in the ROI. A 0.5-cm^2 ROI was measured at the neck of the gallbladder. A single point of interest was obtained for the cystic duct and bile duct where the structures were clearly visible. The cystic duct is dorsally directed and was defined as the region from the neck of the gallbladder to the insertion of the hepatic ducts in the region of the porta hepatis. The bile duct was defined as the portion of the duct distal to the union of the cystic duct and hepatic ducts and extending to its opening onto the major duodenal papilla.

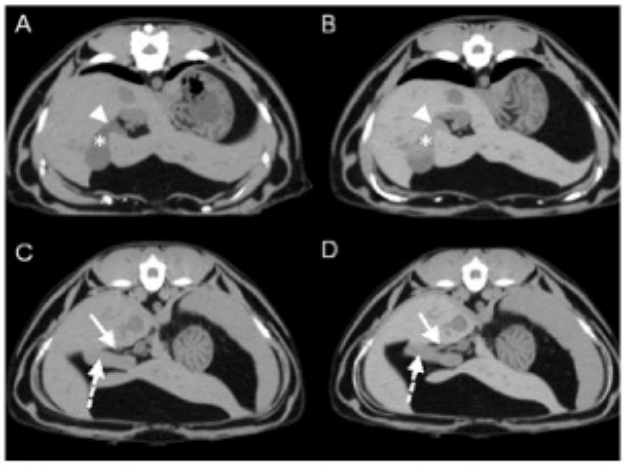

Figure 2—Transverse plane CT images obtained by use of a soft tissue kernel of the cystic duct (A and B) and bile duct (C and D) in a cat before (A and C) and 65 minutes after (B and D) IV administration of a high dose of Gd-EOB-DTPA (0.3 mmol/kg). In panels A and B, the neck of the gallbladder (asterisk) and the cystic duct (arrowhead) are indicated. In panels C and D, notice the bile duct (arrow with solid line) immediately proximal to the point at which it enters the duodenum (arrow with dashed line).

anatomic structure (gallbladder, cystic duct, bile duct, and hepatic ducts; **Figure 5**). In the gallbladder, visual assessment scores were 9.5 times as likely to be higher for the medium dose ($P = 0.007$) and 14.2 times as likely to be higher for the high dose ($P = 0.002$), compared with the visual assessment score for the low dose. Visual assessment scores for the cystic duct were 10.1 and 20.0 times as likely to be higher for the medium ($P = 0.014$) and high ($P = 0.002$) dose, respectively, compared with the visual assessment score for the low dose. Visual assessment scores for the bile duct were 10.4 and 5.8 times as likely to be higher for the medium ($P = 0.005$) and high ($P = 0.029$) dose, respectively, compared with the visual assessment score for the low dose. Visual assessment scores for the hepatic duct were 14.3 and 21.3 times as likely to be higher for the medium ($P = 0.005$) and high ($P = 0.002$) dose, respectively, compared with the visual assessment score for the low dose. However, there was not a significant difference in visual assessment scores between the medium and high dose for any of the anatomic structures (gallbladder, OR = 1.5; cystic duct, OR = 2.0; bile duct, OR = 0.6; and hepatic ducts, OR = 1.5).

The best visual assessment scores were for 1 cat at the high dose of contrast agent. That cat had 8 of 12 scores that indicated moderate enhancement and 4 of 12 scores that indicated poor enhancement of all biliary structures (gallbladder, cystic duct, bile duct, and hepatic ducts). For the same dose of contrast agent, another cat had 4 of 12 scores that indicated poor enhancement and 8 of 12 scores that indicated absent enhancement.

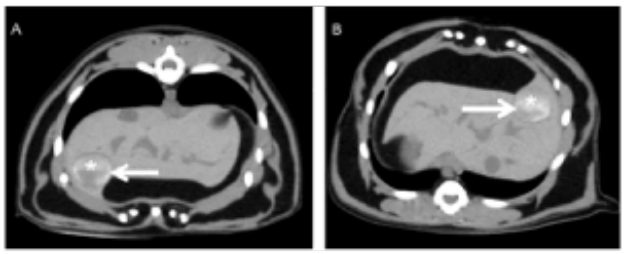

Figure 3—Transverse plane CT images obtained by use of a soft tissue kernel of the liver and gallbladder after CT cholangiography performed with a high dose of Gd-EOB-DTPA (0.3 mmol/kg, IV) for a cat positioned in sternal (A) and dorsal (B) recumbency. Notice that the contrast agent redistributes nonhomogenously to the nondependent portion of the gallbladder (asterisk), delineating the contrast agent from bile in the dependent portion of the gallbladder (arrow).

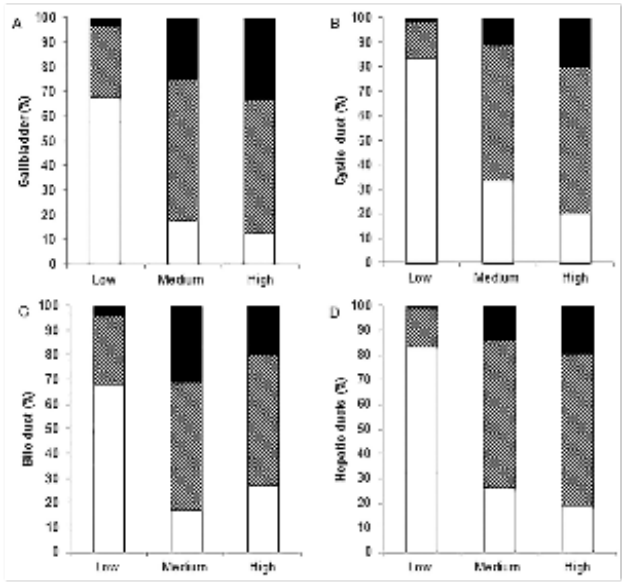

Figure 4—Combined subjective visual assessment scores of 3 investigators for the gallbladder (A), cystic duct (B), bile duct (C), and hepatic ducts (D) at 65 minutes after IV injection of a low (0.0125 mmol/kg; n = 4), medium (0.1 mmol/kg; 5), and high (0.3 mmol/kg; 5) dose of Gd-EOB-DTPA to cats. Visual assessment scores were graded on a scale of 0 to 3 (0 = absent [white bars], 1 = poor contrast enhancement with ill-defined borders [diagonal-striped bars], 2 = moderate contrast enhancement with incomplete delineation of borders [black bars], and 3 = excellent contrast enhancement along the length of the duct with well-defined borders throughout the entire length of the duct [gray bars]). The low dose had a higher percentage of scores that indicated absent contrast for all anatomic structures than did the medium and high doses. The medium and high doses provided improved visual assessment scores, with a high percentage of scores indicative of poor to moderate contrast enhancement in the biliary tract and a low percentage of scores indicative of absent contrast enhancement. Notice that none of the biliary structures had excellent contrast enhancement.

Discussion

The study reported here provided evidence that Gd-EOB-DTPA can be safely administered IV as a contrast agent in healthy cats and that use of Gd-EOB-DTPA resulted in some degree of enhancement of the hepatobiliary system. No acute major adverse effects were identified after IV injection of Gd-EOB-DTPA in cats of the present study. Adverse effects are rare in humans (0.1% to 1%) and include nausea, vasodilation, headache, taste perversion, rash, vomiting, increases in blood pressure, respiratory disorders, feeling hot, and injection site pain.[46] In dogs, a transient prolonged corrected QT interval has been reported at doses of Gd-EOB-DTPA of 0.1 mmol/kg.[46] Although nephrogenic systemic fibrosis has not been reported for Gd-EOB-DTPA, cautious use is recommended in human patients with a reduced glomerular filtration rate because nephrogenic systemic fibrosis reportedly can develop within days to weeks following administration of other gadolinium agents.[37,46,47] The cats in the present study did not have any adverse effects. This may have been attributable to the fact that there was a small study population, cats were anesthetized at the time of injection, or the study ended too soon to enable us to evaluate cats for nephrogenic systemic fibrosis. There were no abnormalities for the physical examinations performed after each phase of the study or for a medical history obtained via verbal communication with research facility personnel 2 weeks after phases 1 and 3 of the study.

All doses of Gd-EOB-DTPA resulted in overall poor visual assessment of the biliary tract in healthy cats by use of CT, which raised questions about the clinical value of this technique for use in cats. In agreement with results of other studies, there were large individual differences in visual assessment scores and objective enhancement characteristics of the biliary structures among cats within the same dose group, which was suspected to have been attributable to individual differences in the number and type of hepatocytes and biliary transport proteins among cats.[41] The difference in results between the study reported here and studies of humans[38] and dogs[41,42] may be related to the manner in which different species accumulate and excrete compounds via the hepatobiliary system. In humans, approximately 50% of Gd-EOB-DTPA is reportedly excreted via the hepatobiliary system,[37,48] whereas

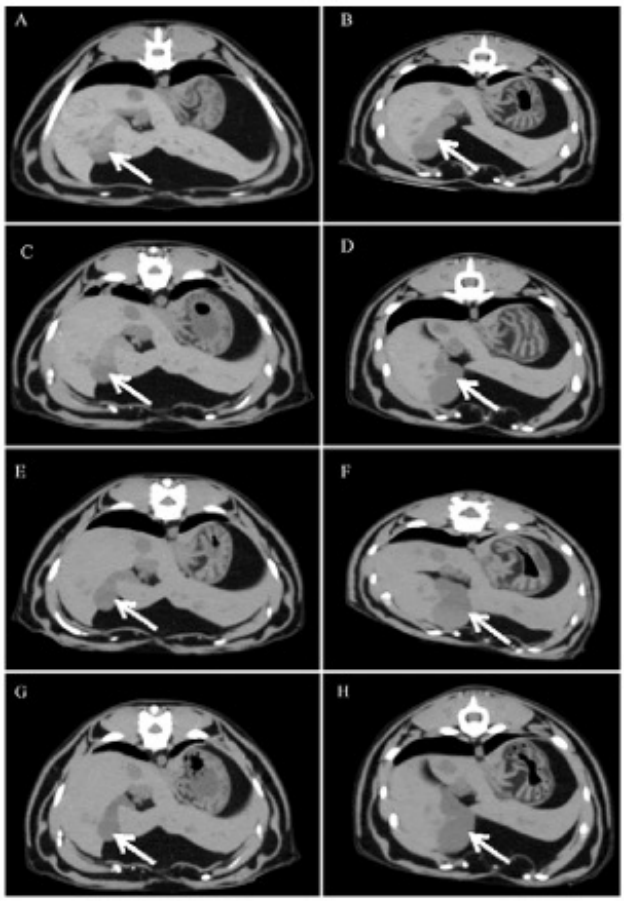

Figure 5—Transverse plane CT images obtained by use of a soft tissue kernel of the gallbladder (arrow) of 2 cats (cat 1 = A, C, E, and G; cat 2 = B, D, F, and H) at 65 minutes after IV injection of a high (0.3 mmol/kg; A and B), medium (0.1 mmol/kg; C and D), and low (0.0125 mmol/kg; E and F) dose of Gd-EOB-DTPA and before administration of contrast agent (G and H). Although there was a similar pattern of an increase in subjective enhancement of the gallbladder with an increase in dose of contrast agent for both cats, there were differences in the number of HU and visual assessment scores between cats for the same dose of contrast agent. There was similar contrast enhancement within the gallbladder of cats 1 and 2 for the high dose (A and B); however, for the medium and low doses, cat 1 (C and E, respectively) had greater contrast enhancement within the gallbladder than did cat 2 (D and F, respectively).

excretion via the same system in rats[48] is 63% to 80% and in monkeys[48] is 32% to 34%. Variability in the excretion rates of contrast agents among species has also been confirmed in other evaluations of nonhepatocyte-specific contrast agents (eg, gadobenate dimeglumine), which are agents that have the highest biliary excretion rate when administered to rats, followed by dogs, rabbits, and monkeys.[49] Although the authors are not aware of any pharmacokinetic evaluations of Gd-EOB-DTPA in cats, it is likely that the biliary excretion rates of cats differ from those reported for other species. A study[50] of biliary excretion of nongadolinium compounds with a molecular weight similar to that of Gd-EOB-DTPA (726 Da) suggested that cats had intermediate biliary excretion of compounds with a high molecular weight (355 to 495 Da), whereas rats and dogs had good biliary excretion and rabbits and monkeys had poor biliary excretion. Thus, it would be expected that cats would excrete Gd-EOB-DTPA at least as well as humans and possibly less well than dogs. Although pharmacokinetic evaluation and a comparison between hepatic and renal enhancement were beyond the scope of the study reported here, they would be beneficial to provide a better understanding of the hepatobiliary and renal excretion properties of Gd-EOB-DTPA in cats.

Dose of Gd-EOB-DTPA had a significant effect on hepatobiliary enhancement. Higher doses were used for the second and third phases of the present study, compared with the dose used for enhanced MRI in humans[46] or dogs.[39,40,51] This was based on the fact that the dose required for CT is higher than the dose required for MRI.[38,42] A low dose was chosen for the first phase of the present study to minimize the risk of adverse effects because use of Gd-EOB-DTPA in cats had not been reported. A significant effect of the dose of contrast agent for each biliary structure was detected between the medium and high doses, compared with results for the low dose; however, there were no significant differences detected between the medium and high doses. This was most likely attributable to the smaller increase in dose (factor of 3) between the medium and high doses, compared with a larger increase (factor of ≥ 10) between the low dose and medium or high dose. Despite this, increases in the dose of contrast agent resulted in higher mean enhancement values (independent of age and body weight) for all anatomic structures in the hepatobiliary system. This is similar to the dose-dependent enhancement seen for dogs in other studies.[41,42] Although the relationship between dose and enhancement in the present study is similar to that detected in studies of dogs[41,42] and humans,[38,45,47] the overall biliary enhancement in the study reported here was lower in cats when considering a similar dose of contrast agent.

Despite the fact there were suboptimal biliary tract visual assessment scores, optimal objective CT contrast enhancement of the cystic and bile ducts was detected at 65 minutes at all doses. This timing is similar to results in a study[41] of dogs in which the time of contrast agent enhancement was also not dose dependent. Therefore, future clinical investigations of biliary pathological conditions of cats by use of Gd-EOB-DTPA could be conducted between 65 and 85 minutes after injection of contrast agent because there was not a significant difference in the number of HU between these times. In the present study, contrast enhancement of the gallbladder differed significantly at each time point and did not reach a plateau by the time of the last scan (85 minutes after injection of contrast agent). Therefore, maximal enhancement of the gallbladder was not determined in the study reported here. In human medicine, Gd-EOB-DTPA–enhanced MRI evaluations revealed intense enhancement of the bile duct from 10 minutes after injection of contrast agent, with scanning and assessment of the biliary tract recommended at 20 to 30 minutes after injection.[35,37,52] However, improved image quality of the bile ducts was detected after a scan delay of 50 to 60 minutes for patients without hepatobiliary dysfunction.[52] It is unclear whether further increasing a delay for image acquisition of cats would result in increased enhancement of the gallbladder.

Clear homogenous contrast enhancement of the liver was detected in the present study. This finding has potential use for the characterization of diffuse or focal hepatic disease in cats by use of CT in clinical studies. The time of contrast enhancement of the liver was similar in all cats, with no significant change in liver enhancement after 45 minutes for all doses of contrast agent. Similar to results of CT and MRI evaluations of dogs with hepatic lesions,[39,40,45] cats with diffuse or focal hepatic pathological conditions may have a reduction in, delay of, or lack of contrast enhancement in affected regions of the liver, compared with values for normal hepatic parenchyma. On the basis of results for the study reported here, these changes may be best visually assessed between 45 and 85 minutes after injection of contrast agent. Despite a continued increase in the number of HU after 45 minutes, it is unclear whether a longer interval after injection of the contrast agent would have improved conspicuity of hepatic lesions given that there was not a significant difference in liver enhancement after 45 minutes. The enhancement curve for the liver of the cats in the present study differed from that described for dogs.[42] In that study,[42] time of maximum enhancement in dogs was dose dependent. It was argued that saturation may have delayed peak enhancement.[42] The reason that the highest dose in the present study did not result in delayed hepatic enhancement is unclear. A possible explanation would be that we may have terminated the study before maximum enhancement was reached. Alternatively, it is possible that the doses in the present study were below the saturation value that results in delayed biliary excretion in dogs.[42] Future studies are needed to investigate higher doses of contrast agents and longer periods of image acquisition.

For all anatomic structures (gallbladder, cystic duct, and hepatic ducts), except for the bile duct, the odds of having a higher visual assessment score were increased when considering the high dose to the low dose and comparing that with the medium dose to the low dose. Interestingly, the OR for the bile duct was higher when comparing the medium dose to the low dose (OR, 10.4) than when comparing the high dose to the low dose (OR = 5.8). The reason for this relationship is unclear, but it may have been attributable to the small size and sinuous shape of the bile duct. In the case of the cystic duct, a possible explanation for the low visual assessment scores may have been related to border effacement with the adjacent hepatic parenchyma. Another reason may have been their tortuosity. In most of the cats, the hepatic ducts were visible only along part of their length (typically just proximal to their entry into the bile duct). This finding is similar to that for a study[41] of dogs in which the hepatic ducts were also found to be the least reliably visible structure with Gd-EOB-DTPA–enhanced CT.

Limitations of the present study included the small number of cats in each phase, particularly because 1 cat was excluded from the first phase of the study. However, because significant differences were detected with the small study population, the use of an additional cat in the first phase was considered unnecessary. A single investigator performed the objective contrast measurements of the hepatobiliary system, which may have introduced bias. Furthermore, because the feline biliary tract is small and tortuous, in particular the bile duct, measurements were difficult to obtain for some cats and may have included additional sampling error or volume averaging. Thinner slices may have reduced this limitation. The study ended at 85 minutes, and the plateau and any decline in enhancement for the gallbladder were not identified. Therefore, we cannot be certain that maximum enhancement was identified. However, additional time for image acquisition and anesthesia did not appear to be warranted, given the data from studies of humans and dogs. Higher doses were not tested in the study reported here because of ethical considerations and cost limitations for implementing additional phases.

In the study reported here, Gd-EOB-DTPA–enhanced hepatic CT and cholangiography provided clear homogenous hepatic enhancement but poor to moderate enhancement of the biliary tract. These results suggested that this technique may be useful for image analysis of the liver parenchyma; however, its value for evaluation of the biliary tract of cats is questionable. No major adverse effects were detected in the healthy cats of the present study. A positive relationship in contrast enhancement was reported

with increases in the dose of contrast agent. Optimal time for imaging of the liver was 45 minutes, whereas optimal time for imaging of the biliary tract was 65 minutes after injection of contrast agent. This information may guide future investigations on the use of Gd-EOB-DTPA–enhanced MRI cholangiography of cats.

Acknowledgments

This manuscript represents a portion of a thesis submitted by Dr. Pilton to the School of Veterinary Science, Faculty of Science at the University of Sydney as partial fulfillment of the requirements for a Master in Veterinary Clinical Studies degree.

The authors declare that there were no conflicts of interest.

Presented in abstract form at the 2017 Australia and New Zealand College of Veterinary Scientists Science Week, Gold Coast, QLD, Australia, July 2017.

Footnotes

a. Eurofins SCEC Agroscience Services Pty Ltd, Lane Cove West, NSW, Australia
b. Siemens Acuson S2000, Siemens AG, Erlangen, Germany.
c Primovist, Bayer Australia Ltd, Pymble, NSW, Australia.
d. Alfaxan, Jurox Pty Ltd, Rutherford, NSW, Australia.
e. Butorgesic, Troy Laboratories Pty Ltd, Smithfield, NSW, Australia.
f. Isoflo, Abbott Australasia Pty Ltd, Botany, NSW, Australia.
g. Hartmann solution, Baxter Healthcare Pty Ltd, Toongabbie, NSW, Australia.
h. Phillips, 16-slice Brilliance CT, version 2.3, Phillips Medical Systems Netherlands, Eindohoven, Netherlands.
i. Pfizer Australia Pty Ltd, West Ryde, NSW, Australia.
j. Osirix, version 4.1.2, 32-bit, Pixmeo SARL, Bernex, Switzerland.
k. Microsoft Excel, version 2010, Microsoft Corp, Redmond, Wash.
l. Genstat, version 17, VSNi, Hemel Hempstead, England.

References

1. Marolf AJ, Stewart JA, Dunphy TR, et al. Hepatic and pancreaticobiliary MRI and MR cholangiopancreatography with and without secretin stimulation in normal cats. *Vet Radiol Ultrasound* 2011;52:415–421.
2. Center SA. Diseases of the gallbladder and biliary tree. *Vet Clin North Am Small Anim Pract* 2009;39:543–598.
3. Smallwood JE. Digestive system. In: Hudson L, Hamilton W, eds. *Atlas of feline anatomy for veterinarians.* Philadelphia: WB Saunders Co, 1993;166–167.
4. Neer TM. A review of disorders of the gallbladder and extrahepatic biliary tract in the dog and cat. *J Vet Intern Med* 1992;6:186–192.
5. Brain PH, Barrs VR, Martin P, et al. Feline cholecystitis and acute neutrophilic cholangitis: clinical findings, bacterial isolates and response to treatment in six cases. *J Feline Med Surg* 2006;8:91–103.
6. Boland L, Beatty J. Feline cholangitis. *Vet Clin North Am Small Anim Pract* 2017;47:703–724.
7. Weiss DJ, Gagne JM, Armstrong PJ. Relationship between inflammatory hepatic disease and inflammatory bowel disease, pancreatitis, and nephritis in cats. *J Am Vet Med Assoc* 1996;209:1114–1116.
8. Cullen JM. Summary of the World Small Animal Veterinary Association Standardization Committee Guide to Classification of Liver Disease in Dogs and Cats. *Vet Clin North Am Small Anim Pract* 2009;39:395–418.
9. Selmic LE. Hepatobiliary neoplasia. *Vet Clin North Am Small Anim Pract* 2017;47:725–735.
10. Bennett SL, Milne M, Slocombe RF, et al. Gallbladder mucocoele and concurrent hepatic lipidosis in a cat. *Aust Vet J* 2007;85:397–400.
11. Woods KS, Brisson BA, Defarges AM, et al. Congenital duplex gallbladder and biliary mucocele associated with partial hepatic cholestasis and cholelithiasis in a cat. *Can Vet J* 2012;53:269–273.
12. Furneaux RW. A series of six cases of sphincter of Oddi pathology in the cat (2008–2009). *J Feline Med Surg* 2010;12:794–801.
13. Della Santa D, Schweighauser A, Forterre F, et al. Imaging diagnosis—extrahepatic biliary tract obstruction secondary to a duodenal foreign body in a cat. *Vet Radiol Ultrasound* 2007;48:448–450.
14. Brioschi V, Rousset N, Ladlow JF. Imaging diagnosis—extrahepatic biliary tract obstruction secondary to a biliary foreign body in a cat. *Vet Radiol Ultrasound* 2014;55:628–631.
15. Linton M, Buffa E, Simon A, et al. Extrahepatic biliary duct obstruction as a result of involuntary transcavitary implantation of hair in a cat. *JFMS Open Rep* 2015;1:2055116915610359.
16. Léveille R, Biller DS, Shiroma JT. Sonographic evaluation of the common bile duct in cats. *J Vet Intern Med* 1996;10:296–299.
17. Sherding RG. Feline jaundice. *J Feline Med Surg* 2000;2:165–169.
18. Newell SM, Selcer BA, Roberts RE, et al. Hepatobiliary scintigraphy in the evaluation of feline liver disease. *J Vet Intern Med* 1996;10:308–315.
19. Newell SM, Graham JP, Roberts GD, et al. Quantitative hepatobiliary scintigraphy in normal cats and in cats with experimental cholangiohepatitis. *Vet Radiol Ultrasound* 2001;42:70–76.
20. Head LL, Daniel GB. Correlation between hepatobiliary scintigraphy and surgery or postmortem examination findings in dogs and cats with extrahepatic biliary obstruction, partial obstruction, or patency of the biliary system: 18 cases (1995–2004). *J Am Vet Med Assoc* 2005;227:1618–1624.
21. Carlisle C. A comparison of technics for cholecystography in the cat. *Vet Radiol* 1977;18:173–176.
22. Larson MM. Ultrasound imaging of the hepatobiliary system and pancreas. *Vet Clin North Am Small Anim Pract* 2016;46:453–480, v–vi..
23. Marolf AJ, Leach L, Gibbons DS, et al. Ultrasonographic findings of feline cholangitis. *J Am Anim Hosp Assoc* 2012;48:36–42.
24. Gaillot HA, Penninck DG, Webster CRL, et al. Ultrasonographic features of extrahepatic biliary obstruction in 30 cats. *Vet Radiol Ultrasound* 2007;48:439–447.
25. Policelli Smith R, Gookin JL, Smolski W, et al. Association between gallbladder ultrasound findings and bacterial culture of bile in 70 cats and 202 dogs. *J Vet Intern Med* 2017;31:1451–1458.
26. Spillmann T, Willard MD, Ruhnke I, et al. Feasibility of endoscopic retrograde cholangiopancreatography in healthy cats. *Vet Radiol Ultrasound* 2014;55:85–91.
27. Marolf AJ. Computed tomography and MRI of the hepatobiliary system and pancreas. *Vet Clin North Am Small Anim Pract* 2016;46:481–497 (vi.).
28. Rosenberg FJ, Ackerman JH, Nickel AR. Iosulamide: a new intravenous cholangiocholecystographic medium. *Invest Radiol* 1980;15:S142–S147.
29. Marolf AJ, Kraft SL, Dunphy TR, et al. Magnetic resonance (MR) imaging and MR cholangiopancreatography findings in cats with cholangitis and pancreatitis. *J Feline Med Surg* 2013;15:285–294.
30. Marolf AJ. Diagnostic imaging of the hepatobiliary system: an update. *Vet Clin North Am Small Anim Pract* 2017;47:555–568.
31. Schindera ST, Nelson RC, Paulson EK, et al. Assessment of the optimal temporal window for intravenous CT cholangiography. *Eur Radiol* 2007;17:2531–2537.
32. Spillmann T, Schnell-Kretschmer H, Dick M, et al. Endoscopic retrograde cholangio-pancreatography in dogs with chronic gastrointestinal problems. *Vet Radiol Ultrasound* 2005;46:293–299.
33. O'Connor OJ, O'Neill S, Maher MM. Imaging of biliary tract disease. *AJR Am J Roentgen* 2011;197:W551–W558.
34. Maccioni F, Martinelli M, Al Ansari N, et al. Magnetic reso-

nance cholangiography: past, present and future: a review. *Eur Rev Med Pharmacol Sci* 2010;14:721–725.
35. Lee NK, Kim S, Lee JW, et al. Biliary MR imaging with Gd-EOB-DTPA and its clinical applications. *Radiographics* 2009;29:1707–1724.
36. Burke C, Alexander Grant L, Goh V, et al. The role of hepatocyte-specific contrast agents in hepatobiliary magnetic resonance imaging. *Semin Ultrasound CT MR* 2013;34:44–53.
37. Van Beers BE, Pastor CM, Hussain HK. Primovist, Eovist: what to expect? *J Hepatol* 2012;57:421–429.
38. Schmitz SA, Häberle J, Balzer T, et al. Detection of focal liver lesions: CT of the hepatobiliary system with gadoxetic acid disodium, or Gd-EOB-DTPA. *Radiology* 1997;202:399–405.
39. Yonetomi D, Kadosawa T, Miyoshi K, et al. Contrast agent Gd-EOB-DTPA (EOB Primovist®) for low-field magnetic resonance imaging of canine focal liver lesions. *Vet Radiol Ultrasound* 2012;53:371–380.
40. Constant C, Hecht S, Craig LE, et al. Gadoxetate disodium (Gd-EOB-DTPA) contrast enhanced magnetic resonance imaging characteristics of hepatocellular carcinoma in dogs. *Vet Radiol Ultrasound* 2016;57:594–600.
41. Chau J, Podadera J, Young A, et al. Use of gadoxetic acid for computed tomographic cholangiography in healthy dogs. *Am J Vet Res* 2017;78:828–839.
42. Schmitz SA, Wagner S, Schuhmann-Giampieri G, et al. A prototype liver-specific contrast medium for CT: preclinical evaluation of gadoxetic acid disodium, or Gd-EOB-DTPA. *Radiology* 1997;202:407–412.
43. Schmitz SA, Wagner S, Schuhmann-Giampieri G, et al. Gd-EOB-DTPA and Yb-EOB-DTPA: two prototypic contrast media for CT detection of liver lesions in dogs. *Radiology* 1997;205:361–366.
44. Shanaman MM, Hartman SK, O'Brien RT. Feasibility for using dual-phase contrast-enhanced multi-detector helical computed tomography to evaluate awake and sedated dogs with acute abdominal signs. *Vet Radiol Ultrasound* 2012;53:605–612.
45. Patel NB, Oto A, Thomas S. Multidetector CT of emergent biliary pathologic conditions. *Radiographics* 2013;33:1867–1888.
46. Eovist (gadoxetate disodium) prescribing information, 2010. Wayne, NJ: Bayer HealthCare Pharmaceuticals Inc. Available at: www.accessdata.fda.gov/drugsatfda_docs/label/2010/022090s004lbl.pdf. Accessed Jun 5, 2017.
47. Mendichovszky IA, Marks SD, Simcock CM, et al. Gadolinium and nephrogenic systemic fibrosis: time to tighten practice. *Pediatr Radiol* 2008;38:489–496.
48. Hamm B, Staks T, Mühler A, et al. Phase I clinical evaluation of Gd-EOB-DTPA as a hepatobiliary MR contrast agent: safety, pharmacokinetics, and MR imaging. *Radiology* 1995;195:785–792.
49. Louvet A, Duconseille A-C. Feasibility for detecting liver metastases in dogs using gadobenate dimeglumine-enhanced magnetic resonance imaging. *Vet Radiol Ultrasound* 2015;56:286–295.
50. Abou-El-Makarem MM, Millburn P, Smith RL, et al. Biliary excretion in foreign compounds. Species difference in biliary excretion. *Biochem J* 1967;105:1289–1293.
51. Marks AL, Hecht S, Stokes JE, et al. Effects of gadoxetate disodium (EOVIST®) contrast on magnetic resonance imaging characteristics of the liver in clinically healthy dogs. *Vet Radiol Ultrasound* 2014;55:286–291.
52. Choi IY, Yeom SK, Cha SH, et al. Diagnosis of biliary stone disease: T1-weighted magnetic resonance cholangiography with Gd-EOB-DTPA versus T2-weighted magnetic resonance cholangiography. *Clin Imaging* 2014;38:164–169.

SECTION 4 - Discussion

This thesis has provided significant insight and understanding in the technical factors affecting multiphase CECT of the abdomen in dogs and cats. It has changed how contrast medium is injected into patients and shaped CT acquisition protocols in veterinary referral hospitals. From the onset of this research project, the aim was to reliably capture multiphase CECT of the liver in dogs and cats and identify a technique that could be easily reproducible in patients that varied in body weight. For every multiple phase CT study, the requirement was to accurately capture an arterial and hepatic phase that clearly met defined radiological criteria; arterial phase at peak enhancement with a minimum peak aortic enhancement of 250HU, and hepatic phase at peak enhancement of the liver parenchyma with a minimum of 50HU increase in CT attenuation compared to pre contrast level.

The pattern of contrast distribution in the body as it flows from the vascular compartment to targets organs was analysed on a bolus geometry curve. The curve is derived from dynamic CT allowing measurement of the attenuation value of contrast in a selected area of interest over time (e.g. aorta or liver). The bolus geometry of the aorta and liver was closely evaluated in Chapter 1 of this thesis, whereby dynamic CT was performed in a canine and feline study population that varied in breed and body weight. The time taken for contrast to flow from the peripheral venous injection site to the aorta (i.e. aortic arrival time) will vary between patients due to inherent differences in patient size, cardiovascular status and also due to the effect of anesthetic drugs and anaesthetic depth as veterinary patients undergoing CT scans are mostly intubated. If cardiac output is decreased, then aortic arrival time is delayed. The aortic arrival time can also be perturbed by the contrast injection technique as a rapid injection rate will hasten the rate of venous inflow to the right heart. The results from this thesis confirm that aortic arrival time is a significant factor that affects time to peak arterial enhancement in dogs and should be taken into consideration when planning an arterial phase scan. This is in agreement with research in humans. An efficient method for measuring aortic arrival time is using bolus tracking which is dynamic CT scan that is integrated into the multiphase CECT study. The dynamic CT is set at the level of the cranial abdominal aorta and initiated from the beginning of contrast medium injection. It allows almost instantaneous detection of contrast arrival in the aorta and an automatic trigger can be set when the attenuation level in the aorta reaches a preset threshold. An aortic density threshold of 150HU was used in our research study and continues to provide reliable results.

The bolus geometry of contrast enhancement in the aorta can also be influenced by external factors such as contrast medium injection rate, injection duration and contrast volume (Bae, 2010). The injection rate affects the early stage of aortic enhancement, contributing to a continuous increase in contrast attenuation of the aorta due to large inflow and relatively small outflow of contrast to visceral organs. Our results in clinical dogs and cats are in agreement with previous experimental research studies, proving that bolus geometry can be disturbed when contrast medium is administered rapidly using a fast injection rate (5ml/s). The bolus

geometry is compressed with the peak of enhancement occurring earlier (Bae, 2010; Makara et al, 2011). Likewise in a canine CT study of the thorax, the bolus geometry of the pulmonary artery was shifted by a rapid injection rate and time to peak enhancement occurred earlier. Small dogs with low body weight were particularly susceptible to this shift. The bolus geometry of the pulmonary artery was significantly different between dogs of different body size when using a fixed, rapid injection rate (Makara et al, 2011) and this also occurred in the abdominal aorta in dogs, and to a lesser extent, the feline abdomen. A rapid injection rate of 5ml/s in dogs that varied in body weight (1.5kg-40kg), resulted in a wide range in time to peak enhancement (7 – 31secs). Conversely, the bolus geometry remained relatively unchanged when contrast medium was administered over a standard duration of 20secs. In our canine study population that received contrast over a standard injection duration weighing from 3-69kg, the time to peak enhancement occurred within a small range (21-27secs). Fixing the injection duration resulted in reproducible time to peak enhancement which is in agreement with experimental studies in dogs and human studies (Tateishi et al, 2008).

The results from Chapter 1 on two clinical studies in both dogs and cats proved that standardising the injection duration (20secs) when administering contrast medium, clearly stabilised the timing of peak arterial enhancement. There was a direct correlation between injection duration and time to peak arterial enhancement. So standardising the injection duration significantly reduced variation in timing of peak arterial enhancement. Regardless if the patient was lightweight or heavy, or if the contrast volume was small or large, fixing the injection duration minimised movement in the peak of arterial enhancement. On the contrary, varying the injection duration when using a fixed injection rate (e.g. 5ml/s) resulted in significant changes in the timing of arterial enhancement between patients. Fixed injection rate led to fluctuations in timing of peak enhancement due to differences in patient body weight and naturally this was more pronounced in the canine study population compared to cats. Body weight is a key variable because the contrast volume is calculated based off body weight, and the contrast volume in turn affects the injection duration when using a fixed injection rate (e.g. fixed injection rate of 5ml/s to administer 10mls of contrast will take 2secs, compared to administering 100mls of contrast would take 20secs). Therefore, a fixed injection rate will inadvertently lead to variation in injection duration due to body weight. If veterinary patients were all the same in body weight, then the volume of contrast medium would be the same for every multiphase CECT study, so a fixed injection rate would not change the injection duration. However, this is not the case and veterinary patients vary significantly in body weight due to species and breed. A contrast injection technique to factor in change in body weight and control timing of contrast enhancement between veterinary patients is necessary. In the veterinary literature, there is no consensus on standard injection duration versus fixed injection rate for the administration of contrast for CT studies. A previously borrowed technique from human radiology (fixed injection rate of 5ml/s) is less suitable compared to standard injection duration in veterinary patients. Results from this thesis indicate that standard injection duration can stabilise and allow prediction of the time to peak arterial enhancement, which is highly desirable when planning multiphase CECT studies.

CT scan start times are pre-set into the machine for multiphase studies and they determine when the scanner will initiate for the arterial and hepatic phases after intravenous contrast medium injection. Accurate timing of the CT scan is necessary to synchronise the arterial and hepatic phase scan with the peak of contrast flow in the splanchnic arteries and liver, respectively. The CT scanner should be triggered before the peak of enhancement, so that the scan phase can ride the peak. Ideally, the middle of the scan phase should be centered on the peak of enhancement. The multiphase CECT scan start time is often referred to as a scan delay, as time 0 marks the beginning of the contrast injection, and a time delay is allowed for contrast to circulate through the body and concentrate in the area of interest. The scan delay can be calculated using the following recommended model:

Time (scan delay in arterial phase) = Time (peak aortic enhancement) – 0.5x Time (scan duration). (Bae, 2010)

The Time (scan duration) is known once the patient is in the scanner and the parameters are set (e.g. scan length, scan speed). Therefore, Time (peak enhancement) is the only unknown variable and predicting time to peak enhancement is key to establishing the correct scan delay times for multiphase CECT studies. From our evaluation of contrast bolus geometry in dogs, we were able to identify methods for predicting time to peak enhancement in the aorta and liver. The most significant variables to consider were injection duration, injection technique and aortic arrival time, which explained 96.1% variation in time to peak aortic enhancement. A regression formula for estimating time to peak enhancement of the aorta in dogs was identified in Chapter 1 of this thesis and this information can be used to individualise the CT scan start time for the arterial phase.

Time (peak aortic enhancement) = 0.8 X [injection duration + aortic arrival time] ± a constant (secs).

When using standard injection duration of 20secs as the injection technique, or fixed injection rate of 5ml/s as the injection technique, the constant in the regression formula was -2.6 secs and +1.6 secs, respectively. The constant in the regression formula was relatively small. The main determinant of time to peak aortic enhancement was 0.8x the sum of injection duration and aortic arrival time. These values can be predetermined during CT scan planning, and then the CT scan delay for the arterial phase can be set accordingly. When using bolus tracking software which is the preferred technique at our institution, we recommend rounding up the value of the aortic arrival time to x1. This is for ease of calculation and because the aortic arrival time is only known after starting the CT scan, while the CT scan delays for the arterial and hepatic phases need to be preset into the machine before starting. If aortic arrival time is presumed as x1, then bolus tracking can be used to take care of aortic arrival time and the scan delay begins after the point of aortic arrival. After contrast medium arrives in the aorta, the Time (peak aortic enhancement) is expected to occur at 0.8x injection duration + constant.

A second option for identifying aortic arrival time is to use the test bolus technique. This technique utilises a small contrast bolus prior to the diagnostic contrast bolus, therefore the aortic arrival time is identified before the diagnostic study and can be used to plan the scan delays for the multiphase CECT study. A third option for estimating the aortic arrival time is to use the mean/median values obtained from our research. Particularly in cats, the aortic arrival time occurred within a narrow range (7-13secs) and did not vary significantly with injection technique (fixed rate of 5ml/s or standard injection duration of 20secs). However, aortic arrival time in dogs did vary significantly (5-19secs). In both cats and dogs, the median aortic arrival time was 11secs. The median aortic arrival time can be inserted into the regression formula [Time (peak aortic enhancement) = 0.8 X [injection duration + aortic arrival time] ± constant].

The formula is further simplified if using a standard injection duration (e.g. 20 secs). The time to peak aortic enhancement can be subsequently estimated and used to calculate the necessary Time (scan delay) for the multiphase CECT study.

Time (peak aortic enhancement) = 0.8 X [20secs + 11 secs] – 2.6 secs.

The timing of peak liver enhancement was relatively constant regardless of the injection technique, injection duration or patient body weight. Estimating Time (peak liver enhancement) was similarly accurate when using the mean Time (peak liver enhancement) compared to the linear regression model. Therefore, we recommended using the mean values. For dogs, this was 45 secs and 50secs, and cats was 22secs and 33 secs for fixed injection rate (5ml/s) and standard injection duration, respectively. A fixed injection rate of 5ml/s did produce a slightly earlier Time(peak liver enhancement), however this was not statistically significant. The bolus geometry of the liver has a very broad and plateaued peak, which provides a wider temporal window for synchronization with the hepatic phase scan. To calculate the scan delay for the hepatic phase, the same model can be used:

Time (scan delay hepatic phase) = Mean time (peak liver enhancement) - 0.5x Time (scan duration).

The University Veterinary Teaching Hospital Sydney (UVTHS) adopted a standard injection duration coupled with bolus tracking technique for multiphase CECT of the abdomen as the routine approach for oncological, surgical, and medical patients. CT scan delays were calculated based on the models described above that allow prediction of time to peak enhancement in the aorta and liver. The technique was efficient, requiring only a single dose of contrast medium and the results were reliable. However, the technique was new and different, with many other veterinary institutions favouring the use of a rapid fixed injection rate and test bolus technique. There was uncertainty about which technique could provide better vascular conspicuity and accurate representation of the arterial and hepatic phases. This was evaluated in Chapter 2 of this thesis, a multi-centre comparison study, triggered by a visiting veterinary radiologist travelling to Sydney from Edinburgh University. Dr T. Schwarz is the first author of a dedicated textbook on Veterinary Computed Tomography and was keen to compare the UVTHS protocol (standardised injection duration of 20secs with bolus tracking) with his technique in Edinburgh University (fixed injection rate of 3ml/s with a test bolus), and the CT protocol from a third

institution, the Istituto Veterinario di Novara in Italy (fixed injection rate of 3ml/s with bolus tracking). These three different CT protocols were performed on different CT scanners (4 row, 16 row and 64 row multidetector CT machines) to evaluate the effect of new technology and rapid machine scan times. Results from our multicentre comparison study supported the fixed-injection duration protocol as the best compromise between an ideal portal vascular enhancement and an easily reproducible protocol on scanners with low and high number of detector rows. Regardless of the type of CT scanner, portal vascular enhancement was superior when using a standardised injection duration with homogenous vascular enhancement of all the portal tributaries. The best technique for the arterial phase varied with the type of CT scanner. When using rapid 64 row CT scanners, bolus tracking to monitor aortic arrival time was superior for capturing the arterial phase compared to the test bolus. There is virtually no delay time from aortic trigger on bolus tracking to the beginning of the diagnostic scan when using 64 row multidetector CT scanners. Older CT scanners had an automatic minimum delay time of 5 secs or more which resulted in a lag phase before the arterial phase scan could initiate. Bolus tracking is logistically easier than the test bolus technique to estimate aortic arrival time, as only a single contrast bolus is required. Whereas the test bolus requires a small contrast dose for the dynamic CT scan, before the full contrast dose can be given during the diagnostic CT scan. Bolus tracking is streamlined with the diagnostic multiphase CECT study and results from this thesis prove that it also improves the accuracy of capturing an arterial phase scan.

This thesis proved that standardised protocols for multiphase CECT of the abdomen are possible in both dogs and cats and so far in this discussion, the technical recommendations have been the same. However, feline patients showed excessive enhancement of the aorta with a mean peak aortic enhancement value of 1907HU when using a fixed injection rate (5ml/s) and 745HU when using a standard injection duration. In comparison, dogs had a median peak aortic enhancement value of 746HU and 549 HU, respectively. Using a 20 sec standard injection duration allowed the contrast medium to be administered relatively slowly compared to the fixed injection rate (5ml/s), which contributed to reduced intensity of aortic enhancement in this group because the contrast medium was given more time to disperse and dilute within the body. However, feline aortic enhancement remained excessive. An aortic enhancement level of 250HU is considered sufficient, whereas some cats showed over 7-fold excess in aortic enhancement. Reducing contrast dose is valuable to avoid the unnecessary administration of a chemical compound to a patient, reduce the risk of potential nephrotoxicity and lower cost. A lower contrast dose proved viable and was further supported by reduced kVp. Reduced contrast dose improved vascular conspicuity within abdominal organs (particularly the liver). A 25% reduction in contrast dose performed better than the standard dose in the arterial and hepatic phases. Lower radiation exposures (90kVp) improved mean CT attenuation values of contrast for the aorta in the arterial phase, and all vascular and parenchymal structures measured in the hepatic phase (except spleen) and delayed phase. The combination of lower radiation exposure and reduced contrast dose can be used in cats for multiphase CECT of the abdomen.

The fundamental goal of multiphase CECT is to improve contrast resolution, which is critical in acute abdomens, peritonitis, peritoneal effusion and mass effect with crowding of the abdomen. However, the integrity of the biliary tract cannot be assessed on multiphase CECT of the abdomen. The intrahepatic bile ducts are inconspicuous. Only the extra hepatic biliary tract is visible in the normal abdomen, and even this may become obscured in acute abdominal disease. In Chapter 4 of this thesis, we explored the feasibility of visualising the biliary tract in dogs and cats on CECT using a novel contrast agent, gadoxetic acid. These were experimental studies in small groups of research dogs and cats. In dogs, CT cholangiography using gadoxetic acid provided adequate contrast enhancement of the gall bladder, bile duct and cystic duct and in more than half of the study population, it allowed visualization of the intrahepatic ducts that are not otherwise seen. Therefore, this imaging technique can be considered as an important diagnostic tool for patients with disruption or leakage of the biliary tree with clinical signs manifesting from bile peritonitis. This can occur because of abdominal trauma or iatrogenic secondary to liver lobectomy or cholecystectomy. In these cases, evidence of biliary leakage on cholangiography that can be expected include extravasation of contrast into the peritoneal cavity. Further research is required on the clinical application of this technique in dogs with bile peritonitis to provide a description of the imaging features. Results from this research thesis demonstrated that CT cholangiography using gadoxetic acid can be performed in sedated animals with no significant compromise to image quality. This avoids the need for general anesthesia which is a desirable option in patients that may be critically ill from peritonitis. The optimal timing of image acquisition was 65 minutes after contrast administration to achieve maximal contrast enhancement of the biliary tree. Maximum contrast enhancement that could be achieved was variable between dogs and this research thesis identified that contrast dose had a positive influence. Although some dogs showed strong contrast enhancement with the low contrast dose, all dogs showed a positive response to a higher contrast dose. Given the wide safety range of gadoxetic acid in dogs, our results suggest that increasing the dose could be considered in cases with suboptimal enhancement. However, increasing the contrast dose can be cost prohibitive especially in heavy body weight patients. An alternative CT cholangiography technique was published in the veterinary literature during the course of this thesis. New veterinary CT studies on drip infusion cholangiography (DIC-CT) have trialled iotroxate meglumine (Biliscopin; 2ml/kg) in dogs and cats. Animals were administered the infusion over 30 mins and CT was performed at 60 mins. In dogs, contrast enhancement of the biliary tract was seen in 9/10 dogs with a gallbladder mucocele (Hayakawa et al, 2018). Iotroxate meglumine also proved to be effective and safe for visualisation of the bile duct in cats with and without biliary disease (obstructive and non-obstructive) (Tanaka et al, 2017). These results outperform gadoxetic acid as a cholangiographic contrast medium in cats in this thesis. Gadoxetic acid had poor excretion into the biliary tract of cats even on the high dose with absent enhancement in 20% and poor enhancement in 57%.

SECTION 5 - Conclusion

This thesis has improved our technical understanding of CECT for hepatobiliary imaging with a focus on optimising the utility of contrast agents and improving image quality. Vascular and parenchymal CT imaging using an iodinated contrast agent is the mainstay for dogs and cats, and a new lower dose is recommended in cats based on our research. Biliary CT imaging using a gadolinium based contrast agent was feasible in dogs but was cost prohibitive, and not feasible in cats. New information gained from this research has been used to standardise protocols used for scanning the abdomen in dogs and cats and has been applied to clinical patients in veterinary radiology. The importance of standardising contrast injection protocols and CT scan timing for multiphase CECT imaging cannot be overlooked and there are unique challenges when facing veterinary patients that differs to human patients. We have proven that patient body weight, contrast injection technique and contrast dose in cats are significant factors to consider when planning multiphase CECT. Standardised protocols for multiphase studies in humans have already been established and is well-recognised in human radiology and is incorporated into The American and European Associations for the Study of Liver disease to ensure performance and quality of imaging. There is certainly strong interest in the veterinary radiology field to extract meaningful information from multiphase CECT studies of the liver, pancreas, spleen and other organ systems. The ability to non-invasively diagnose tumours such as hepatocellular carcinoma, hepatoma or pancreatic insulinoma using multiphase CECT is desirable, and routinely used in human radiology. We are yet to achieve a clear consensus in veterinary radiology on the classic CT enhancement characteristics of these types of tumours, possibly because scan protocols have varied widely between veterinary referral centres. Standardised protocols for contrast injection and CT scan times derived from this research may provide renewed hope for using multiphase CECT to non-invasively diagnose certain cancers. Further research on the sensitivity and specificity of this multiphase imaging technique for screening patients with focal or multifocal liver disease could be considered. The rate of lesion detection using our standardised protocol could be assessed compared to other previously described CT scan protocols. Additionally, the contrast enhancement characteristics of focal liver lesions could be analysed in large retrospective clinical case studies with histopathology to correlate with the aim of accurately classifying tumour type based on multiphase CECT imaging.

SECTION 6 – Bibliography

1. Allan GS and Dixon RT. 1975 'Cholecystography in the dog: the choice of contrast media and optimum dose rates'. *Veterinary Radiology and Ultrasound,* Vol, 16, pp. 98–104.
2. Awai K and Hori S. 2003 'Effect of contrast injection protocol with dose tailored to patient weight and fixed injection duration on aortic and hepatic enhancement at multidetector-row helical CT.' *European Radiology,* Vol. 13, pp. 2155-2160.
3. Bae KT. 2010 'Intravenous contrast medium administration and scan timing at CT: considerations and approaches.' *Radiology*, Vol. 256, No. 1, pp. 32–61.
4. Bertolini, G. 2017 'Body MDCT in small animals – basic principles, technology and clinical applications' *Springer International Publishing, Padua, Italy.*
5. Bertolini, G., Rolla, E.C, Zotti, A. and Caldin, M. 2006 'Three dimensional multislice helical computed tomography techniques for canine extra-hepatic portosystemic shunt assessment' *Veterinary Radiology and Ultrasound,* Vol 47, No. 5, pp 439-443.
6. Blaser, A, Dennler, M, Mosing, M, Gent, T.C, Santner, G, Imhasly, S, Boretti, F.S, Reusch, C.E, Kircher, P. and Sieber-Ruckstuhl, N.S. 2016 'Effects of contrast medium injection technique on attenuation values of adrenal glands in healthy dogs during contrast-enhanced computed tomography' *American Journal of Veterinary Research,* Vol. 77, pp. 144-150.
7. Bouma, J.L, Aronson, L.R, Keith, D.G. and Saunders, H.M. 2003 'Use of computed tomography renal angiography for screening feline renal transplant donors' *Veterinary Radiology and Ultrasound,* Vol. 44, No. 6, pp. 636-641.
8. Buishand, F.O, Gross, F.R.V, Kirpensteijn, J. and van Nimwegen, S.A. 2018 'Utility of contrast-enhanced computed tomography in the evaluation of canine insulinoma location' *Veterinary Quarterly,* Vol 38, No. 1, pp. 53-62.
9. Burti, S, Zotti, A, Bonsembiante, F, Contiero, B. and Banzato, T. 2021 'Diagnostic accuracy of delayed phase post contrast computed tomographic images in the diagnosis of focal liver lesions in dogs: 69 cases' *Frontiers in Veterinary Science,* Vol. 8, pp. 1-10.
10. Burti, S, Zotti, A, Bonsembiante, F, Contiero, B. and Banzato, T. 2021 'Diagnostic accuracy of delayed phase post contrast computed tomographic images in the diagnosis of focal liver lesions in dogs: 69 cases' *Frontiers in Veterinary Science,* Vol. 8, Article 611556.
11. Cao, S.E, Zhang, L.Q, Kuang, S.C, Shi, W.Q, Hu, B, Xie, S.D, Chen, Y.N, Liu, H, Chen, S.M, Jiang, T, Ye, M, Zhang, H.X. and Wang, J. 2020 'Multiphase convolutional dense network for the classification of focal liver lesions on dynamic contrast enhanced computed tomography' *World Journal of Gastroenterology,* Vol, 26, No. 25, pp. 3660-3672.
12. Carlson, S.K, Johnson, C.D, Bender, C.E. and Welch, T.J. 2000 'CT of focal nodular hyperplasia of the liver' *American Journal of Roentgenology,* Vol. 174, pp. 705-712.
13. Cordella, A, Caldin, M. and Bertolini, G. 2020 'Splenic extramedullary hematopoiesis in dogs is frequently detected on multiphase multidetector-row CT as hypervascular nodules.' *Veterinary Radiology and Ultrasound,* Vol. 61, No. 5, pp. 512-518.

14. Cordella, A. and Bertolini, G. 2021 ‘Multiphase multidetector-row CT reveals different patterns of hepatic portal venous gas and pneumobilia.’ *Veterinary Radiology and Ultrasound,* Vol. 62, pp. 68-75.
15. Courtice, F.C. 1943 ‘The blood volume of normal animals.’ *Journal of Physiology,* Vol. 102, pp. 290-305.
16. De Magistris, A.V, Rossi, F, Valenti, P, Anson, A, Penninck, D.G, Agut, A. and Specchi, S. 2022 ‘CT feaures of gastrointestinal spindle cell, epithelial and round cell tumours in 41 dogs’ *Veterinary Radiology and Ultrasound,* Vol. 64, pp. 271-282.
17. Döhr, O, Hofmeister, R, Treher, M. and Schweinfurth, H. 2007 ‘Preclinical safety evaluation of Gd-EOB-DTPA (Primovist).’ *Investigative Radiology,* Vol. 42, pp. 830–841.
18. Feeney, D.A, Barber, D.L. and Osborne, C.A. 1982 *‘The functional aspects of the nephrogram in excretory urography: a review’ Veterinary Radiology and Ultrasound,* Vol. 23, No. 2, pp.42-45.
19. Fernando, J.L, Loughin, C.A, Dewey, C.W, Marino, D.J, Akerman, M and Lesser M.L. 2018 ‘Histopathologic characteristics of biopsies from dogs undergoing surgery with concurrent gross splenic and hepatic masses: 125 cases (2012-2016)’ *BMC Research Notes* Vol 11, No 122.
20. Fields, E.L, Robertson, I.D, Osborne, J.A and James C. 2012 ‘Comparison of abdominal computed tomography and abdominal ultrasound in sedated dogs’ *Veterinary Radiology and Ultrasound,,* Vol. 53, pp. 513-517.
21. Fischetti, A.J. and Kovak, J. 2008 ‘Imaging diagnosis: azygous continuation of the caudal vena cava with and without portocaval shunting’ *Veterinary Radiology and Ultrasound,* Vol, 49, No. 6, pp. 573–576.
22. Fujita, M. and Orima, H. 1994 ‘Effect and safety of meglumine iotroxate or cholangiocystography in normal cats.’ *Veterinary Radiology and Ultrasound,* Vol. 35, pp. 79–82.
23. Fukushima, K, Kanemoto, H, Ohno, K, Takahashi, M, Nakashima, K, Fujino, Y, Uchida, K, Fujiwara, R, Nishimura, R. and Tsujimoto, H. 2012 ‘CT characteristics of primary hepatic mass lesions in dogs’ *Veterinary Radiology and Ultrasound,* Vol. 53, No. 3, pp. 252-257.
24. Fukushima, K., Fujiwara, R, Yamamoto, K, Kanemoto, H, Ohno, K, Tsuboi, M, Uchida, K, Matsuki, N, Nishimura, R. and Tsujimoto, H. 2015 ‘Characterisation of triple-phase computed tomography in dogs with pancreatic insulinoma,’ *Journal of Veterinary Medical Science,* Vol. 77, No. 12, pp. 1549-1553.
25. Gaschen L. 2009 ‘Update on hepatobiliary imaging’. *Veterinary Clinics North American Small Animal Practoce*, Vol 39, pp. 439–467.
26. Gbande, P, N’timon, B, Tchakpedeou, D.A, Tchaou, M, Adambounou, K, Sonhaye, L, Agoda-Koussema, L.K. and Adjenou, K. 2023 ‘Evaluation of iodinated contrast media use in abdominal CT scans in cancer assessments: a cross sectional study in Lome (Togo).’ *Hindawi Radiology Research and Practice.*
27. Gregori, T, Mantis, P, Benigni, L, Priestnall, S.L. and Lamb, C.R. 2015 ‘Comparison of computed tomographic and pathologic findings in 17 dogs with primary adrenal neoplasia’ *Veterinary Radiology and Ultrasound,* Vol. 56, No. 2, pp. 153-159.
28. Griebie, E.R, David, F.H, Ober, C.P, Feeney, D.A, Anderson, K.L, Wuenschmann, A. and Jessen, C.R. 2017 ‘Evaluation of canine hepatic

masses by use of triphasic computed tomography and B-mode, color flow, power and pulsed wave Doppler ultrasonography and correlation with histopathologic classification' *American Journal of Veterinary Research,* Vol. 78, No. 11, pp. 1273-1283.
29. Han, J.K, Kim, A.Y, Lee, K.Y, Seo, J.B, Kim, T.K, Choi, B.I, Lhee, C.S. and Han, M.C. 2000 'Factors influencing vascular and hepatic enhancement at CT: experimental study on injection protocol using a canine assisted model' *Journal of Computed Assisted Tomography,* Vol, 24, No. 3, 400-406.
30. Hayakawa, S, Sato, K, Sakai, M, Kutara, K, Asano, K. and Watari, T. 2018 'CT cholangiography in dogs with gallbladder mucocele' *Journal of Small Animal Practice,* Vol 59; pp. 490-495.
31. Hollett MD, Jeffrey RB, Nino-Murcia M, Jorgensen M.J. and Harris, D.P. 1995 'Dual-phase helical CT of the liver: value of arterial phase scans in the detection of small (<1.5cm) malignant hepatic neoplasms' *American Journal of Roentgenology*, Vol, 164, No. 4, pp. 879–884.
32. Hsieh, C.C, Zeng, A.B, Chen, C.H, Jhou, Z.Y, Wang, C.D, Yang, Y.L, Hsieh, F.C, Lin, J.K, Yeh, J.Y. and Huang, C.C. 2021 'A practical biphasic contrast media injection protocol strongly enhances the aorta and pulmonary artery simultaneously using a single CT angiography scan'. *BMC medical Imaging,* Vol 21, 160.
33. Huda, W, Scalzetti, E.M. and Levin, G. 2000 'Technique factors and image quality as functions of patient weight at abdominal CT' *Radiology,* Vol. 217, no. 2.
34. Ichikawa, T, Federle, M.P, Grazioli, L. and Nalesnik, M. 2000 'Hepatocellular adenoma: multiphasic CT and histopathologic findings in 25 patients' *Radiology,* Vol. 214, pp. 861-868.
35. Irausquin, R.A, Scavelli, T.D, Corti, L, Joseph, D, Stefanacci, J.D, Demarco, J, Flood, S and Rohrbach, B.W. 2008 'Comparative evaluation of the liver in dogs with a splenic mass by using ultrasonography and contrast-enhanced computed tomography' *Canadian Veterinary Journal, Vol* 49, pp. 46–52.
36. Iseri, T, Yamada, K, Chijiwa, K, Nishimura, R, Matsunaga, S, Fujiwara, R. and Sasaki, N. 2007 'Dynamic computed tomography of the pancreas in normal dogs and in a dog with pancreatic insulinoma'. *Veterinary Radiology and Ultrasound,* Vol. 48, No. 4, pp. 328-331
37. Janq, H.J, Kim, T.K, Khalili, K, Yazdi, L, Menezes, R, Park, S.H. and Sherman, M. 2013 'Characterisation of 1 to 2cm liver nodules detected on HCC surveillance ultrasound according to the criteria of the American association for the study of liver disease: is quadriphasic CT necessary?' *Gastrointestinal imaging,* Vol. 201, pp. 314-321.
38. Jones, I.D, Lamb, C.R, Drees, R, Priestnall, S.L. and Mantis, P. 2016 'Associations between dual-phase computed tomography features and histopathologic diagnoses in 52 dogs with hepatic or splenic masses.' *Veterinary Radiology and Ultrasound,* Vol. 57, No. 2, pp. 144-153.
39. Kim, T.H, Kim, S.Y, Tang, A. and Lee, J.M. 2019 'Comparison of international guidelines for noninvasive diagnosis of hepatocellular carcinoma: 2018 update' *Clinical and Molecular Hepatology,* Vol. 25, pp. 245-263.
40. Kulkarni, N, Fung, A, Kambadakone, A.R. and Yeh, B.M. 2021 'CT techniques, protocols, advancements and future directions in liver diseases' *Magnetic Resonance Imaging Clinics of North America,* Vol. 29, No. 2, pp. 305-320.

41. Kutara, K, Seki, M, Ishikawa, C, Sakai, M, Kagawa, Y, Iida, G, Ishigaki, K, Teshima, K, Edamura, K, Nakayama, T. and Asano, K. 2013 'Triple-phase helical computed tomography in dogs with hepatic masses.' *Veterinary Radiology and Ultrasound,* Vol. 55, No. 1, pp 7-15.
42. Latimer, H.B. 1967 'Variability in body organ weights in the newbody dog and cat compared with that in the adult' *The Anatomical Record,* vol. 157, no. 3, pp. 449-456.
43. Lee N.K, Kim S, Lee J.W, Lee, S.H, Kang, D.H, Kim, G.H. and Seo, H.I. 2009 'Biliary MR imaging with Gd- EOB-DTPA and its clinical applications' *Radiographics,* Vol, 29, pp. 1707–1724.
44. Leela-Arporn, R, Ohta, H, Shimbo, G, Hanazono, K, Osuga, T, Morishita, K, Sasaki, N. and Takiguchi, M. 2019 'Computed tomographic features for differentiating benign from malignant liver lesions in dogs' *Journal of Veterinary Medical Science,* Vol. 81, No. 12, pp. 1697-1704.
45. Li, B, Ren, M, Abouelfetouh, M.M, Guo, P, Ding, M.X, Yang, D, Wu, Y. and Ding, Y. 2022 'Optimal delay for triple-phase hepatic computed tomography using a bolus-tracking technique in cats' *Animal Diseases,* Vol. 2, pp. 1-9.
46. Mahesh, M. 2002 'Search for isotropic resolution in CT from conventional through multiple-row detector' *Radiographics,* Vol 22, pp. 949-962
47. Mai W, Suran JN, Caceres AV. And Feetz, J.A. 2013 'Comparison between bolus tracking and timing- bolus techniques for renal computed tomographic angiography in normal cats.' *Veterinary Radiology and Ultrasound,* Vol. 54, No. 4, pp.343-350
48. Mai, W. and Caceres, A.V. 2008 'Dual-phase computed tomographic angiography in three dogs with pancreatic insulinoma' *Veterinary Radiology and Ultrasound,* Vol. 49, No. 2, pp. 141-148.
49. Maiti SK, Ajith P, Dutta A, Kumar, N. and Sharma, A.K. 2011 'Laparoscopic-assisted cholecystocentesis and cholecystocholangiography in canines'. *Journal of Applied Animal Research,* Vol 39, No. 1, pp. 29–32.
50. Makara. M, Dennler. M, Kuhn. K, Kalchofner, K. and Kircher, P. 2011 'Effect of contrast medium injection duration on peak enhancement and time to peak enhancement of canine pulmonary arteries.' *Veterinary Radiology and Ultrasound,* Vol. 52, No. 6, pp. 605–610.
51. Marks, A.L, Hecht, S, Stokes J.E, Conklin, G.A. and Deanna, K.H. 2014 'Effects of gadoxetate disodium (Eovist) contrast on magnetic resonance imaging char- acteristics of the liver in clinically healthy dogs.' *Veterinary Radiology and Ultrasound* Vol. 55, pp, 286–291.
52. Marolf A.J, Stewart J.A, Dunphy T.R. and Kraft, S.L. 2011 'Hepatic and pancreaticobiliary MRI and MR cholangiopancreatography with and without secretin stimulation in normal cats'. *Veterinary Radiology and Ultrasound,* Vol, 52, pp. 415–421.
53. Marrero, J.A, Kulik, L.M., Sirlin, C.B, Zhu, A.X, Finn, R.S, Abecassis, M.M, Roberts, L.R. and Heimbach, J.K. 2018 'Diagnosis, staging, and management of hepatocellular carcinoma: 2018 practice guidance by the American association for the study of liver diseases' *Hepatology,* Vol. 68, No. 2, pp. 723-750.
54. Mitchell, D, Bruix, J, Sherman, M. and Sirlin, C.B. 2015 'LI-RADS (Liver imaging reporting and data system): summary, discussion, and consensus of the LI-RADS management working group and future directions' *Hepatology,* Vol. 61, pp. 1056-1065.

55. Mortele, K.J, Oliva, M.R, Ondategui, S, Ros, P.R. and Silverman, S.G. 2004 'Universal Use of Nonionic Iodinated Contrast Medium for CT: Evaluation of Safety in a Large Urban Teaching Hospital' *American Journal of Roentgenology,* Vol, 185, pp. 31-34
56. Noh, D, Shim, J, Choi, S, Choi,H. and Lee, Y. 2022 'Computed tomographic findings of primary renal tumours in dogs and cats' *Thai Journal of Veterinary Medicine,* Vol. 52, No. 3, pp. 499-505.
57. Ohashi I, Hanafusa K and Yoshida T. 1993 'Small hepatocellular carcinomas: two-phase dynamic incremental CT in detection and evaluation' *Radiology,* Vol. 189, No. 3, pp. 851– 855.
58. Ohlerth, S. and Scharf, G. 2007 'Computed tomography in small animals – basic principles and state of the art applications' *The Veterinary Journal,* Vol 173, no.2, pp. 254-271.
59. Oliver J.H, Baron R.L, Federle M.P and Rockette, H.E. 1996 'Detecting hepatocellular carcinoma: value of unenhanced or arterial phase CT imaging or both used in conjunction with conventional portal venous phase contrast-enhanced CT imaging' *American Journal of Roentgenology,* Vol 167, No. 1, pp. 71–77.
60. *Prullage, M.L, Scwendenwein, I, Eberspacher-Schweda, E. and Kneissl, S.* 2022 'Does intravenous contrast medium administration result in altered renal biomarkers? A study in clinically stable cats with and without azotemia.' *Journal of Feline medicine and surgery,* Vol. *24, No. 6, pp. 656-579*
61. Ross, L. 2011 'Acute kidney injury in dogs and cats'. *Veterinary Clinics of North America: Small Animal Practice,* Vol 41, pp. 1-14.
62. Sabarudin A, Sun, Z. and Ng, K.H. 2012 'A systematic review of radiation dose associated with different generations of multidetector CT coronary angiography' *Journal of Medical Imaging and Radiation Oncology,* Vol 56, pp. 5-17.
63. Schmitz SA, Wagner S, Schuhmann-Giampieri G, Krause, W, Bollow, M. and Wolf, K.J. 1997b 'Gd- EOB-DTPA and Yb-EOB-DTPA: two prototypic contrast media for CT detection of liver lesions in dogs.' *Radiology,* Vol. 205, pp. 361–366.
64. Schmitz SA, Wagner S, Schuhmann-Giampieri G, Krause, W. and Wolf, K.J. 1997a 'A prototype liver-specific contrast medium for CT: preclinical evaluation of gadoxetic acid disodium, or Gd-EOB-DTPA.' *Radiology,* Vol. 202, pp. 407–412.
65. Schwarz, T. and Saunders, J. 2011 'Veterinary computed tomography' *Wiley-Blackwell Publishing,* West Sussex, UK.
66. Secrest, S, Sharma, A. and Bugbee, A. 2018 'Triple phase computed tomography of the pancreas in healthy cats' *Veterinary Radiology and Ultrasound,* Vol. 59, pp. 163-168.
67. Shaker, R, Wilke, C, Ober, C. and Lawrence, J. 2021 'Machine learning model development for quantitative analysis of CT heterogeneity in canine hepatic masses may predict histologic malignancy' *Veterinary Radiology and Ultrasound,* Vol. 62, pp. 711-719.
68. Shanaman, M.M, Hartman, S.K and O'Brien, R.T. 2012 'Feasibility for using dual-phase contrast-enhanced multi-detector helical computed tomography to evaluate awake and sedated dogs with acute abdominal signs' *Veterinary Radiology and Ultrasound,* Vol 53, pp 605-612.

69. Shanaman, M.M, Schwarz, T, Gal, A. and O'Brien, R. 2013 'Comparison between survey radiography, B-mode ultrasonography, contrast enhanced ultrasonography and contrast enhanced multi-detector computed tomography findings in dogs with acute abdominal signs. *Veterinary Radiology and Ultrasound,* Vol, 54, pp.591-604.
70. Shi, W, Kuang, S, Cao, S, Hu,B, Xie, S, Chen, S, Chen, Y, Gao, D, Chen, Y, Zhu, Y, Zhang, H, Liu, H, Ye, M, Sirlin, C.B. and Wang, J. 2020 'Deep learning assisted differentiation of hepatocellular carcinoma from focal liver lesions: choice of four-phase and three-phase CT imaging protocol' *Abdominal Radiology,* Vol 45, pp. 2688-2697.
71. Spillmann T, Willard M.D, Ruhnke I, Suchodolski, J.S. and Steiner, J.M. 2013 'Feasibility of endoscopic retrograde cholangiopancreatography in healthy cats'. *Veterinary Radiology and Ultrasound*, Vol, 55, No. 1, pp. 85–91.
72. Stehlik, L, Tommaso M.D, Signore, F.D, Paninarova, M, Terragni, R, Magni, T, Pontonutti, L, Carloni, A, Alberti, M, De Magistris, A.V. and Vignoli, M. 2020 'Triple-phase multidetector computed tomography in distinguishing canine hepatic lesions' *Animals,* Vol. 11, pp. 1-12.
73. Stokes, J.E. and Bartges, J.W. 2006 'Causes of acute renal failure.' *Compendium* https://www.researchgate.net/profile/Joe-Bartges-2/publication/235676917_Causes_of_Acute_Renal_Failure/links/02e7e514c3859d9bb8000000/Causes-of-Acute-Renal-Failure.pdf
74. Suter P.F. and Olsson S.E. 1970 'The diagnosis of injuries to the intes- tines, gallbladder and bile ducts in the dog' *Journal of Small Animal Practice,* Vol, 11, pp. 575–584.
75. Szucs-Farkas, Z, Strautz, T, Patak, M.A, Kurmann, L, Vock, P. and Schindera, S.T. 2009 'Is body weight the most appropriate criterion to select patients eligible for low-dose pulmonary CT angiography? Analysis of objective and subjective image quality at 80 kVp in 100 patients'. *European Radiology,* Vol. 19, pp. 1914-1922
76. Tanaka, T, Akiyoshi, H, Mie, K, Okamoto, M, Yoshida, Y. and Kurokawa, S. 2019 'Contrast-enhanced computed tomography may be helpful for characterising and staging canine gastric tumours' *Veterinary Radiology and Ultrasound,* Vol. 60, No. 1, pp. 7-18.
77. Tanaka, T., Akiyoshi, H., Mie, K, Shimazaki, H. and Ohashi, F. 2017 '*Drip infusion cholangiography with CT in cats' Journal of feline medicine and surgery,* Vol. 20, No. 12, pp. 1173-1176.
78. Tang, A, Cruite, I, Mitchell, D.G. and Sirlin, C.B. 2018 'Hepatocellular carcinoma imaging systems; why they exist, how they evolved, and how they differ' *Abdominal Radiology,* Vol 43, pp. 3-12.
79. Taniura, T, Marukawa, K, Yamada, K, Hikasa, Y. and Ito, K. 2009 'Differential diagnosis of hepatic tumour-like lesions in dog by using dynamic CT scanning' *Hiroshima Journal of Medical Science,* Vol. 58, No. 1, pp. 17-24.
80. Tateishi, K, Kishimoto, M, Shimizu, J. and Yamada, K. 2008 'A comparison between injection speed and iodine delivery rate in contrast-enhanced computed tomography (CT) for normal beagles' *Journal of Veterinary Medical Science,* Vol. 70, No. 10, pp. 1027-1030.
81. Veterinary CT Scanner Market 2017, *Veterinary CT scanner market by type (multi-slice CT scanner, portable CT scanner), Animal (small animals, equine,*

livestock), Application (neurology, oncology, orthopedic, traumatology), End user (animal hospital, clinic) – Global Forecast to 2022. https://www.marketsandmarkets.com/Market-Reports/veterinary-ct-scanner-market-39631288.html

82. Wintersperger, B, Jakobs, T, Hezog, P, Schaller, S, Nikolaou, K, Suess, C, Weber, C, Reiser, M. and Becker, C. 2005 'Aorto-iliac multidetector-row CT angiography with low kV settings: improved vessel enhancement and simultaneous reduction of radiation dose' *European Radiology,* Vol. 15, pp 334-341.
83. Wise, M. 1982 'Nonselective angiocardiography in the normal dog and cat' *Veterinary Radiology and Ultrasound,* Vol. 23, No. 4, pp. 144-151.
84. Wrigley RH and Reuter RE. 1982 'Percutaneous cholecystography in normal dogs'. *Veterinary Radiology and Ultrasound,* Vol, 23, pp. 239–242.
85. Yonetomi, D, Kadosawa, T, Miyoshi, K, Nakao, Y, Homma, E, Hanazono, K, Yamada, E, Nakamura, K, Ijiri, A, Minegishi, N, Maetani, S, Hirayama, K, Taniyama, H. and Nakede, T. 2012 'Contrast agent Gd-EOB-DTPA (EOB-Primovist) for low-field magnetic reso- nance imaging of canine focal liver lesions.' *Veterinary Radiology and Ultrasound,* Vol. 53, pp. 371–380.
86. Yoshida, O, Kutara, K, Seki, M, Ishigaki, K, Teshima, K, Ishikawa, C, Iida, G, Edamura, K, Kagawa, Y. and Asano, K. 2016 'Preoperative differential diagnosis of canine adrenal tumours using triple-phase helical computed tomography' *Veterinary Surgery,* Vol. 45, pp. 427-435.
87. Yoshinobu, Y, Iwamoto, Y, Han, X, Lin, L, Hu, H, Zhang, Q. and Chen Y.W. 2020 Proceedings of *IEEE International Conference on Consumer Electronics (ICCE)*
88. Zwingenberger A.L, McLear R.C, Weisse C. 2005 'Diagnosis of arterioportal fistulae in four dogs using computed tomographic angiography' *Veterinary Radiology and Ultrasound,* Vol, 46, No. 6, pp. 472–477.
89. Zwingenberger AL, Schwarz T. 2004 'Dual-phase CT angiography of the normal canine portal and hepatic vasculature' *Veterinary Radiology and Ultrasound,* Vol 45. No. 2, pp. 117-124.